DISS. ETH NO. 17632

DEVELOPMENT OF NEW NUCLEOSIDE ANALOGUES AS PET IMAGING AGENTS FOR MONITORING GENE EXPRESSION

A dissertation submitted to

ETH ZURICH

for the degree of

Doctor of Sciences

presented by

MILJEN MARTIĆ

Dipl. Ing. Kemije, University of Zagreb, Croatia

born on January 14th, 1979

citizen of Zagreb, Croatia

accepted on the recommendation of

Prof. Dr. P.A. Schubiger, examiner
Prof. Dr. L. Scapozza, co-examiner
Prof Dr. S.M. Ametamey, co-examiner

2008

Acknowledgements

First of all, I would like to thank Prof. August Schubiger and Prof. Simon Ametamey for their support and understanding during entire duration of the thesis. I certainly hope they didn't regret waiting for me two years to start the Ph.D.

… Prof. Leonardo Scapozza, Dr. Remo Perozzo, Anja Stoeffel and Yvonne Westermeier from the University of Geneva for their support regarding enzyme kinetics and for docking countless numbers of molecules.

… Dr. Anass Johayem for introducing me into the field and help at the beginning of the synthesis.

… Dr. Jean-Fred Salazar and Sabine Baumann for teaching me basics of cell culture and ex-vivo studies. Thank you for your patience.

… Dr. Michael Honer and Claudia Keller for help during animal experiments, even when the wrong solvent was used ;-)

… Sandha Keller who helped me so many times with those "easy" administrative issues.

… Aileen Höhne, a "personal secretary", without whom I would be lost in schedule. Thank you for the friendship and those 3 nice years in the lab ☺

… Dr. Jessica Becaud for the nice friendship and support with so many scientific and technical issues ☺

… my dear "Boss", Dr. Tobias Ross, a good friend with a lot of ideas and positive energy! ☺

… Dr. Linjing Mu for many fruitful scientific and deep spiritual discussions in the train.

… Keith Graham for the friendship and giving me different, industrial, point of view on the science and everything around it ☺

… Mathias Nobst for the help on all those technical issues in which I am completely lost!

… Lab-mates Miray Demirer, Phoebe Lam, Marianne Kehl and Cindy Baumann, for the friendship and making those long hours in the lab very interesting ☺

… Dr. Christophe Lucatelli, Dr.Thomas Mindt and Dr. Meri De Angelis for many good ideas how to overcome chemistry problems.

… Dominic Franck, Simon Schwarz, Eva Geissler, Dr. Samson Fabrice, Dr. Thomas Ebenhan, Dr. Thomas Nauser, Dr. Volkmar Uhlendorf and everybody else for the nice atmosphere in the lab.

… Tanasis Galiciadis and Tibor Kovacs, for excellent professional IT support and advices.

… Sanja for the unlimited support, even when "why the hell not" is not an easy option! But the only right one ;-)

… a very special thanx goes to mysterious CS for making my life interesting ;-)

At the end I would like to express a big THANK YOU to my parents who kept me going and kept believing in me my whole life! Hvala vam! ☺

Table of Contents

List of Abbreviations

[^{18}F]FHBG	9-[4-[^{18}F]fluoro-3-(hydroxymethyl)butyl]guanine
[^{18}F]FLT	[^{18}F]fluoro-3'-deoxy-3'-L-fluorothymidine
[^{18}F]Fluoromethyl HHT	6-(2-hydroxy-hydroxypropyl)-5-[^{18}F]fluoromethyl (1H,3H)-pyrimidine-2,4-dione
[^{18}F]N-Me DHBT	6-(3-[^{18}F]fluoro-2-(hydroxymethyl)propyl)-1,5-dimethylpyrimidine-2,4(1H,3H)-dione
3D	three dimensional
Ac	acetyl
AcOH	acetic acid
ACV	acyclovir, 9-(2-hydroxymethyl)guanine
ADP	adenosine 5'-diphosphate
AIBN	2,2'-azobis(isobutyronitrile)
ATP	adenosine 5'-triphosphate
AZT	azidothymidine
BLI	bioluminescence imaging
Boc	*tert*-butoxycarbonyl
br	broad
BrUdR	bromodeoxyuridine
Cbz	benzyloxycarbonyl
CCD	charge coupled device
d	doublet
DAD	diode array detector
DAST	diethylaminosulfur trifluoride
dC	deoxycitidine
DHBT	6-(3-hydroxy-2-(hydroxymethyl)propyl)-5-methyl-pyrimidine-2,4(1H,3H)-dione
DMAP	4-dimethylaminopyridine
DMF	dimethylformamide
DMSO	dimethylsulfoxide
DNA	deoxyribonucleic acid

dT	deoxythymidine, 2'-deoxythymidine
dTDP	deoxythymidine 5'-diphosphate
dTMP	deoxythymidine 5'-monophosphates
dTTP	deoxythymidine 5'-triphosphate
dU	2'-deoxyuridine
dUDP	deoxyuridine 5'-diphosphate
dUMP	deoxyuridine 5'-monophosphate
dUTP	deoxyuridine 5'-triphosphate
EDTA	ethylenediamine tetraacetic acid
ELISA	enzyme linked immunosorbent assay
FGCV	8-fluoroganciclovir
FHBT	6-(3-fluoro-2-(hydroxymethyl)propyl)-5-methyl-pyrimidine-2,4(1H,3H)-dione
FHPG	9-[3-fluoro-1-hydroxy-2-propoxymethyl]guanine
FIAU	2'-fluoro-2'-deoxy-1-ß-D-arabinofuranosyl-5-iodouracil
FIRU	1-(2-fluoro-2-deoxy--D-ribofuranosyl)-5-iodouracil
FLI	fluorescent imaging
FMAU	1-(2'-deoxy-2'-fluoro-β-D-arabinofuranosyl)thymine
FPCV	8-fluoropenciclovir
GCV	ganciclovir, 9-(1,3-dihydroxy-2-propoxy-methyl)-guanine
GFP	green fluorescent protein
GOLD	genetic optimisation for ligand docking
HPLC	high performance liquid chromatography
HSV1	herpes simplex virus type 1
hTK	human thymidine kinase
hTK1	human thymidine kinase 1
hTK2	human thymidine kinase 2
IUdR	5-iodo-2'-deoxyuridine
IVFRU	(E)-5-(2-iodovinyl)-2'-fluoro-2'-deoxyuridine
K_{cat}	turnover number
K_i	inhibition constant
K_m	Michaelis-Menten constant
LB-Medium	Luria-Bertani medium
LDA	lithium diisopropylamide

LDH	lactate dehydrogenase
LOR	line of response
m	multiplet
MeOH	methanol
MS	mass spectroscopy
MTr	4-methoxytrityl
MW	microwave
n	neutron
n.c.a.	non carrier added
NADH	nicotinamide-adenine dinucleotide, reduced form
N-Me DHBT	6-(3-hydroxy-2-(hydroxymethyl)propyl)-1,5-dimethyl-pyrimidine-2,4(1H,3H)-dione
NMR	nuclear magnetic resonance
OD	optical density
p	proton
p	para
PAGE	polyacrylamide gel electrophoresis
PCV	penciclovir, 2-amino-9-[4-hydroxy-3-(hydroxymethyl)-butyl]-3H-purin-6-one
PDB	protein data bank
PEP	phosphoenolpyruvate
PET	positron emission tomography
PK	pyruvate kinase
PMB	*p*-methoxybenzyl
PMSF	phenyl methyl sulfonyl fluoride
POCl$_3$	phosphorous oxychloride
PSF	penicillin streptomycin fungizone
q	quartet
RCY	radiochemical yield
RMSD	root mean square deviation
RNA	ribonucleic acid
ROI	region of interest
RPMI	Roswell Park Memorial Institute
s	singlet

SDS	sodium dodecyl sulfate
S_N2	bimolecular nucleophilic substitution
SPECT	single-photon emission computed tomography
t	triplet
TBAF	tertabutylammonium fluoride
Tf	triflate, trifluoromethanesulfonyl
THF	tetrahydrofurane
TK	thymidine kinase enzyme
tk	thymidine kinase gene
TK1	human cytosolic thymidine kinase
TK2	human mitochondrial thymidine kinase
TLC	thin layer chromatography
Tris	tris(hydroxymethyl)aminomethane
Ts	tosyl, p-toluensulfonyl
UV	ultra violet
V_{max}	rate of enzyme catalyzed reaction at infinite concentration of substrate
XTT	2,3-bis(2-methoxy-4-nitro-5-sulfophenyl)-2H-tetrazo-lium-5-carboxanilide

Summary

Gene therapy offers a promising new treatment modality for a variety of inherited and acquired disorders. All of the gene therapy approaches are based on the common strategy to use gene delivery to effect production of a therapeutic protein in a target tissue. For application in humans as well as for research purposes, it is critically important to have a noninvasive imaging modality such as positron emission tomography (PET), which offers the possibility of monitoring the location, magnitude, and duration over time of the expression of delivered therapeutic genes. One of the most promising approaches in imaging gene expression uses the gene of the viral enzyme herpes simplex virus thymidine kinase (HSV1 *tk*) as a reporter gene in combination with an appropriate reporter probe. Several pyrimidine and purine analogues labeled with F-18 or I-124 have been synthesized and evaluated as potential imaging agents for the HSV1 TK expression *in vivo*. These two classes of substrates are selectively phosphorylated by HSV1 TK to their monophosphates and thereby metabolically trapped in transfected cells.

Our investigations were prompted by the need to develop PET imaging agents that lack the disadvantages of already existing reporter probes such as cytotoxicity, unfavorable pharmacokinetics, and by-stander effect. The major advantage of pyrimidine analogues over the purine ones is that pyrimidine analogues do not show any or a very low by-stander effect.

The first chapter of this thesis gives a brief introduction on PET, HSV1 TK and its substrate acceptance properties, comparison of HSV1 TK to human TK, and basic approaches to gene therapy monitoring. Finally, a short introduction on molecular modeling, especially docking procedure concludes the first chapter.

Chapter 2 describes the synthetic attempts made to prepare FHBT, a fluoro analogue of the lead compound, 6-(1,3-dihydroxy-isobutyl)thymine (DHBT). Several synthetic strategies that were designed to prepare FHBT starting from DHBT or its two intermediates were not successful. In most cases, the anticipated reaction products were not formed, either because the intermediates or the starting material decomposed, or underwent intramolecular cyclization. The use of different protecting groups such as PMB, Cbz and Boc did not lead to the expected results. In one case, by protecting a hydroxyl group in DHBT with MTr and reacting with DAST, traces of the target compound, FHBT, were detected. An attempt was

made to prepare the [18F]FHBT starting from a tosyl precursor. Although the F-18 labeled MTr-protected intermediate was synthesized, no traces of [18F]FHBT could be found after the deprotection step since the radiolabeled intermediate decomposed or underwent intramolecular cyclization.

In Chapter 3 the focus is on the preparation of a novel C-6 substituted radiolabeled HSV1 TK substrate. In order to prevent intramolecular cyclization and undesired side reactions described in Chapter 2, a methyl group at the N-1 position of the pyrimidine ring was introduced. Molecular modeling studies were employed to explore the outcome of the substitution in the N-1 position. It was found that the introduction of a methyl group in the N-1 position of the pyrimidine ring should not have any detrimental effects on the binding properties of the methylated non-fluorinated ligand, N-Me DHBT.

The total synthesis of the novel non-fluorinated key intermediate, N-Me DHBT, was accomplished in a 10-step reaction sequence in 13 % overall yield. Enzymatic tests confirmed that N-Me DHBT is indeed a substrate for HSV1 TK. Additionally, cytotoxicity experiments on B16F1 cell lines showed that N-Me DHBT is not cytotoxic up to a concentration of 1 mM. Encouraged by these promising *in vitro* results, the fluoro analogue, N-Me FHBT was prepared. The introduction of a methyl group in the N-1 position of pyrimidine ring effectively prevented intramolecular cyclization and undesired side reactions, making the synthesis of the "cold" reference N-Me FHBT possible.

A suitable precursor for the radiosynthesis of [18F]N-Me FHBT was prepared in 30 % yield. The radiolabeling was carried out under classical conditions with potassium [18F]fluoride and kryptofix 2.2.2 in acetonitrile at 90°C and the fluorinated intermediate was produced in 35 % conversion. The cleavage of the MTr protecting group was accomplished by using 5% HCl in methanol. Radiochemically pure [18F]N-Me FHBT (>99 %) was obtained in 25 % RCY (decay corrected) after the HPLC purification.

Further *in vitro* validation (cell uptake studies) as well as *in vivo* studies are necessary to fully assess the applicability of [18F]N-Me FHBT for the monitoring of HSV1 TK expression *in vivo*. Although only N-Me DHBT was validated *in vitro*, the literature suggests that the binding affinities of N-Me DHBT and N-Me FHBT should be in the same range. Therefore, it can be concluded that [18F]N-Me FHBT is a promising candidate for monitoring HSV1 TK expression *in vivo*.

Zusammenfassung

Die Gentherapie ist eine vielversprechende neue Behandlungsmethode für eine Vielzahl von vererbten und erworbenen Erkrankungen. Alle Ansätze zur Gentherapie basieren auf der gemeinsamen Strategie, genetisches Material in Zellen einzuschleusen, um die Herstellung eines therapeutischen Proteins im betroffenen Gewebe auszulösen. Für die Anwendung am Menschen und auch für Forschungszwecke ist es entscheidend, über ein nicht-invasives bildgebendes Verfahren wie die Positronen-Emissions-Tomography zu verfügen, dass die Möglichkeit bietet, Ort, Ausmass und Dauer der Expression der eingeschleusten Gene zu überwachen. Einer der vielversprechensten Ansätze für die bildliche Darstellung der Genexpression nutzt das Gen für die Thymidinkinase des Herpes Simplex Virus (HSV1 *tk*) als Reportergen in Kombination mit einem geeigneten Reportersubstrat. Diverse F-18 oder I-124 markierte Pyrimidin- und Purin-Analoga wurden bereits synthetisiert und als potentielle Radiodiagnostika für die Expression des Enzyms HSV1 TK *in vivo* getestet. Diese zwei Substratklassen werden durch HSV1 TK selektiv zu Monophosphaten phosphoryliert und dadurch in den transfizierten Zellen metabolisch angereichert.

Die Motivation unserer Untersuchungen ist der Bedarf an PET-Reportersubstanzen ohne die Nachteile bisheriger Reportersubstrate wie Zytotoxizität, ungünstige Pharmakokinetik und den sogenannten Bystander-Effekt. Der Vorteil der Pyrimidin- gegenüber den Purin-Analoga ist hierbei der nicht vorhandene oder allenfalls sehr geringe Bystander-Effekt.

Das erste Kapitel dieser Arbeit enthält eine kurze Einführung in PET, HSV1 TK und seine Substratspezifität, einen Vergleich von HSV TK1 mit der humanen TK, und grundlegende Ansätze der Gentherapieüberwachung. Eine kurze Einführung ins Molecular Modeling mit Schwerpunkt auf die Docking-Methode beschliesst das erste Kapitel.

Kapitel 2 beschreibt die synthetischen Ansätze zur Herstellung von FHBT, des Fluor-Analogs der Leitstruktur 6-(1,3-Dihydroxy-isobutyl)thymin (DHBT). Keine der etlichen synthetischen Strategien, die zur Darstellung von FHBT aus dem Ausgangsstoff DHBT oder einer seiner zwei Vorstufen führen sollten, war erfolgreich. Im Allgemeinen wurden die erwarteten Reaktionsprodukte nicht gebildet, entweder aufgrund Zersetzung der Zwischenstufen oder des Ausgangsmaterials, oder ihrer intramolekularen Zyklisierung. Die Verwendung verschiedener

Schutzgruppen wie zum Beispiel PMB, Cbz oder Boc führte nicht zu den erwarteten Resultaten. In einem Fall, in welchem MTr-geschütztes DHBT mit DAST umgesetzt wurde, war es möglich, Spuren der Zielstruktur FHBT zu detektieren. Es wurde der Versuch unternommen, [^{18}F]FHBT ausgehend vom Tosyl-Vorläufer herzustellen. Obwohl die F-18 markierte, MTr-geschützte Zwischenstufe synthetisiert werden konnte, war es nicht möglich, nach dem Entschützungsschritt [^{18}F]FHBT nachzuweisen, da währenddessen die Zersetzung oder intramolekulare Zyklisierung der radiomarkierten Zwischenstufen auftrat.

Im Kapitel 3 liegt der Schwerpunkt auf der Herstellung eines neuartigen C-6 substituierten radiomarkierten HSV1 TK Substrates. Um die intramolekulare Zyklisierung und die unerwünschten Nebenreaktionen, welche im Kapitel 2 beschrieben wurden, zu umgehen, wurde eine Methylgruppe an der N-1 Position des Pyrimidinrings eingeführt. Molecular-Modeling-Studien wurden durchgeführt, um die Auswirkungen der Substitution der N-1 Position zu untersuchen. Es wurde festgestellt, dass die Einführung einer Methylgruppe in der N-1 Position des Pyrimidinrings keine nachteiligen Auswirkungen auf die Bindungseigenschaften des methylierten nicht-fluorierten Liganden, N-Me DHBT, haben sollte.

Die Totalsynthese der neuartigen nicht-fluorierten zentralen Zwischenstufe N-Me DHBT wurde in einer zehnstufigen Reaktionssequenz mit einer Gesamtausbeute von 13% erreicht. Enzymatische Tests bestätigten, dass N-Me DHBT tatsächlich ein Substrat für HSV1 TK ist. Zytotoxizitätstests mit B16F1 Zelllinien zeigten, dass N-Me DHBT in Konzentration bis zu 1 mM nicht zytotoxisch wirkt.

Aufgrund der vielverprechenden *in vitro* Resultate mit N-Me DHBT wurde das Fluoranalog, N-Me FHBT, synthetisiert. Die Einführung einer Methylgruppe an der N-1 Position des Pyrimidinrings verhinderte wirksam die intramolekulare Zyklisierung und unerwünschte Nebenreaktionen und ermöglichte dadurch die Synthese der „kalten" Referenzverbindung N-Me FHBT. Ein geeigneter Präkursor für Die Radiosynthese von [^{18}F]N-Me FHBT wurde in 30% Ausbeute hergestellt. Die Radiomarkierung wurde unter klassischen Bedingungen mit [^{18}F]Kaliumfluorid und Kryptofix 2.2.2. in Acetonitril bei 90°C durchgeführt und die [^{18}F]fluorierte Zwischenstufe mit 35% Umsetzung produziert. Die Abspaltung der MTr-Schutzgruppe wurde mit 5% HCl in Methanol erreicht. Nach HPLC-Reinigung wurde radiochemisch-reines (> 99%) [^{18}F]N-Me FHBT in 25% radiochemischer Ausbeute (zerfallskorrigiert) erhalten.

Eine weitere *in vitro* Evaluation (Zellaufnahmestudien) sowie *in vivo* Studien sind notwendig, um die Eignung von [^{18}F]N-Me FHBT zur Überwachung der HSV1 TK Expression *in vivo* vollständig abzuschätzen. Obwohl lediglich N-Me DHBT *in vitro* validiert wurde, gibt es Hinweise in der Literatur, dass die Bindungsaffinitäten von N-Me DHBT und N-Me FHBT im selben Bereich liegen sollten. Deshalb kann geschlussfolgert werden, dass [^{18}F]N-Me FHBT ein vielversprechender Kandidat für die Kontrolle der HSV1 TK Expression *in vivo* ist.

1 Introduction

1.1 Positron Emission Tomography (PET)

Positron Emission Tomography (PET) is a nuclear medicine, quantitative imaging modality that produces a three-dimensional (3D) image or a map of functional processes in the body. Image map is reconstructed based on the coincidence detection of two gamma ray photons produced in annihilation process. In the process of annihilation, a positron (ejected from positron emitting radionuclide) and an electron from the surrounding medium are annihilated and two gamma ray photons are formed.

1.1.1 Positron Decay and Positron Emitting Radionuclides

The positron is the antiparticle or the antimatter counterpart of the electron. The positron has an electric charge of +1, a spin of 1/2, and the same mass as an electron. Nuclei that are "proton rich" (i.e., have an N/Z ratio less than that of the stable nuclei) can decay by β^+-particle emission accompanied by the emission of a neutrino. After β^+ particle emission, the daughter nuclide has an atomic number 1 less than the parent nuclide (Figure 1.1).

Beta plus decay can only happen inside nuclei when the absolute value of the binding energy of the daughter nucleus is higher than that of the mother nucleus. The difference between these energies goes into the reaction of converting a proton (p^+) into a neutron (n^0), a positron (e^+) and a neutrino (ν_e) and into the kinetic energy of these particles.

$$p^+ \rightarrow n^0 + e^+ + \nu_e$$
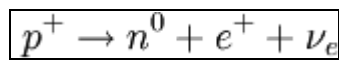
In the annihilation process energy and momentum are conserved. Therefore, the result is emission of 2 gamma rays, each having an energy equal to the rest-mass energy of electron or positron (mc^2 = 511 keV), which propagate in the opposite direction of each other. In the Table 1.1 are listed positron emitting radionuclides commonly used in research.
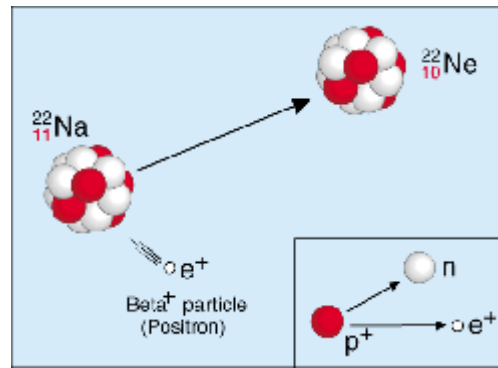
Figure 1.1. Graphical interpretation of beta plus decay [1]

Table 1.1. Most commonly used positron emitting radionuclides [2]

Radionuclide	Half-life	β^+ fraction (%)	Max Energy (MeV)
^{11}C	20.4 min	99	0.96
^{13}N	9.96 min	100	1.20
^{15}O	123 sec	100	1.74
^{18}F	109.8 min	97	0.63
^{38}K	7.6 min	100	2.68
^{62}Cu	9.74 min	98	2.93
^{64}Cu	12.7 hrs	19	0.65
^{68}Ga	68.3 min	90	1.83
^{72}As	26 hrs	88	2.52
^{73}Se	7.1 hrs	65	1.32
^{75}Br	98 min	75.5	1.74
^{76}Br	16.1 hrs	100	1.90
^{82}Rb	78 sec	96	3.15
^{86}Y	14.7 hrs	34	1.30
^{120}I	1.35 hrs	64	4.10
^{124}I	4.18 days	0.22	1.50

1.1.2 Data Acquisition and Image Reconstruction

Reconstruction of the three-dimensional image is based on the coincidence detection of two 511 keV gamma ray photons emitted after the annihilation of positron, from the positron emitter, and an electron, form the surrounding medium. Since formed photons travel in 180° to each other, only the coincidence of simultaneous photon detection on the opposite sides of the detector is recorded and stored for later processing. The virtual line connecting those two detection sites is called the line of response (LOR). The more lines of response, the higher resolution can be obtained. The position of the radioisotope within the investigated subject can be computed based on the intersections of LORs (Figure 1.2). Therefore, it is crucial to inject enough radioactive tracer to obtain sufficient resolution of the PET images.
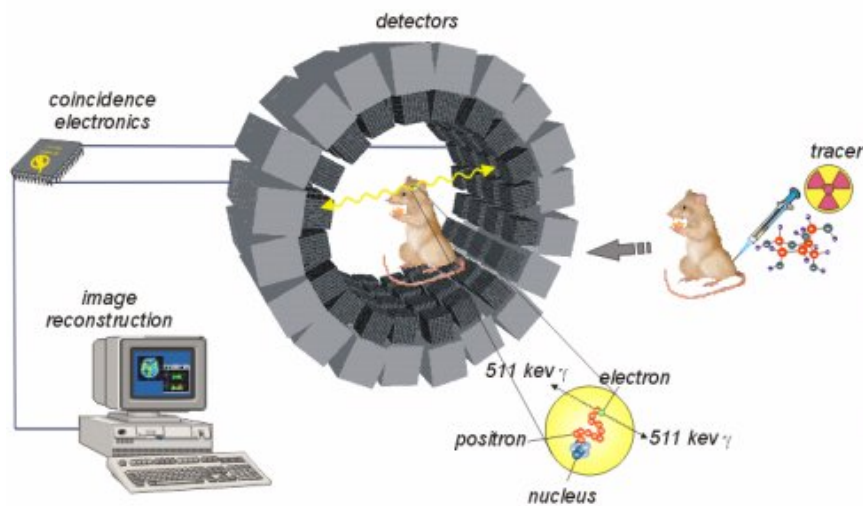
Figure 1.2. Animal experimental setup for the tracer evaluation with PET [3]. The radiolabeled compound is injected into an animal, after which the animal is anaesthetized and placed inside the PET scanner. Emitted gamma rays are detected and the image is reconstructed by intersecting lines of response.

1.1.3 Commonly Used Radionuclides for Radiolabeling of Organic Compounds for PET

Most commonly used PET radionuclides are ^{11}C and ^{18}F (Figure 1.3). The choice of these two radionuclides lies in their properties: short half-life, easy incorporation into organic molecules and the convenient on-site cyclotron production. In the case of carbon-11, stable ^{12}C can be replaced with β^+ emitter ^{11}C without changing the properties of the compound since all chemical properties remain intact. The disadvantage of C-11 is the in short half-life of 20.4 minutes which requires short radiosynthesis time and fast purification procedures [4].
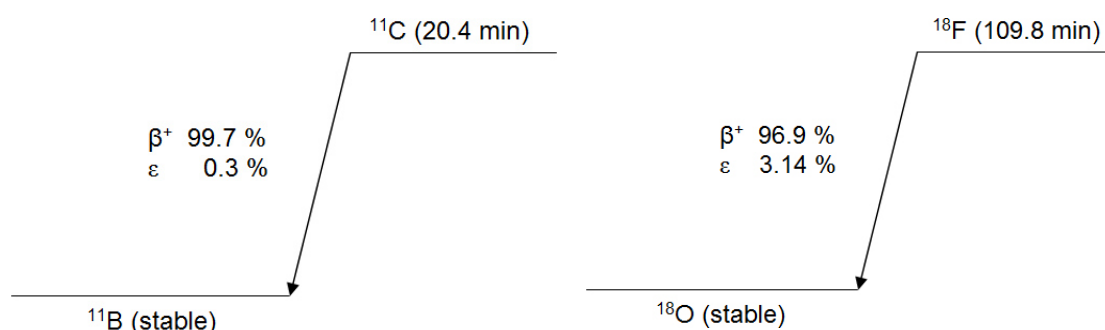
Figure 1.3. Decay schemes of C-11 and F-18

In the case of ^{18}F, chemical properties of the molecule are changed (unless ^{19}F is substituted with ^{18}F). The van der Waals' radius of the fluorine (1.35 Å) is similar to that of hydrogen (1.20 Å), which means that the size of the molecule would not be affected. However, differences in the electronic character are very pronounced. The half-life of 109.8 minutes allows multi-step radiosynthesis as well as extended PET studies of slower biochemical processes [4]. In addition, the radionuclide has low β^+ energy of 635 keV, essential for high resolution down to 1 mm in PET images [4].

1.1.4 ^{18}F Labeling Strategies

The F-18 can be incorporated into organic molecule either by electrophilic or via nucleophilic substitution [5]. Produced radiotracers can be obtained with very high specific radioactivies (50-500 GBq μmol^{-1}). However, the maximum theoretical value of 6.3 x 10^4 GBq μmol^{-1} is never reached due to contamination with the stable

isotope originating from the radionuclide production, the solvents, chemicals and other sources [5].

Electrophilic Radiofluorination

The simplest fluorinating reagent is $[^{18}F]F_2$ which provides a facile mean of introducing ^{18}F into electron-rich compounds. However, electrophilic fluorination of aromatic compounds using F_2 is a non-selective method since the oxidizing strength of fluorine may lead to exothermic radical chain reactions with the formation of side products and tars. Methods of $[^{18}F]F_2$ production require carrier fluoride (0.1% in neon) [6-9]. As a consequence, $[^{18}F]F_2$ cannot be used for the synthesis of radiopharmaceuticals with high specific activity.

Nucleophilic Radiofluorination

Nucleophilic substitution reactions with $[^{18}F]$fluoride have been largely developed both for aromatic and aliphatic systems [10]. Usually, they do not require a carrier and thus enable the synthesis of products with high specific activities. The nucleophilic substitution can be performed either directly on a suitable precursor of the target molecule or indirectly via a small labeled precursor [11].

$[^{18}F]$Fluoride anion in its highly solvated form is a poor nucleophile, but a strong base. The need for a reactive naked fluoride requires its combination to large cations, such as tetrabutylammonium, cesium, rubidium, or the presence of the crown ester or aminopolyether with potassium [12-16].

In nucleophilic aliphatic substitution, a leaving group is substitute with ^{18}F in a S_N2-type reaction [17]. Commonly used leaving groups are mesylate, tosylate, nosylate, triflate, iodide or bromide. The choice of a leaving group is strongly dependent on the substrate which is labeled and the optimization of radiochemical yield (RCY) requires testing of several different leaving groups.

1.2 Thymidine Kinase (TK)

1.2.1 Human Thymidine Kinase (hTK)

Thymidine kinase (EC 2.7.1.75) can be found in most living cells. In mammalian cells, it is present in two forms, hTK1 and hTK2. They are coded by different genes, have different substrate specificity and different substrate kinetics, differ in phosphate donor specificity and are located in different cellular compartments. TKs have a key function in the synthesis of DNA and thereby in the cell proliferation, thus making it a excellent potential target for measuring the cell proliferation.
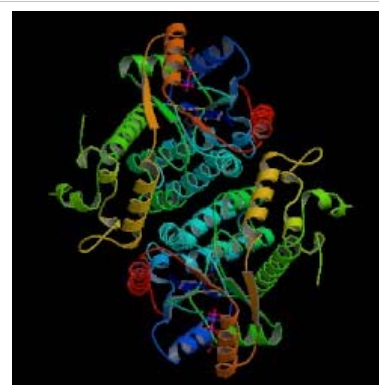
Figure 1.4. X-ray structure of hTK (PDB ID: 1W4R)

Thymidine kinase 1 (hTK1), also know as "soluble" or human cytosolic thymidine kinase is the most studied among the salvage pathway enzymes. hTKl, is widely distributed in human tissues, but being S-phase correlated, it is only detected in proliferating cells, either normally growing or malignant. It is characterized by a high substrate specificity, accepting only close analogues of thymidine. Especially important thymidine analogue is PET tracer [^{18}F]FLT, which is used to image cell proliferation [18].
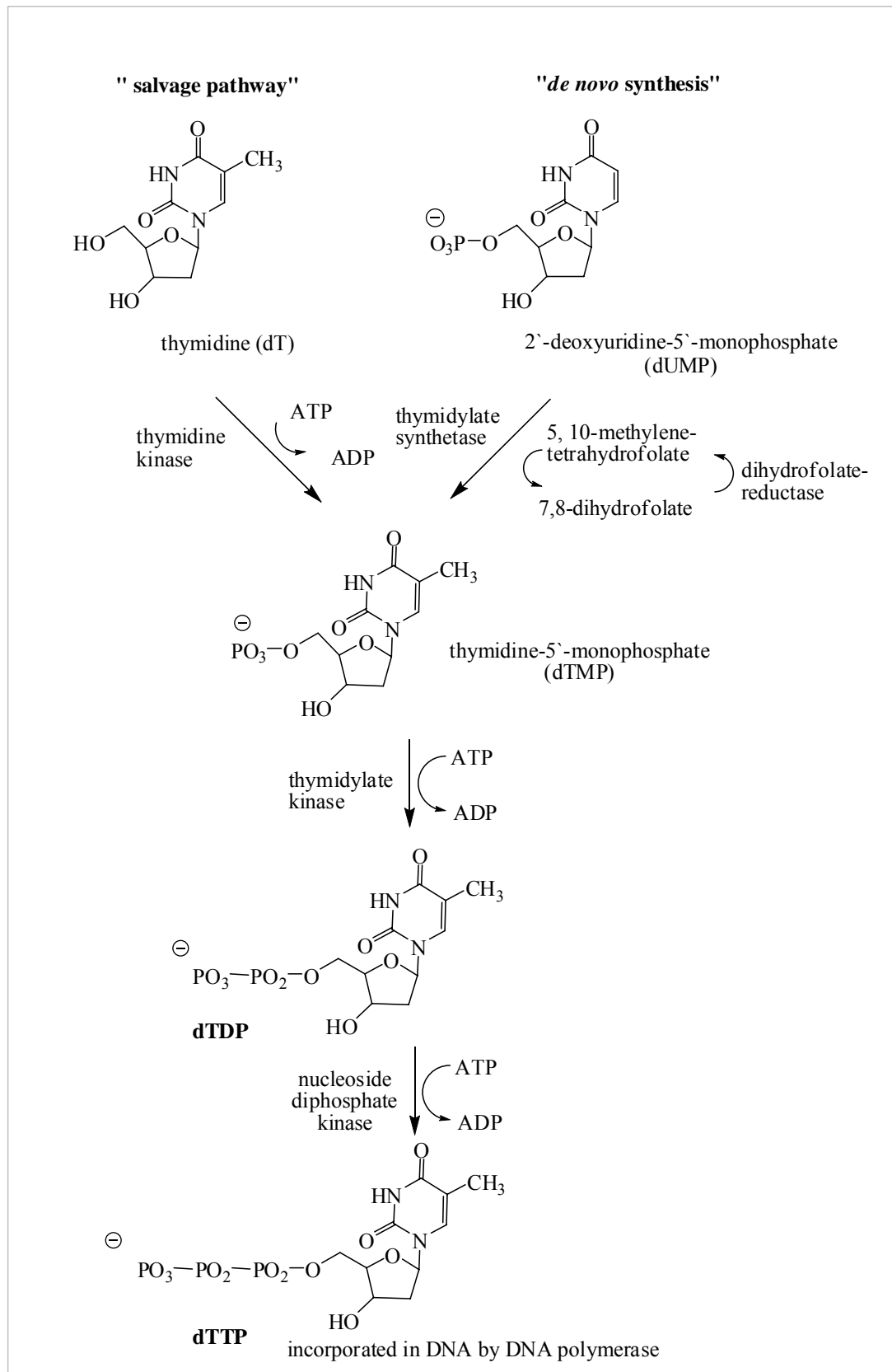
After the crystallization of hTK in 2005 [19], structure and binding mode have been revealed (Figure1.4). Unexpectedly, thymidine as a natural substrate is tied by a hydrogen bond network to a protein backbone. Amino acids which form interactions with thymidine are: Met28, Phe101, Leu124, Phe128, Phe133, Thr163, Val172, Val174, Tyr181. This binding mode of thymidine is in contrast with most of the other nucleoside/nucleotide kinases, which bind it via side chains. The adaptation of the active site to substrate is clearly not possible since substrate is bound via backbone. However, X-ray structure revealed that N-3 position of thymidine points out of the active site, making it the most promising site for analogue preparation.

Thymidine kinase 2 (hTK2), or mitochondrial thymidine kinase is present in most tissues. The amount of enzyme is in the correlation to the number of mitochondria and is independent of the growth state of the cell [20]. When compared to the level of TK1 in proliferating cells, the level of TK2 is low, but TK2 becomes significant in resting and terminally differentiated cells, such as muscle or brain and unstimulated lymphocytes, where TK1 activity is barely detectable [21, 22]. In tissues, where de novo synthesis of DNA precursors is undetectable, TK 2 is likely to be responsible for the supply of deoxynucleotides required for the mitochondrial DNA synthesis due to the low penetration of thymidine monophosphate (dTMP) through the mitochondrial membrane [23]. Unlike hTK1, hTK2 phosphorilates wider range of pyrimidine analogues as well as deoxycitidine (dC), deoxyuridine (dU), azidothymidine (AZT) and fluroarabino-furalosyl-iodouracil (FIAU) [24].

1.2.2 Salvage Pathway

Salvage pathways are used to recover bases and nucleosides that are formed during degradation of RNA and DNA. Thymidine kinase is one of the salvage pathway enzymes. In the presence of adenosine triphosphate (ATP) and Mg^{2+}, it catalyzes the phosphorylation of the thymidine (dT) into thymidine monophosphate (dTMP). The γ-phosphate group of the ATP is transferred to the 5`-OH group of thymidine thus producing dTMP. Thymidine monophosphate is subsequently further phosphorylated to the corresponding diphosphate (dTDP) and finally to triphosphate (dTTP) which is used as a DNA building block (Scheme 1.1). In addition to the salvage pathway, cells can synthesize phosphorylated nucleotides via *de novo* synthetic pathway. In the *de novo* pathway, thymidine monophosphate is produced by the methylation of deoxyuridine monophosphate (dUMP) in the reaction catalyzed by thymidylate synthetase in the presence of methylene tetrahydrofolate (Scheme 1.1).

" salvage pathway"

thymidine (dT)

"*de novo* synthesis"

2`-deoxyuridine-5`-monophosphate
(dUMP)

ATP

ADP

thymidine
kinase

thymidylate
synthetase

5, 10-methylene-
tetrahydrofolate

7,8-dihydrofolate

dihydrofolate-
reductase

thymidine-5`-monophosphate
(dTMP)

ATP

ADP

thymidylate
kinase

dTDP

ATP

ADP

nucleoside
diphosphate
kinase

dTTP incorporated in DNA by DNA polymerase

Scheme 1.1. Graphical representation of "salvage pathway" and "de novo synthesis"

1.2.3 Herpes Simplex Virus Type 1 Thymidine Kinase (HSV1 TK)

HSV1 TK (EC 2.7.1.21) is a multifunctional cellular enzyme characterized by the wide substrate acceptance (Figure 1.5). The size and the shape of its active site make it possible to accommodate and phosphorylate large number of pyrimidine as well as purine analogues. Based on the X-ray analysis of the compounds co-crystallized with HSV1 TK , single-point mutations and molecular modeling studies, it is known that following amino acids influence the binding properties and the catalytic activity of viral

Figure 1.5. X-ray structure of HSV1 TK (PDB ID: 2VTK)

TK: His58, Glu83*, Trp88, Ile100*, Tyr101*, Met121, Gln125*, Met128, Tyr132, Arg163*, Tyr172, Arg220, Arg222, Glu225*. While amino acids marked with (*) form H-bond interactions with the natural substrate thymidine, the remaining amino acids form H-bond interactions with other known substrates, such as penciclovir (PCV), ganciclovir (GCV) and DHBT. Differences in binding modes between thymidine and GCV are shown in Figure 1.6 [25, 26].
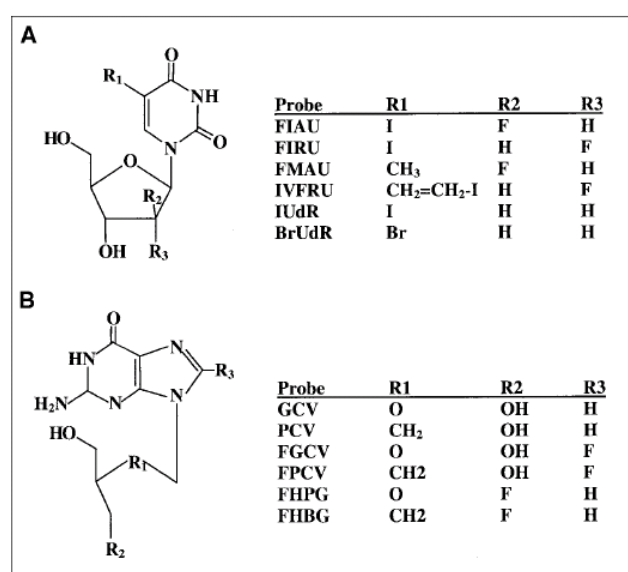
A
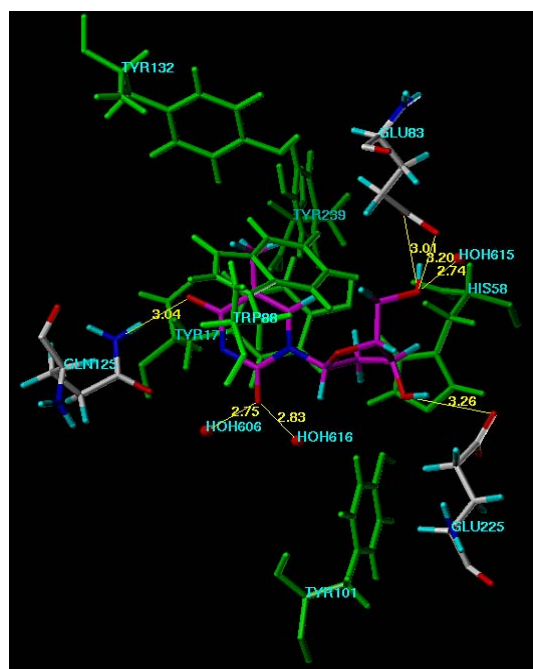
B
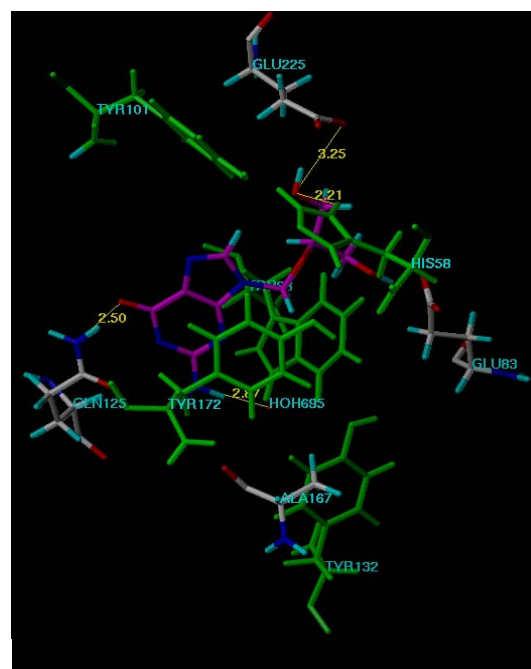
Figure 1.6. Different binding modes of the natural substrate thymidine (A) and the most widely used anti-viral drug ganciclovir (B)

Additionally, careful analysis of the X-ray crystal structures of HSV1 TK with different ligands reveal that HSV1 TK active site is very flexible and adopts its conformation to maximize protein-ligand interactions (Figure 1.7).

A　　　　　　　　**B**　　　　　　　　**C**
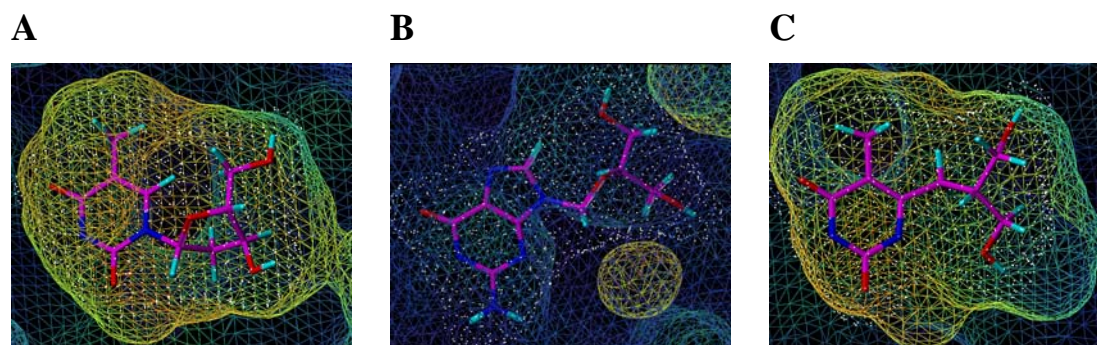
Figure 1.7. Different conformations of the HSV1 TK active site with thymidine (A), ganciclovir (B) and DHBT (C).

These differences in substrate diversity between hTK and HSV1 TK are the crucial molecular basis for a wide field of possible applications [27]. Since HSV1 TK phosphorylates wider range of compounds than hTK it can be used for selective phosphorylation of the investigated compound *in vivo*. However, almost all of the developed HSV1 TK substrates (several shown in Figure 1.8) have several disadvantages such as cytotoxicity, unfavorable pharmacokinetics, and by-stander effect.

A

Probe	R1	R2	R3
FIAU	I	F	H
FIRU	I	H	F
FMAU	CH3	F	H
IVFRU	CH2=CH2-I	H	F
IUdR	I	H	H
BrUdR	Br	H	H

B

Probe	R1	R2	R3
GCV	O	OH	H
PCV	CH2	OH	H
FGCV	O	OH	F
FPCV	CH2	OH	F
FHPG	O	F	H
FHBG	CH2	F	H

Figure 1.8. Developed HSV1 TK substrates for gene therapy monitoring [28]

1.2.4 Anti-Herpes Viral Therapy

In order to be effective, antiviral agents must be capable of reaching the infected organ(s) and preventing viral replication without affecting the function of the host cell. As previously stated, HSV1 TK has broader substrate acceptance than hTK. Compounds like aciclovir (ACV), penciclovir (PCV) and ganciclovir (GCV) are exclusively phosphorylated only by HSV1 TK (Figure 1.9). Subsequently, di- and triphosphorylated analogues are formed by cellular enzymes which, in turn, block the viral replication process by terminating DNA elongation at the viral DNA polymerase [29].

aciclovir   **penciclovir**   **ganciclovir**
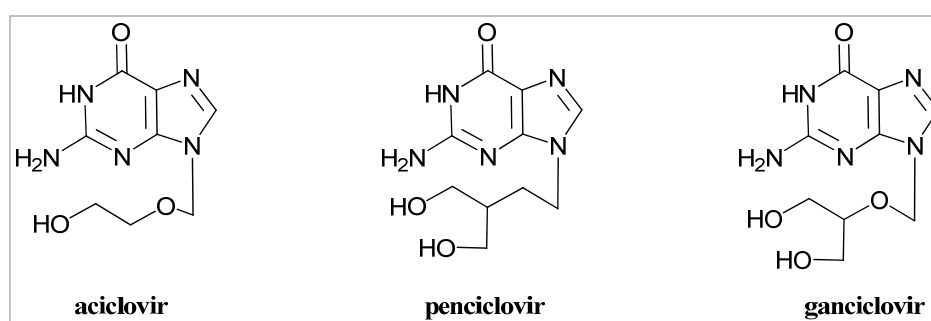
Figure 1.9 Most widely used anti-herpes viral agents.

1.2.5 Gene Therapy

Gene therapy is a technique for correcting defective genes responsible for the disease development. In other words, it is the insertion of genes into an individual's cells and tissues to treat a disease and hereditary diseases by complementing a defective mutant allele with a functional one. There are several approaches for correcting faulty genes:

- A normal gene may be inserted into a non-specific location within the genome to replace a non-functional gene (the most common approach).
- An abnormal gene could be swapped for a normal gene through homologous recombination.
- The abnormal gene could be repaired through selective reverse mutation, which returns the gene to its normal function.
- To alter the regulation (the degree to which a gene is turned on or off) of a particular gene.

A carrier molecule, vector, must be used to deliver the therapeutic gene to the patient's target cells or tissue. The most common vector is a genetically modified virus to carry normal human DNA. Viruses are preferred mean of carrier due to their ability to encapsulate and deliver their genes to human cells. Some of the different types of viruses used as gene therapy vectors are modified retroviruses, adenoviruses, adenoassociated viruses and herpes simplex viruses. In addition to virus-mediated gene-delivery systems, there are several non-viral options for gene delivery. They include delivery of naked DNA via plasmid, oligonucleotides, lipoplexes and polyplexes.

1.3 *In vivo* Imaging of Gene Expression

1.3.1 Reporter Gene Constructs

Reporter gene is a gene that is attached to a gene of interest (usually therapeutic gene) to monitor its activity. Several genes are chosen as reporter genes since they could easily be identified and measured, or because they are selectable markers.

Reporter genes are used to indirectly provide the information whether a gene of interest is being expressed, as well as, the duration and the position of the expression. It is crucially important that a gene of interest and a reporter gene are simultaneously expressed, since only simultaneous expression of both genes can provide an accurate information on expression of gene of interest. In our case, HSV1 tk serves both as a gene of interest and as a reporter gene.

1.3.2 Available Technologies

There are several technologies which could be used to monitor gene expression in vivo: fluorescent imaging (FLI), bioluminescence imaging (BLI), single photon emission computed tomography (SPECT) and positron emission tomography (PET). Some of the characteristics of these imaging technologies are summarized in Table 1.2.

Table 1.2. Properties of several non-invasive in vivo imaging modalities of gene expression [30]

Imaging modality	Form of energy used	Spatial resolution (mm)	Acquisition time per frame (s)	Molecular probe mass required (ng)	Molecular sensitivity (mol/l)	Tissue penetration depth (mm)	Mainly small animal or clinical?	Signal quantification capabilities	Cost (equipment and usage)
FLI	Visible to infrared light	2–10	10–2,000	10^3–10^6	10^{-9}–$10^{-11}*$	1–20	Small animal	Low–medium	Low
BLI	Visible to infrared light	3–10	10–300	10^3–10^6	10^{-13}–$10^{-16}*$	1–10	Small animal	Low–medium	Low
SPECT	Gamma rays	0.5–5 (animal), 7–15 (clinical)	60–2,000	1–100	10^{-10}–10^{-11}	>300	Both	Medium–high	Medium–high
PET	Annihilation photons	1–4 (animal), 6–10 (clinical)	1–300	1–100	10^{-11}–10^{-12}	>300	Both	High	High

Fluorescence Imaging (FLI)

Green fluorescent protein (GFP) is a perfect example of the "fluorescence imaging target" which was first isolated from the jellyfish *Aequorea Victoria*. GFP comprises of 11 β-sheets and a single α-helix containing the chromophore [31, 32] (Figure 1.10). It possesses unique property to fluorescent green when exposed to blue light which enables to monitor cellular processes in animals transparent to light [33, 34]. In other subjects, green fluorescence is efficiently absorbed by tissues limiting the usage

Figure 1.10. X-ray structure of GFP (PDB ID: 1F0B)

of GFP only to qualitative observations for subcutaneous tissues up to depth of 3-4 mm.

Bioluminescence Imaging (BLI)

Bioluminescence imaging exploits the emission of visible photons at specific wavelengths on the basis of energy-dependent reactions catalyzed by luciferases. Luciferase genes have been cloned from several organisms, including bacteria, firefly (fluc, from Photinus pyralis) and a coral (rluc, from Renilla) [35] (Figure 1.11). A photon is produced by the oxydation of luciferin in the presence of ATP.
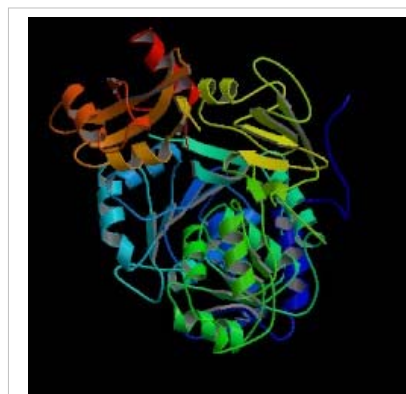
Figure 1.11 X-ray structure of luciferase (PDB ID: 1LCI)

Spontaneous rate of the this reaction is extremely slow. However, if the reaction is catalyzed by the luciferase, the rate of the reaction increases several folds. The reaction takes place in two steps:

Luciferin+ATP → luciferyl adenylate + PP$_i$

Luciferyl adenylate + O$_2$ → oxyluciferin + AMP + photon
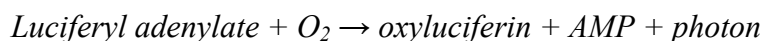
Luciferin and luciferase are not specific molecules, but are generic terms used to describe a substrate and its associated enzyme (or protein) that catalyzes a photon-producing reaction. The gene for luciferase is incorporated into DNA of cells or animal model of disease. In case ATP is available for the enzyme, the result is emission of photons that can be used to monitor cellular and genetic activity of every cell that expresses luciferase enzyme [35, 36]. Emitted photons can be detected and counted using low-light charge-coupled device (CCD) or photon-counting cameras.

Single-Photon Emission Computed Tomography (SPECT)

Molecular imaging using SPECT requires a molecular probe that is labeled with a radionuclide that results in the emission of gamma-ray or high-energy X-ray photons. In contrast to PET, only one photon is emitted making the determination of LORs and photon quantification in SPECT more difficult than in PET (Figure 1.12). Most common radionuclides used in SPECT are ^{123}I, ^{111}In and ^{99m}Tc.

Figure 1.12. SPECT used in our laboratories

Positron Emission Tomography (PET)

As mentioned in Chapter 1.1, PET is based on the simultaneous detection of two gamma rays emitted during the annihilation process. Possibility of quantification of the radioisotope in the ROI makes PET an excellent modality for monitoring biological processes *in vivo*. Example of PET instrument is shown on Figure 1.13.


Figure 1.13. PET used in our laboratories

1.3.3 HSV1 TK PET Reporter Probes

PET reporter genes encode proteins that are either receptors that bind and sequester "positron-emitting PET reporter ligand probes" or enzymes that metabolize "PET reporter substrate probes" to sequestered products [37, 38].

The HSV1 tk gene has its roots in a therapeutic approach as a suicide gene, since it is less substrate specific than hTK and phosphorylates not only thymidine, but also a wide range of nucleoside analogues by activating them *in situ* to drugs. After the phosphorylation of a substrate, negatively charged formed metabolite remains trapped inside the transduced cells. Thus a specific signal, derived from the trapped radiolabeled reporter probe, provides an indirect measurement of transgene expression (Figure 1.14).
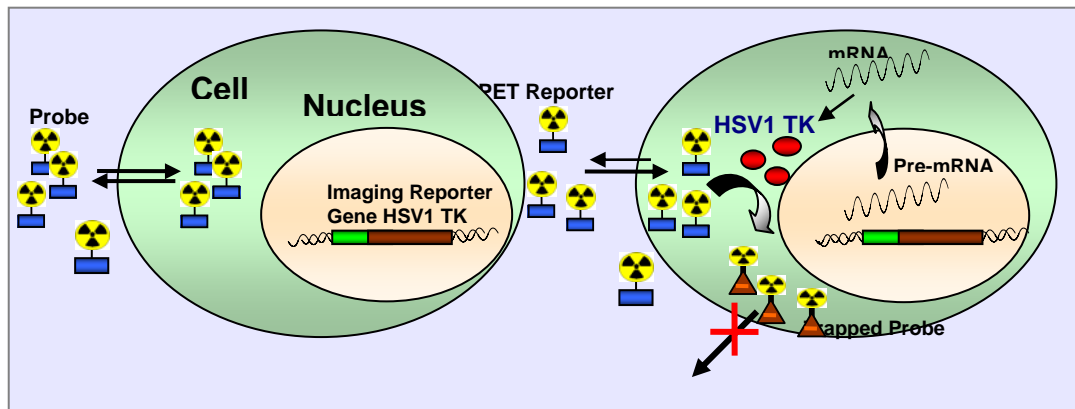
Figure 1.14: Schematic illustration of a reporter gene approach. Initially, an imaging reporter gene has to be introduced into the cell. Transcription of the imaging reporter gene (HSV1 *tk*) with subsequent translation of the mRNA leads to the expression of an enzyme HSV1 TK. HSV1 TK can selectively phosphorylate reporter probe, which due to the negative charge stays trapped inside the cell. The imaging reporter probe will be phosphorylated in tk transfected cells only, while in non-transfected cells, the probe should freely move in and out of the cell. Thus the signal obtained from the reporter probe should be cell type specific, providing an indirect measurement of transgene expression.

1.4 Molecular Modeling

1.4.1 Introduction

Molecules, like all other objects that surround us have three dimensions (3D). Properties of the molecule are set by the position of its atoms in the space. Good examples are biological systems where the activity of an enzyme depends on its conformation. Since, the structure of the active site is well defined, the main condition any molecule must possess to be a substrate of certain enzyme is the ability to fully or partially enter the enzyme's active site. Development of computers and computational methods gave us the opportunity to simulate a part of the biological system on computer. When enzyme structure and the position of its active site are known, we can estimate the complementarity between the ligand and the macromolecule. The first step is the determination of the geometric structure of the selected molecule, followed by the simulation and calculation to determine whether the selected molecule will be a good substrate or not.

Determination of the geometric structure can be made most precisely with X-Ray structural analysis of a crystal, while 3D structure of a molecule can be determined using theoretical approaches such as quantum-chemical *ab initio*, semi-empirical methods and molecular mechanics.

1.4.2 Molecular Mechanics

Molecular mechanics treats molecules applying laws of classical physics on atomic nuclei, while electrons are neglected. This approach can be even more simplified in the explanation that molecular mechanic treats atoms as solid balls, bonds as harmonic oscillators, while non-bonding interactions are described by potential functions derived from classical mechanics. Molecular mechanics describes the energy of a system by a set of functions of potential energy applied from classical mechanics, which together with parameters used for their scoring are called "force fields". Many force fields have been developed during the years which in general term for energy of the molecule

Esum=Estretch+Ebend+Etorsion+Enon-bonding interactions

add certain values for specific types of molecules, increasing the accuracy of the model. Especially interesting force field is MMFF94, developed as combined field for organic molecules and proteins, and parameterized on large number of different chemical systems. These characteristics make application of MMFF94 suitable to different types of molecules [39]. Beside previously mentioned energy terms, which are used in all force fields, MMFF94 uses extra interaction energy between bond stretching and bending, energy outside the plane, van der Walls interaction energy and electrostatic interactions for better accuracy [40].

Conformational space of the molecules can be explored by random search (RS) method which is used for finding molecule's global energy minimums [41-43]. Exploration of the conformational space is done by random changes of torsion angles inside the molecule, after which energy minimization follows. This cycle is repeated certain number of times. After each cycle, the obtained conformation is compared with those previously calculated: the new conformation is saved, while previously encountered ones are counted how many times they appeared [44]. It is important to emphasize that high energy conformations are discarded. Random search method is a very powerful tool for finding the minimum energy conformations because it is about an order of the magnitude more efficient than using dynamics for that purpose [45].

1.4.3 Docking

The docking process involves the prediction of ligand conformation and orientation (or posing) within a targeted binding site [46]. It is generally devised as a multi-step process in which each step introduces one or more additional degrees of complexity [47]. The process begins with the application of docking algorithms that pose small molecules into active site. Posing is the process of determining whether a given conformation and orientation of a ligand fits the active site [46]. The process itself is challenging since even relatively simple organic molecules can contain many conformational degrees of freedom. Algorithms are complemented by scoring functions that are designed to predict the biological activity through the evaluation of interactions between compounds and potential targets. Pre-selected conformers are usually additionally evaluated using more complex scoring schemes with more detailed treatment of electrostatic and van der Waals interactions, as well as inclusion of salvation or entropic effects [48].

Challenges to accurately predict binding conformations and compound activity include limited resolution of crystallographic targets, inherent flexibility, induced fit or other conformational changes that occur on binding and the participation of water molecules in protein-ligand interactions. Many docking programs have been developed in recent years. The most commonly used ones are DOCK, FlexX, AutoDock, GOLD which differ in used algorithms and scoring functions.

The choice of the docking program was made based on a study of Kellenberger et al. (2004) [49] stating that both the capacity of reproducing the X-ray pose (accuracy) as well as the discrimination of known thymidine kinase ligands was best with GOLD.

GOLD (Genetic Optimisation for Ligand Docking) is an automated ligand docking program that uses a genetic algorithm to explore the full range of ligand conformational flexibility with partial flexibility of the protein. Additionally, it satisfies the fundamental requirement that the ligand must displace loosely bound water on binding [50]. GOLD performs automated docking with full acyclic ligand flexibility, partial cyclic ligand flexibility and partial protein flexibility in the neighborhood of the protein active site. In order to search the space of available binding modes efficiently, hydrogen bond motifs have been directly encoded into the genetic algorithm. A scoring function was used to rank generated binding modes. This comprised a term for hydrogen bonding (which took account of the fundamental requirement that water must be displaced from both donor and acceptor before a bond is formed); a pair wise dispersion potential that was able to describe a significant contribution to the hydrophobic energy of binding; and a molecular mechanics term for the internal energy of the ligand.

1.5 References

[1] Image taken from the web site of the Forschungszentrum Jülich in der Helmholtz Gemeinschaft http://www.fz-juelich.de/zel/index.php?index=136

[2] European Nuclear Agency http://www.nea.fr/

[3] Image taken from web site of the European Nuclear Society, http://www.euronuclear.org/info/encyclopedia/betaplusdecay.htm

[4] PA Schubiger, L Lehmann, M Friebe. Fluorine-18 Labeling Methods: Features and Possibilities of Basic reactions In: PET Chemistry – The Driving Force in Molecular Imaging

[5] Lasne M-C, Perrio C, Rouden J, Barré L, Roeda D, Dolle F, Crouzel C. Chemistry of ß$^+$-Emitting Compounds Based on Fluorine-18. In: Topics in Current Chemistry: Contrast Agents II -/- Optical, Ultrasound, X-Ray and Radiopharmaceutical Imaging. Springer Berlin / Heidelberg 2002;222: 203-58

[6] Crouzel C, Comar D. Production of carrier-free ^{18}F-hydrofluoric acid. Int J Appl Radiat Isot 1978;29:407-8

[7] Fowler JS, Wolf AP (1986) Positron emitter-labelled compounds: priorities and problems. In: Phelps M, Mazziotta J, Schelbert H (eds) Positron emission tomography and autoradiography: principles and applications for the brain and heart. Raven Press.New York, chap 9, p 341

[8] Kilbourn MR (1990) Fluorine-18 labelling of radiopharmaceuticals. Nuclear Science Series,NAS-NS-3203 National Academy Press,Washington DC

[9] Halpern DF (1995) 18F-Labelled radiopharmaceuticals. In: Hudlicky M, Pavlath AE (eds) Chemistry of organic fluorine compounds. II.ACS Monogr 187. The American Chemical Society,Washington DC, p 1126

[10] Clark JH, Miller JM. Hydrogen bonding in organic synthesis. 3. Hydrogen bond assisted reactions of cyclic organic hydrogen bond electron acceptors with halogenoalkanes in the presence of potassium fluoride. J Am Chem Soc 1977;99:498-504

[11] Clark JH. Fluoride ion as a base in organic synthesis. Chem Rev 1980; 80:429-452

[12] Brodack JW,Dence CS, Kilbourn MR,Welch MJ (1988) Appl Radiat Isot 39:699

[13] Attina M, Cacace F, Wolf A. Labeled aryl fluorides from the nucleophilic displacement of activated nitro groups by 18F-F⁻. J Labelled Compd Radiopharm 1983;20:501-14

[14] Irie T, Fukushi K, Ido T,Nozaki T,Kasida Y. 18F-Fluorination by crown ether—metal fluoride: (I) On labeling ^{18}F-21-fluoroprogesterone. Int J Appl Radiat Isot 1982;33:1449-52

[15] Brodack JW,Dence CS, Kilbourn MR,Welch MJ (1988) Appl Radiat Isot 39:699

[16] Hamacher K, Coenen HH, Stöcklin G (1986) J Nucl Med 27:2351

[17] Lasne M-C, Perrio C, Rouden J, Barré L, Roeda D, Dolle F, Crouzel C. Chemistry of ß⁺-Emitting Compounds Based on Fluorine-18. In: Topics in Current Chemistry: Contrast Agents II -/- Optical, Ultrasound, X-Ray and Radiopharmaceutical Imaging. Springer Berlin / Heidelberg 2002;222: 203-58

[18] Cobben DC, Jager PL, Elsinga PH, Maas B, Suurmeijer AJ, Hoekstra HJ. 3'-18F-fluoro-3'-deoxy-L-thymidine: a new tracer for staging metastatic melanoma? J Nucl Med 2003;44:1927-32

[19] Birringer MS, Claus MT, Folkers G, Kloer DP, Schulz GE, Scapozza L. Structure of a type II thymidine kinase with bound dTTP. FEBS Lett. 2005;579:1376-82

[20] Arner ES, Eriksson S. Mammalian deoxyribonucleoside kinases. Pharmacol Ther 1995;67:155-86

[21] Tyrsted G, Munch-Petersen B. Early effects of phytohemagglutinin on induction of DNA polymerase, thymidine kinase, deoxyribonucleoside triphosphate pools and DNA synthesis in human lymphocytes. Nucleic Acids Res 1977;4:2713-23

[22] Wang J, Eriksson S. Phosphorylation of the anti-hepatitis B nucleoside analog 1-(2'-deoxy-2'-fluoro-1-beta-D-arabinofuranosyl)-5-iodouracil (FIAU) by human cytosolic and mitochondrial thymidine kinase and implications for cytotoxicity. Antimicrob Agents Chemother 1996; 40: 1555-7

[23] Arner ES, Eriksson S, Mammalian deoxyribonucleoside kinases. Pharmacol Ther 1995;67:155-86

[24] Johansson M., Karlsson A. Cloning of the cDNA and chromosome localization of the gene for human thymidine kinase 2. J Biol Chem 1997; 272:8454-8.

[25] Sulpizi M, Schelling P, Folkers G, Carloni P, Scapozza L. The rational of catalytic activity of herpes simplex virus thymidine kinase. a combined biochemical and quantum chemical study. J Biol Chem 2001;276:21692-7.

[26] Protein Data Bank (PDB) ID: 2VTK

[27] Pilger BD, Perozzo R, Alber F, Wurth C, Folkers G, Scapozza L. Substrate diversity of herpes simplex virus thymidine kinase. Impact Of the kinematics of the enzyme. J Biol Chem 1999;274:31967-73.

[28] Tjuvajev JG, Doubrovin M, Akhurst T, Cai S, Balatoni J, Alauddin MM, et al. Comparison of radiolabeled nucleoside probes (FIAU, FHBG, and FHPG) for PET imaging of HSV1-tk gene expression. J Nucl Med 2002;43:1072-83.

[29] Hannigan BM, Barnett YA, Armstrong DB, McKelvey-Martin VJ, McKenna PG. Thymidine kinases: the enzymes and their clinical usefulness. Cancer Biother, 1993;8:189-97

[30] Levin CS. Primer on molecular imaging technology. Eur J Nucl Med Mol Imaging 2005;32:S325–45

[31] Phillips G. Green fluorescent protein--a bright idea for the study of bacterial protein localization. FEMS Microbiol Lett 2001;204:9-18

[32] Ormö M, Cubitt A, Kallio K, Gross L, Tsien R, Remington S. Crystal structure of the Aequorea victoria green fluorescent protein. Science 1996;273:1392-5

[33] Prendergast F, Mann K. Chemical and physical properties of aequorin and the green fluorescent protein isolated from Aequorea forskålea. Biochemistry 1978; 17:3448-53

[34] Tsien R. The green fluorescent protein. Annu Rev Biochem 1998;67: 509-44

[35] Contag CH, Jenkins D, Contag PR, Negrin RS. Use of reporter genes for optical measurements of neoplastic disease in vivo. Neoplasia 2000;2:41–52

[36] Contag CH, Contag PR, Mullins JI, et al. Photonic detection of bacterial pathogens in living hosts. Mol Microbiol 1995;8:593–603

[37] Herschman HR, MacLaren DC, Iyer M, Namavari M, Bobinski K, Green LA, et al. Seeing is believing: non-invasive, quantitative and repetitive imaging of reporter gene expression in living animals, using positron emission tomography. J Neurosci Res, 2000;59:699-705

[38] MacLaren, D.C., et al., PET imaging of transgene expression. Biol Psychiatry, 2000. 48(5): p. 337-48

[39] Halgren AT. MMFF VII. Characterization of MMFF94, MMFF94s, and other widely available force fields for conformational energies and for intermolecular-interaction energies and geometries. J Comput Chem 1999;20:730-43

[40] Halgren TA. Merck molecular force field .1. Basis, form, scope, parameterization, and performance of MMFF94. J Comp Chem 1996;17:490-519

[41] Saunders M., U.S. Patent 4,855,931

[42] Chang G, Guida WC, and Still WC, An internal-coordinate Monte Carlo method for searching conformational space. J Am Chem Soc; 1989;111:4379-86

[43] Li Z and Scheraga HA, Monte Carlo-minimization approach to the multiple-minima problem in protein folding. Proc Natl Acad Sci USA;1987;84:6611-6615

[44] Saunders M, Stochastic exploration of molecular mechanics energy surfaces. Hunting for the global minimum. J Am Chem Soc;1987;109:3150-2

[45] Saunders M, Houk KN, Wu YD, Still WC, Lipton M, Chang G, Guida WC, Conformations of cycloheptadecane. A comparison of methods for conformational searching. J Am Chem Soc;1990;112: 1419-27

[46] Kitchen DB, Decornez H, Furr JR, Bajorath J. Docking and scoring in virtual screening for drug discovery: methods and applications. Nat Rev Drug Discov 2004;3:935-49

[47] Brooijmans N, Kuntz ID. Molecular recognition and docking algorithms. Annu Rev Biophys Biolmol Struct 2003;32:335–73

[48] Gohlke H, Klebe G. Approaches to the description and prediction of the binding affinity of small-molecule ligands to macromolecular receptors. Angew Chem Int Ed 2002;41:2644–76

[49] Kellenberger E, Rodrigo J, Muller P, Rognan D. Comparative Evaluation of Eight Docking Tools for Docking and Virtual Screening Accuracy. Proteins 2004;57: 225-42.

[50] Jones G, Willett P, Glen RC, Leach AR, Taylor R. Development and validation of a genetic algorithm for flexible docking. J Mol Biol 1997; 267:727-48

Aim and Scope of This Study

Several imaging modalities, such as optical, magnetic resonance and radionuclide-based techniques are currently under investigation as tools for gene therapy monitoring in living subjects. Positron Emission Tomography (PET) is a radionuclide-based imaging modality which allows non invasive, repetitive and quantifiable imaging of biological processes with highest available sensitivity. The most studied system for the visualization of the gene expression in animals and humans is Herpes Simplex Virus type 1 Thymidine Kinase (HSV1 TK), the enzyme product of the reporter gene HSV1 tk. Several pyrimidine and purine analogues labeled with F-18 or I-124 have been synthesized and evaluated as potential imaging agents for HSV1 TK expression *in vivo*. However, almost all of the reporter probes, including the most commonly used ^{18}F-9-[4-fluoro-3-(hydroxymethyl)butyl]guanine ([^{18}F]FHBG), have several disadvantages such as cytotoxicity, unfavorable pharmacokinetics, and by-stander effect. Due to the broad substrate acceptance, HSV1 TK phosphorylates both purine and pyrimidine classes of compounds to their corresponding monophosphates which are metabolically trapped inside the transfected cells. The major advantage of pyrimidine derivatives over purine ones is that pyrimidine analogues do not show any or a very low by-stander effect.

An ideal reporter probe for monitoring the gene expression should have the following characteristics:

1. High V_{max}/Ki for HSV1 TK and good catalytic efficacy (K_{cat}>0.1 s-1).

3. The reporter probe should be stable *in vivo* and not be converted to peripheral metabolites that complicate the development of a quantitative assay.

4. The reporter probe should be cleared rapidly from the blood and non-specific sites. Additionally, it should preferably have an elimination route that does not interfere with the detection of a specific signal.

5. When the reporter gene is not expressed, there should be no significant accumulation of reporter probe in cells.

6. The reporter probe should be conveniently radiolabeled with an appropriate PET radioligand without significant changes in its properties, and should be labeled with an appropriate specific activity.

7. The reporter probe or its metabolites should not be cytotoxic at the concentrations used.

In a previous work a series of new C-6 substituted pyrimidine derivatives as HSV1 TK substrates was identified. Initial experiments suggested that these novel compounds do not exhibit cytotoxicity and show better *in vitro* binding affinities for HSV1 TK than already existing PET reporter probes. When labeled with appropriate PET radionuclide, such as ^{18}F, these new analogues could be useful as PET reporter probes for monitoring HSV1 tk gene expression *in vivo*.

One such C-6 substituted pyrimidine derivative which was identified through the random synthesis is DHBT. A close analogue of DHBT, 6-(2-hydroxy-hydroxypropyl)-5-^{18}F-fluoromethyl (1H,3H)-pyrimidine-2,4-dione ([^{18}F]Fluoromethyl HHT) was synthesized and evaluated for suitability as a PET reporter probe *in vivo*. Although [^{18}F]Fluoromethyl HHT was superior to [^{18}F]FHBG in terms of specificity of the accumulation in TK+ vs. TK- cells, [^{18}F]Fluoromethyl HHT lacked *in vivo* stability.

The aim of this study is to synthesize novel non-cytotoxic fluorinated DHBT analogues and their respective precursors for radiolabeling with F-18 for PET imaging. Specifically, two new compounds, FHBT and N-Methyl DHBT, were selected based on the results obtained from docking studies. The new compounds should be evaluated *in vitro* to estimate their suitability as PET imaging agents for monitoring HSV1 tk expression *in vivo*.

2 Synthetic Approaches Toward FHBT

2.1 Introduction

After the ground-breaking work by Tjuvajev et al. in 1995 [1] , numerous groups worldwide started the development of radiolabeled substrates for Herpes Simplex Virus 1 thymidine kinase (HSV1 TK), thus focusing research on non-invasive gene expression monitoring *in vivo* using positron emission tomography (PET). To be considered a suitable TK substrate for PET imaging a compound has to fulfill several requirements [2]:

- Good catalytic efficacy (K_{cat});
- High specificity towards the HSV1-TK enzyme;
- Low cytotoxicity in normal and TK-transfected cells;
- Suitable structure for radiolabeling, and
- Favorable pharmacokinetics.

A

Probe	R1	R2	R3
FIAU	I	F	H
FIRU	I	H	F
FMAU	CH_3	F	H
IVFRU	$CH_2=CH_2-I$	H	F
IUdR	I	H	H
BrUdR	Br	H	H

B

Probe	R1	R2	R3
GCV	O	OH	H
PCV	CH_2	OH	H
FGCV	O	OH	F
FPCV	CH2	OH	F
FHPG	O	F	H
FHBG	CH2	F	H
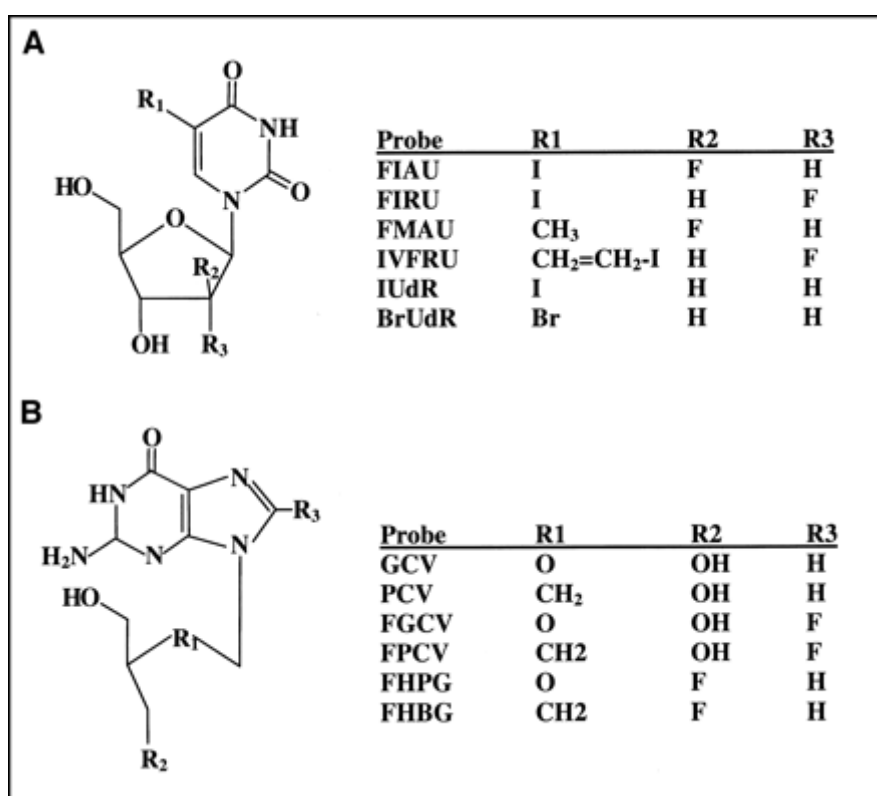
Figure 2.1: List of most successful HSV1 TK analogues developed for gene therapy monitoring by PET [1]

Target compounds developed since 1995 can be divided into two main groups: purine-type nucleoside analogues; and pyrimidine-type nucleoside analogues. Although several hundreds of TK substrates have been successfully synthesized, most of them failed *in vitro* or *in vivo* validation. Additionally, even the most successful ones (listed in Figure 2.1) have numerous disadvantages such as very slow pharmacokinetics, cytotoxicity and, the most common one, unspecific cell uptake [3].

We have decided to take an innovative approach to prepare a series of C-6 substituted pyrimidine derivatives (Figure 2.2) and to test their suitability as PET imaging agents for gene expression monitoring. The lead compound should preferably have two free hydroxyl groups; one to be replaced by a fluorine atom and the second for the phosphorylation by HSV1 TK.
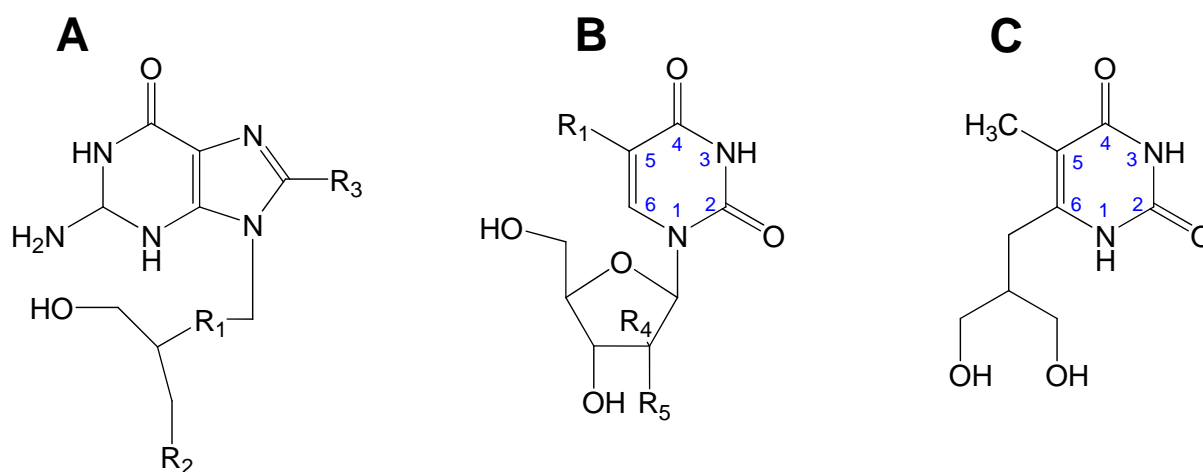
Figure 2.2: A: Purine derivatives; B: N-1 substituted pyrimidine derivatives, C: C-6 substituted pyrimidine derivative, DHBT

The lead structure, DHBT, was discovered in random reaction between thymine and several alcohols induced by gamma irradiation. Since it was proven by enzyme kinetics that DHBT is indeed a TK substrate, a lot of effort was made to develop a total synthesis of the compound whereby an overall yield of around 2.5% was obtained. To be useful as a PET tracer, DHBT has to be additionally modified in a way that one of its two hydroxyl groups is substituted by fluorine (Scheme 2.1).
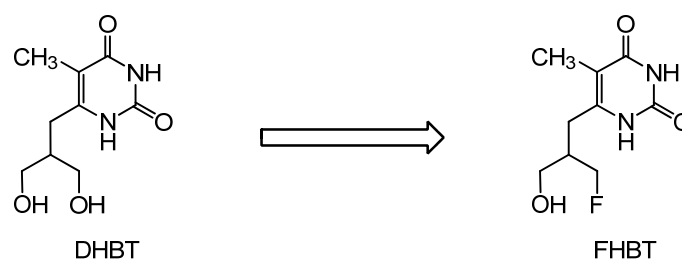
Scheme 2.1: Lead molecule DHBT and its fluoro derivative FHBT

Some attempts were made to obtain FHBT [4], and one such attempt is shown in Scheme 2.2.
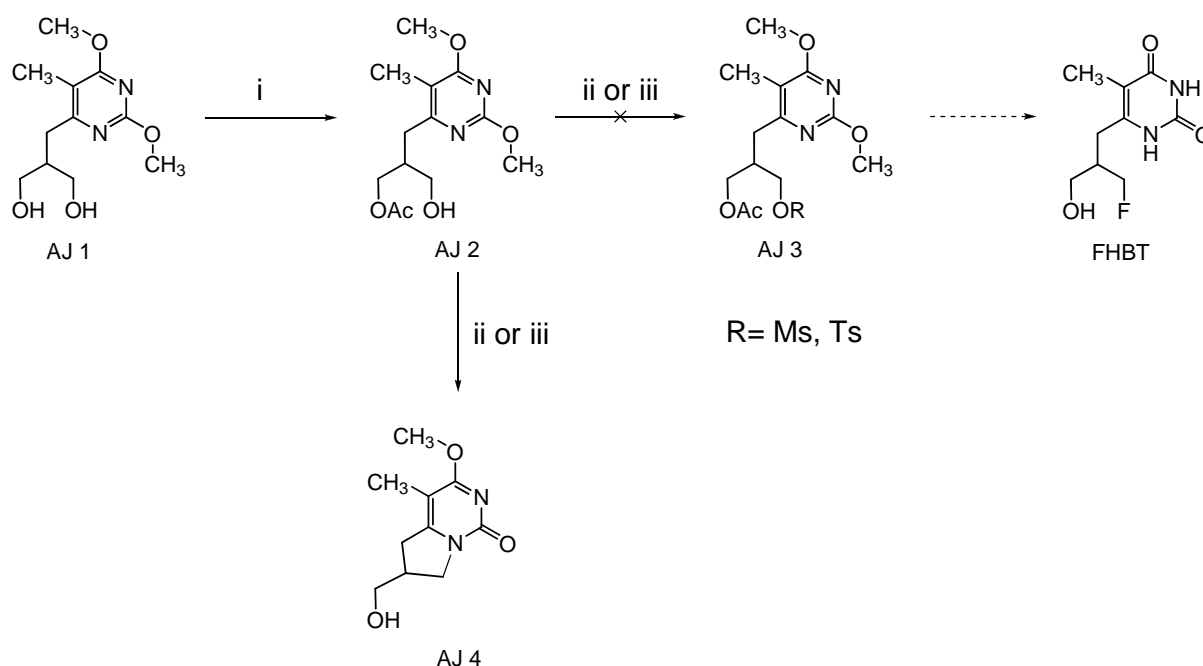
Scheme 2.2: Synthetic scheme of a previous attempt to prepare FHBT which was unsuccessful due to intramolecular cyclization; Reagents and conditions: (*i*) Bu$_2$SnO/toluene, AcCl/THF-CH$_2$Cl$_2$; (*ii*) TsCl, pyridine; (*iii*) MsCl, pyridine

AJ 1 was used as a starting point for the preparation of FHBT. It was treated with dibutyl tin oxide to give the cyclic cyclostannioacetate intermediate which in a subsequent reaction with acetyl chloride gave the mono-acetylated compound **AJ 2** in 49% yield. Reaction of **AJ 2** with either tosyl chloride or mesyl chloride did not lead to the expected sulfonate **AJ 3.** Instead of **AJ 3,** a bicyclic compound **AJ 4** was formed. Consequently, in this work new synthetic strategies were sought.

2.2 Novel Synthetic Strategies to FHBT

2.2.1 Optimization of DHBT Synthesis

As mentioned earlier, the overall yield of DHBT was 2.5%. Therefore, initially it was necessary to improve on the yield of DHBT prior to introducing novel synthetic strategies towards the synthesis of FHBT. Special focus was on increasing the yield of reaction steps *i*, *iv*, *vii* and *viii*, (Scheme 2.3) since these steps were critical for the overall reaction yield.

In step *i*, recrystallization was omitted and the crude product was used for the next reaction step in which dimethoxy compound **3** was prepared. As indicated in Scheme 2.3, the reaction yield for the first two steps increased from 56% to 95%.

Corey oxidation was used in step *iv* to convert secondary hydroxide **5** into ketone **6**. By simply using column chromatography instead of recrystallization, an increase of 10% in the yield of compound **6** was achieved.

For the radical deoxygenation in step *vii*, schlenk line was used, which allowed almost a 2-fold higher yield (from 25% to 45%).

The best condition for the deprotection of benzyl groups was found by extending reaction time from 2 to 3 hours after which the reaction went to completion. Compound **10** was obtained in 90% yield after column chromatography.

Other reactions used in the pathway remained the same, or were only slightly modified.

As a result of these optimized synthetic procedures, the overall reaction yield was increased 10-fold, from 2.5 to 25%.
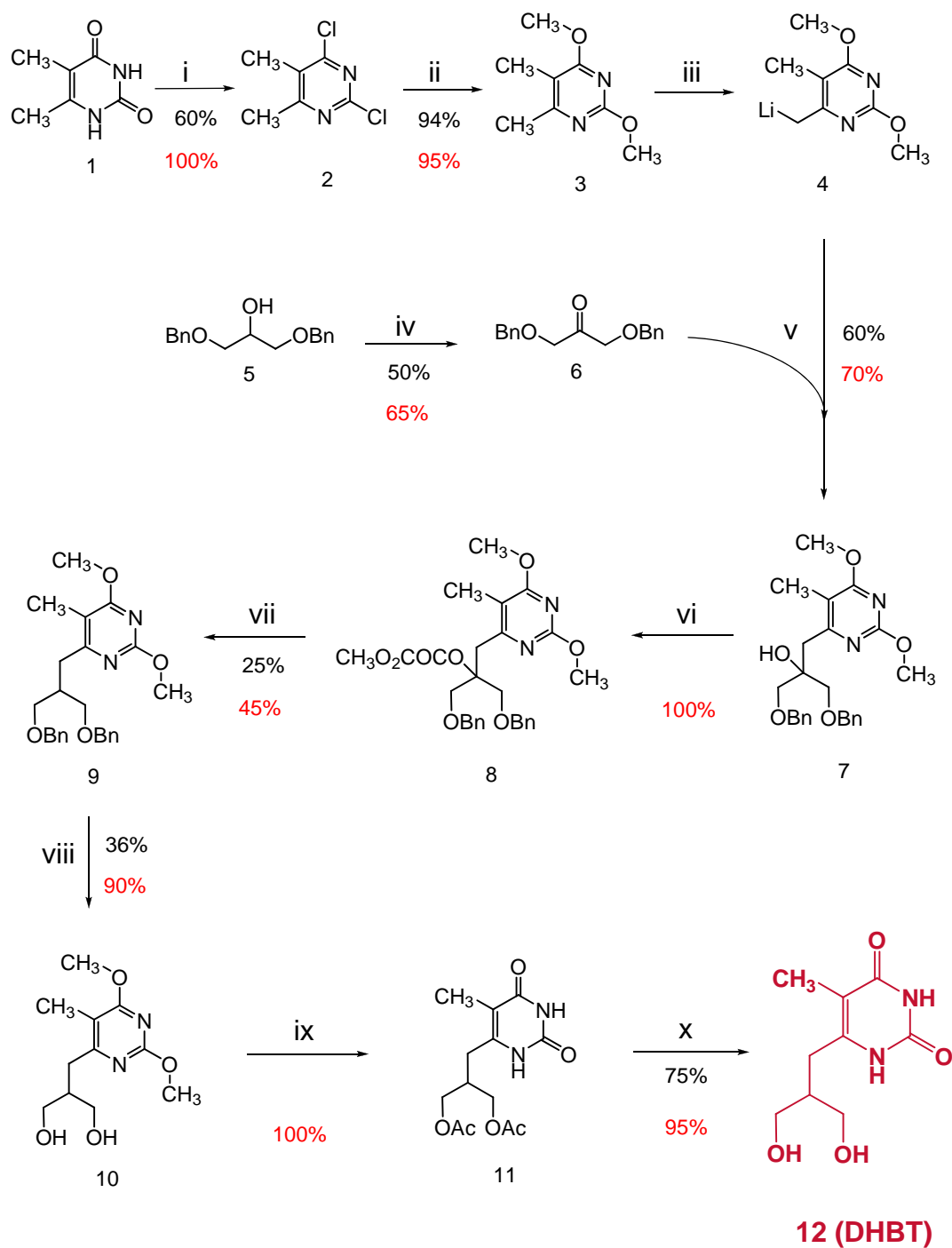
Scheme 2.3: Synthetic pathway toward lead molecule, DHBT with initial (black) and optimized (red) reaction yields; Reagents and conditions: (*i*) POCl$_3$, reflux; (*ii*) NaOCH$_3$, MeOH; (*iii*) LDA, THF; (*iv*) N-Chlorosuccinimide, Et$_3$N, Toluene ; (*v*) -55°C, THF; (*vi*) C$_3$H$_3$ClO$_3$, DMAP, CH$_3$CN; (*vii*) Bu$_3$SnH, AIBN, Toluene; (*viii*) -78°C, BCl$_3$, CH$_2$Cl$_2$; (*ix*) AcCl, H$_2$O; (*x*) NH$_3$, MeOH.

2.2.2 Synthetic Strategies Towards FHBT

For the design of the synthesis of FHBT, several key issues have to be taken into consideration:

1. *Solubility of the starting material*

   DHBT is highly soluble in water; partly in methanol, dioxane and DMSO. Therefore a limited choice of reaction solvents is available for the preparation of the intermediates of FHBT. As a consequence, acetylated compound **11** and dimethoxy compound **10** (Scheme 2.4) were additionally selected as starting compounds due to their sufficient solubility in organic solvents.

2. *Suitability of reagents*

   The choice of appropriate reagents was especially crucial when starting from compound **10** and **11** since both compounds contain protecting groups (two methoxy groups in compound **10** and two acetyl groups in compound **11**) and their stability is of great importance for subsequent reactions.
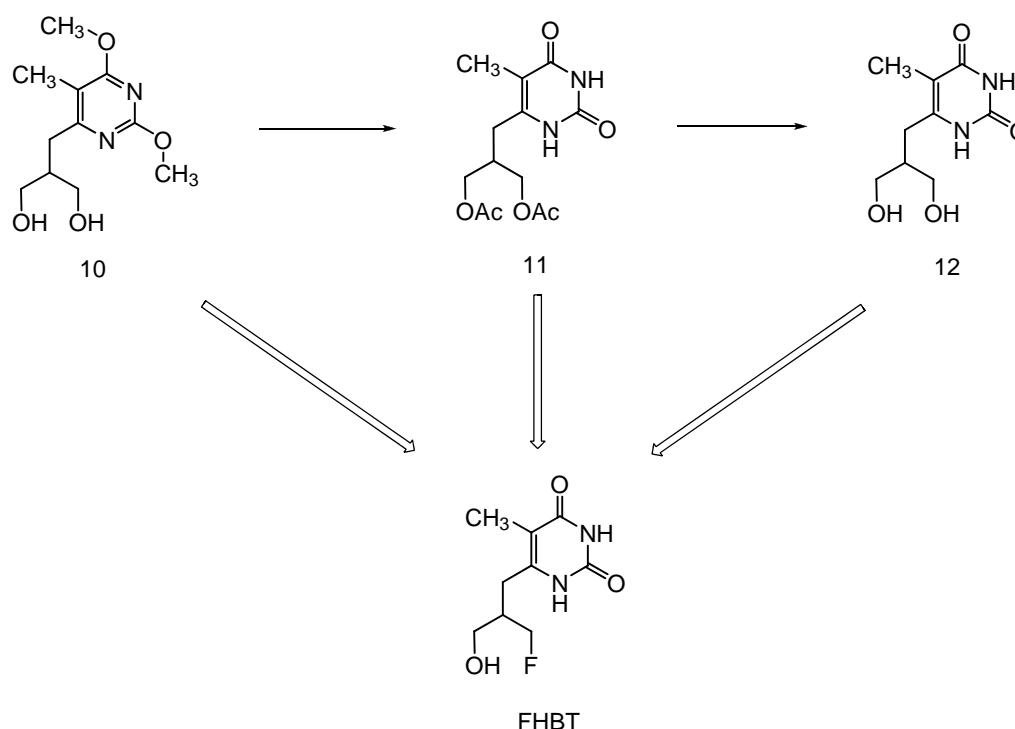
Scheme 2.4: Possible synthetic pathways toward FHBT

2.2.3 Synthetic Strategies via Cyclic Sulfate

Cyclic sulfates have been used as precursors for the synthesis of fluorinated compounds [5-8]. These sulfates could be obtained via the corresponding sulfite followed by the oxidation with potassium permanganate, or directly with sulfuryl chloride [9-14]. We adopted a similar strategy for the preparation of FHBT (Scheme 2.5).
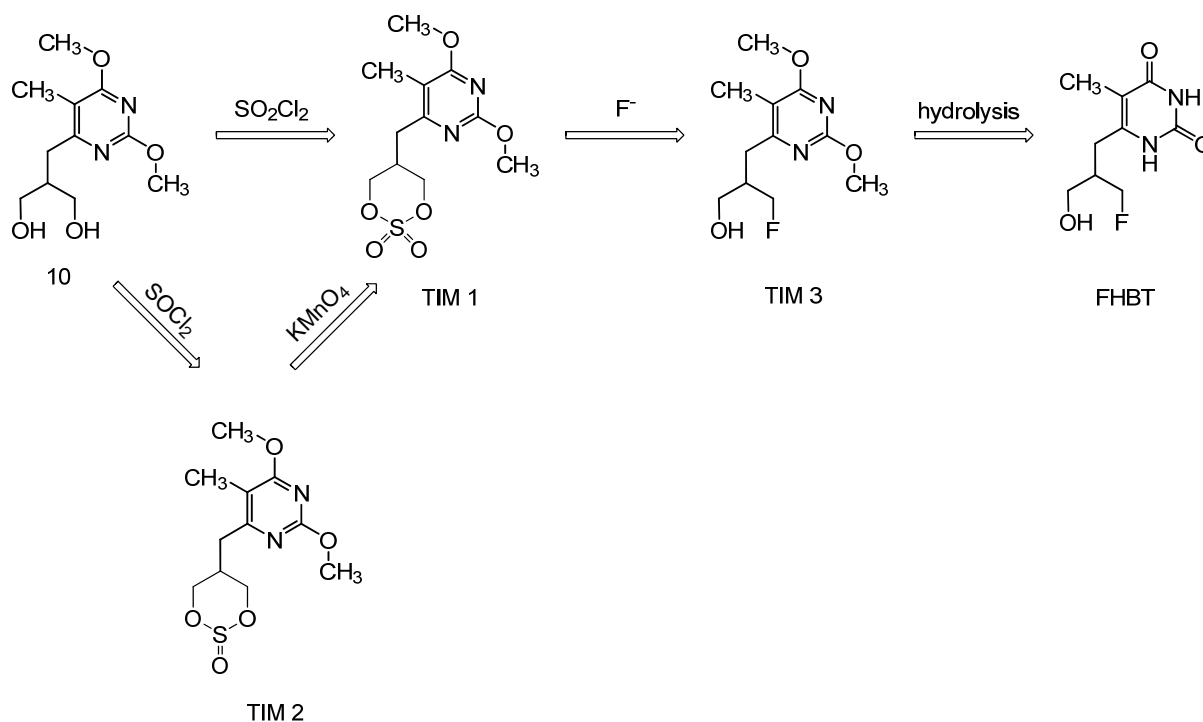
Scheme 2.5. Proposed synthetic approach via cyclic sulfate

Starting from compound **10**, several reaction conditions (Table 2.1) were tried, but unfortunately no traces of the sulfate **TIM 1** were found.

Table 2.1: List of reaction conditions used for the preparation of cyclic sulfate

Temperature	Reaction time
rt	0.5h, 2h, 24h, 48h
-78°C gradually to rt	15 min, 30 min, 60 min
-35°C gradually to 0°C	1h, 3h, 24h
0°C (constant)	0.5h, 1.5h, 2h, 3h

Additionally, we tried to prepare sulfite **TIM 2**, but when treated with thionyl chloride, compound **10** decomposed.

2.2.4 Synthetic Strategies using Direct Fluorination with DAST

Direct fluorination with DAST would provide another quick and convenient method for the preparation of FHBT (Scheme 2.6) [15-23]. The reaction of **10** with DAST was tried using different conditions (Table 2.2), however all attempts were futile since no fluoro intermediate **TIM 4** was formed.
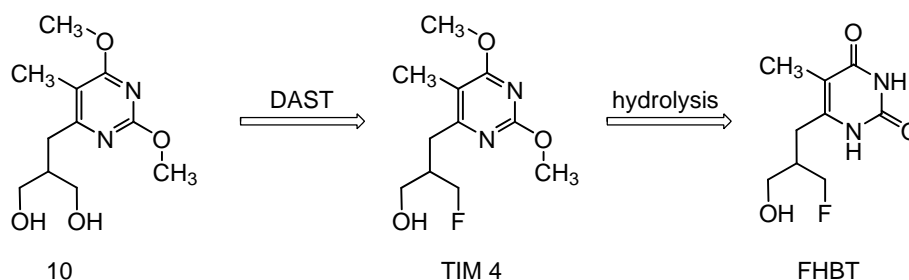
Scheme 2.6. Synthetic approach with DAST starting from compound **10**

Compound **10** either decomposed or the isolated products did not correspond to the target compound.

Table 2.2: Tested reaction condition for the reaction of **10** with DAST

Temperature	Reaction time (in min)
-78°C (constant)	25
-78°C and gradually warming to rt	15, 30, 60

2.2.5 Synthetic Strategies using Protecting Groups

After several unsuccessful attempts to prepare FHBT from compound **10**, new synthetic strategies were proposed starting from acetylated compound **11**. The synthetic pathway, as shown on Scheme 2.7 involves the following steps:

1. Protection of the –NH groups
2. Selective removal of the acetyl groups
3. Fluorination with DAST
4. Removal of the N-protecting groups
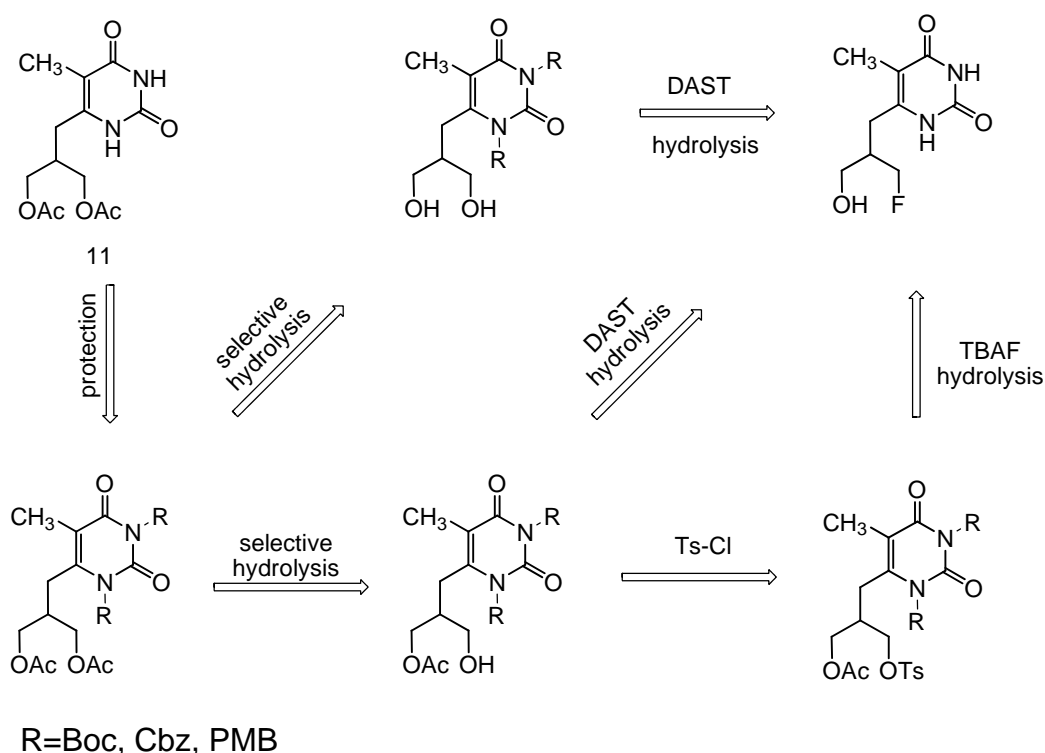
Scheme 2.7: Proposed synthetic route to FHBT starting from compound **11**

Protection of –NH functionality with *p*-methoxybenzyl (PMB) protecting group is well described in the literature [24-34]. For our purposes, the best approach was found in the publication by Smith et al. [25] since it was shown that PMB group could be selectively cleaved or retained in compounds with similar structure. However, treatment of **11** with PMB-Cl using conditions described by Smith et al., did not lead to the expected compound (Scheme 2.8). Similar results were obtained with benzyloxycarbonyl (Cbz) protecting group (Scheme 2.8).
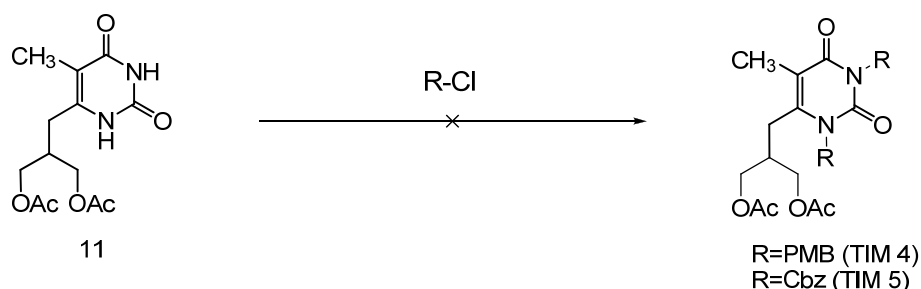
Scheme 2.8: Reaction of **11** with PMB-Cl and Cbz-Cl

Successful protection with *tert*-butoxycarbonyl (Boc) group was achieved using the procedure developed by Martin et al. [35] for the synthesis of [^{18}F]FLT. Compound **13** (Scheme 2.9) was obtained in 94% yield after column chromatography purification.
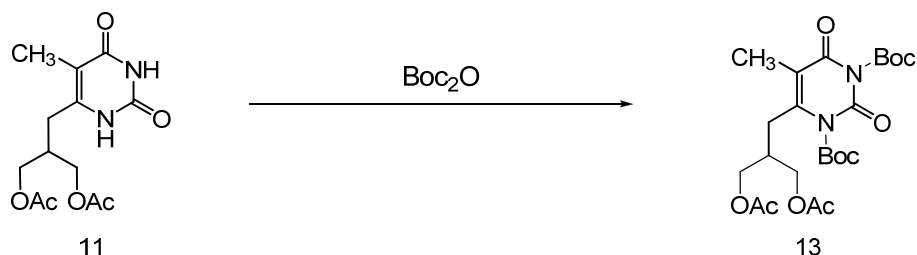
Scheme 2.9: Reaction of compound **11** with Boc$_2$O

After the successful preparation of the Boc protected compound **13**, the next step was to selectively remove the acetyl groups making two hydroxyl groups available for possible modification. Detailed literature search suggested that the acetyl group should not be stable under slightly basic conditions (pH=7-10), while the Boc group should be stable [36-40].

However, instead of the acetyl groups, deprotection of the Boc groups occurred. Such an outcome was not favorable since the reaction led to compound **11** (Scheme 2.10). By extending the reaction time, both acetyl groups were slowly cleaved from the molecule and the final compound was, in fact, DHBT (Scheme 2.10). The progress of the reaction was followed by HPLC and the products were analyzed by MS and ^{1}H NMR. The results obtained by ^{1}H NMR confirmed that the Boc group was cleaved much faster from N-3 than N-1 position. Reaction conditions used for the hydrolysis are shown in Table 2.3.
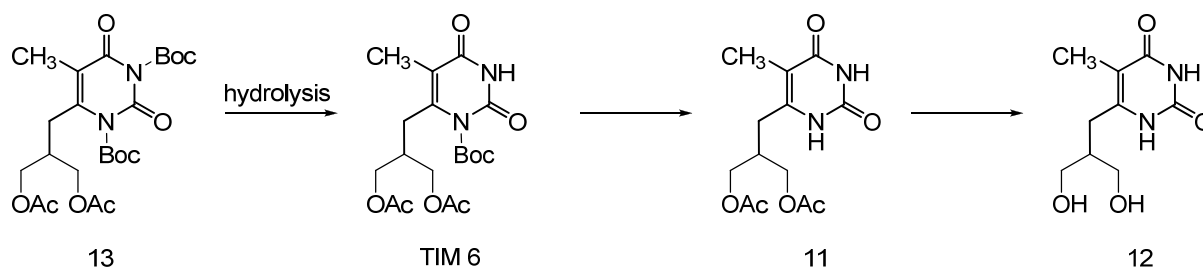
Scheme 2.10: Deprotection of Boc and acetyl groups of compound **13**

Table 2.3: Reaction conditions tried for the selective removal of acetyl protecting groups from compound **13**

Base	Solvent	Temperature	Reaction time
NH$_3$	MeOH	rt	1h, 2h, 3h
0.1 M NaOH	ACN	rt	0 min, 30 min, 60 min, 90 min, 100 min
		0°C	0 min
		-20°C	0 min, 30 min
NaOH$_{(s)}$	ACN	rt	2 min, 60 min, 24 h
K$_2$CO$_3$	MeOH/	rt	30 min, 60 min, 90 min
	H$_2$O	0°C	0 min, 30 min
-	H$_2$O	rt	0 min, 30 min, 60 min

A similar approach was used for the preparation of FHBT starting from compound **12** (DHBT). The synthetic strategy (Scheme 2.11) comprised of:

1. Selective protection of the –NH groups

2. Protection of the –OH and –NH groups with the same protecting group, followed by selective deprotection of hydroxyl groups, if step 1 fails

3. Fluorination using DAST or via introduction of the leaving group

4. Removal of the N-protecting groups
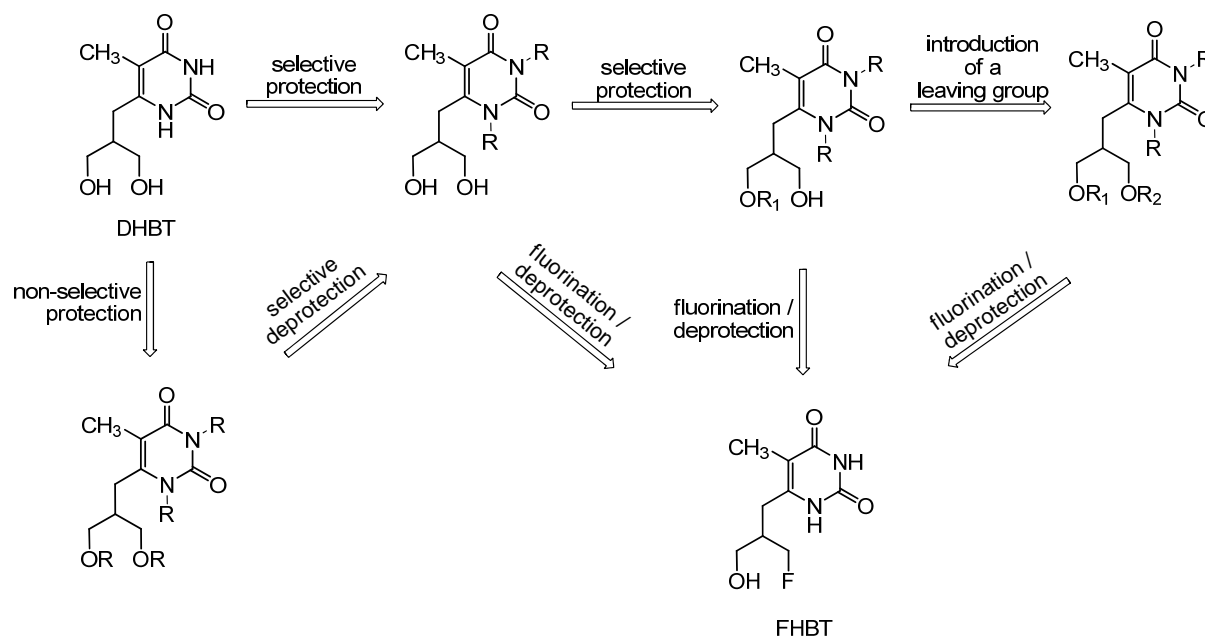
Scheme 2.11: Possible reaction pathways to FHBT from DHBT

The protection of DHBT with the PMB protecting group was performed using previously described procedures [24-34] however, no new traces of the desired compound were formed. The same result was obtained with the Cbz protecting group (Scheme 2.12) [41-54].
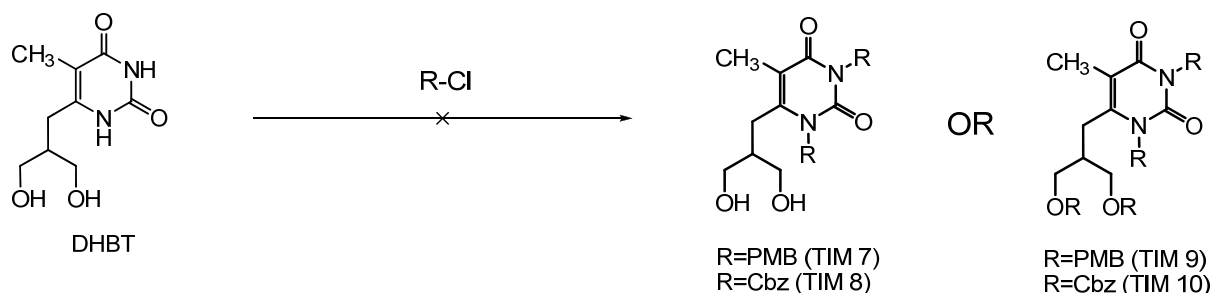
Scheme 2.12: Reaction of DHBT with PMB-Cl and CBZ-Cl

Generally, for the Boc protecting group it was not clear whether selective cleavage from the –OH groups would be feasible. The literature [55-61] suggested that the –NH groups should be more reactive than –OH groups, but this turned out not to be the case.

The reaction of DHBT with 2 equivalents of Boc_2O gave exclusively compound **14** (Scheme 2.13). The selective protection of both hydroxyl groups and the presence of two free –NH groups were confirmed by ^1H NMR. Resonance peaks at 9.6 and 10.4 ppm corresponded to unprotected N-1 and N-3 amino groups, respectively. When DHBT was treated with 6 equivalents of Boc_2O, the tetra-Boc-protected compound **16** was obtained (Scheme 2.13). The reaction was followed by HPLC and each component of the reaction mixture was isolated and analyzed by ^1H NMR. Immediate formation of intermediate **14** was observed. This was followed by the formation of compound **15** and finally the tetra-Boc-protected product **16**.
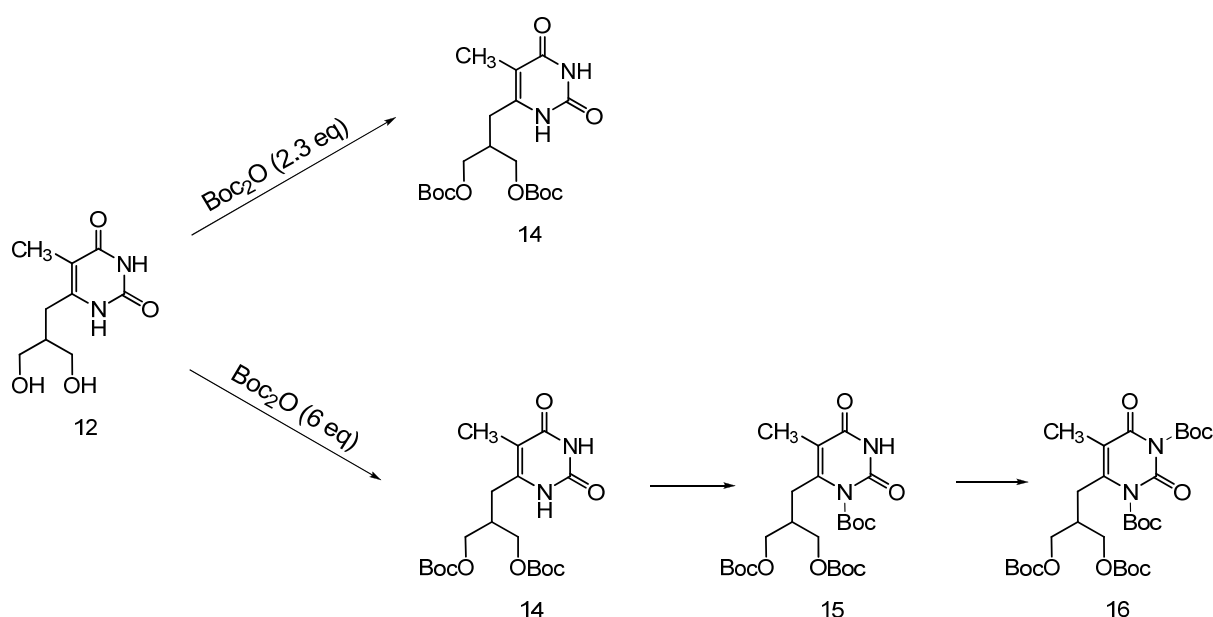
Scheme 2.13: Reaction of DHBT with Boc_2O

Unfortunately, neither compound **14** nor compound **16** could be used in subsequent synthetic steps since the Boc protecting group turned out to be more stable on –OH than on –NH functionalities.

As a last possibility, we examined the synthetic strategy shown in Scheme 2.14. The strategy involved:

1. Selective protection of one hydroxyl group with R_3
2. Fluorination
3. Removal of protecting group R_3
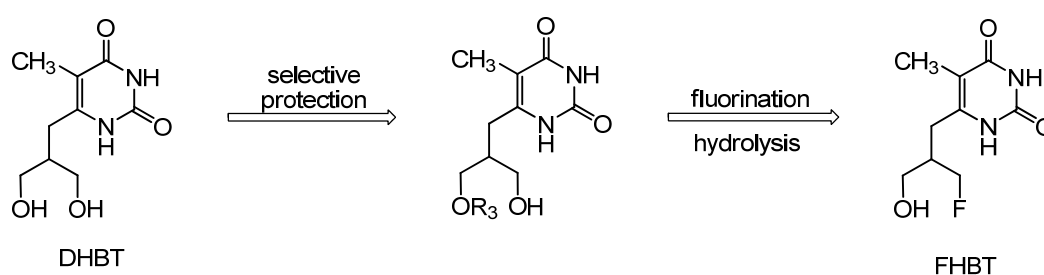
Scheme 2.14: Synthetic strategy involving the selective protection of one hydroxyl group starting from DHBT

MTr-Cl (4-Methoxytrityl chloride) is a protecting group used in the synthesis of [^{18}F]FHBG [34]. It is generally stable under fluorination conditions and does not require harsh deprotecting conditions [35, 62-64]. The reaction of DHBT with MTr-Cl successfully gave compound **17** in 54% chemical yield (Scheme 2.15).
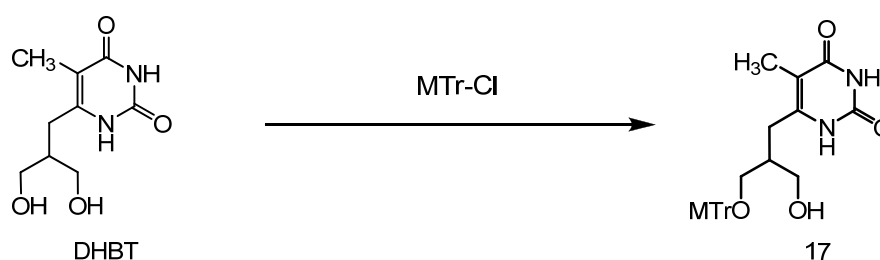
Scheme 2.15: Reaction of DHBT with MTr-Cl

Direct fluorination of **17** was successfully achieved by reaction with DAST to produce the fluorinated intermediate **18**. However, deprotection of the MTr group using 5% HCl in methanol failed to produce the expected results. This is possibly due to decomposition or intramolecular cyclization of intermediate **18** (Scheme 2.16). Evidence for decomposition was obtained from HPLC analysis, while evidence for intramolecular cyclization was obtained by ^{1}H NMR from the isolated product.
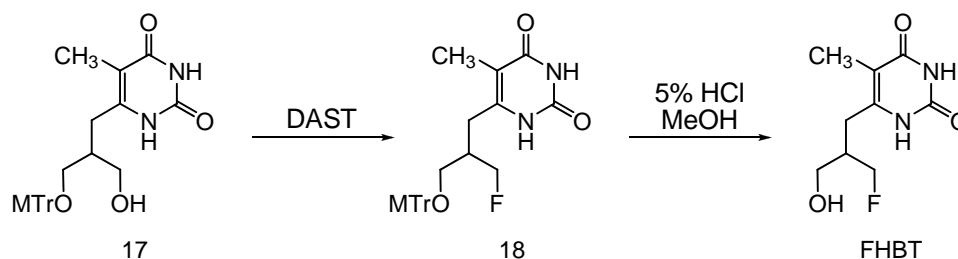
Scheme 2.16: Reaction of compound **17** with DAST and deprotection with HCl

In one case, a trace of a compound potentially corresponding to FHBT was detected when the reaction was followed by HPLC. This was based on the retention time and the absorption pattern observed within the reaction mixture (Figure 2.3).
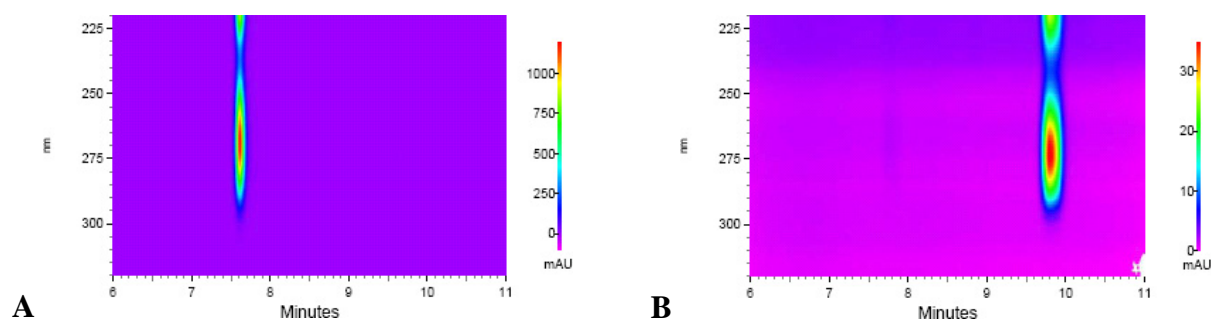

Figure 2.3: Diode array chromatogram showing different retention times and same absorption pattern of (A) DHBT; and (B) possible FHBT

Another synthetic approach was to introduce a good leaving group such as the trifluoromethanesulfonate functionality which would be substituted for fluorine in an S_N2-type reaction (Scheme 2.17), but for unknown reasons this strategy also failed.
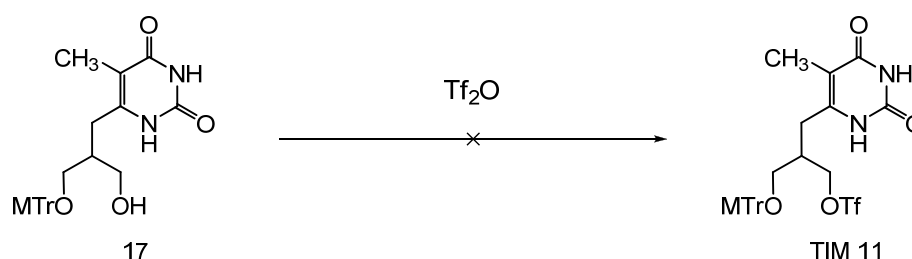
Scheme 2.17: Reaction of **17** with Tf$_2$O

Finally, it was possible to prepare compound **19** (Scheme 2.18) after the catalytic amount of trimethylamine hydrochloride was added to the reaction mixture.
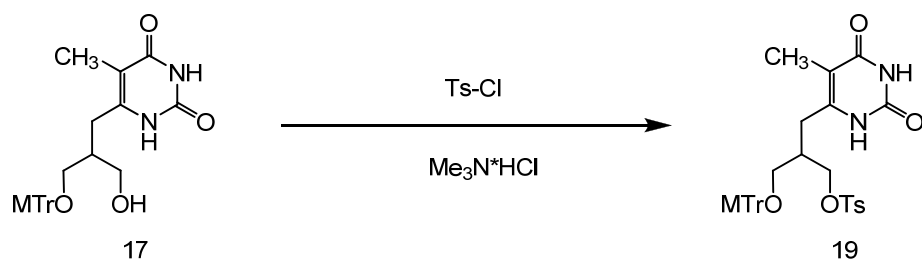
Scheme 2.18: Synthesis of the tosyl intermediate **19**

By preparing compound **19**, a very important milestone was achieved since it could be used for the preparation of "cold reference" compound FHBT by reaction with TBAF. Additionally, compound **19** could be used as a precursor for the radiolabeling of ^{18}F-labeled FHBT.
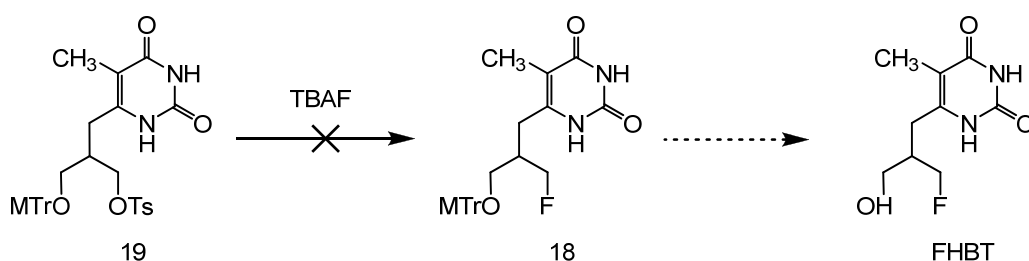
**Scheme 2.19:** Reaction of tosylated compound **19** with TBAF

The reaction with TBAF unfortunately did not produce the desired fluorinated product **18** (Scheme 2.19). Compound **19** completely decomposed under the reaction conditions used.

2.3 Fluorine-18 Radiolabeling of [^{18}F]FHBT

Even though we were unsuccessful in preparing the reference compound, we decided to investigate whether radiolabeling with ^{18}F would be feasible. The two questions to be answered were:

1. Would the radiofluorination step work with K2.2.2/[^{18}F]F$^-$ complex and whether it would be possible to prepare compound **20** (Scheme 2.20)
2. If the radiolabeling of **19** was possible, what would be the fate of the intermediate **20** after the hydrolysis?

The radiolabeling (Scheme 2.20) was performed in acetonitrile at 90°C in a reaction time of 30 minutes. As indicated from HPLC chromatograms (Figure 2.4 and 2.5), the fluorination reaction with K2.2.2/[^{18}F]F$^-$ was successful. The desired intermediate **20** was produced with 10 % conversion (Figure 2.6). However, attempts to cleave MTr group were not successful. An unknown compound was obtained in 6 % conversion (Figure 2.5).
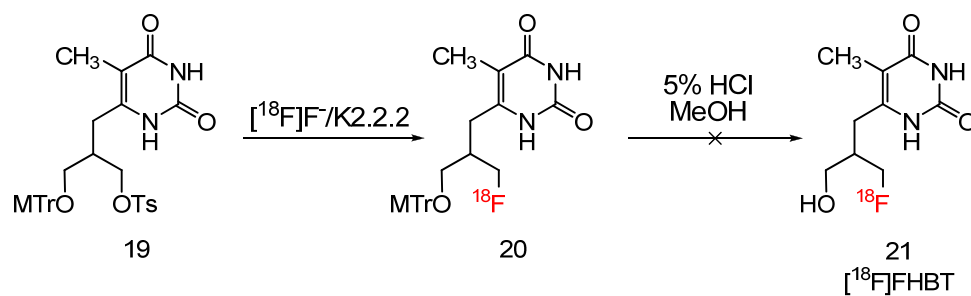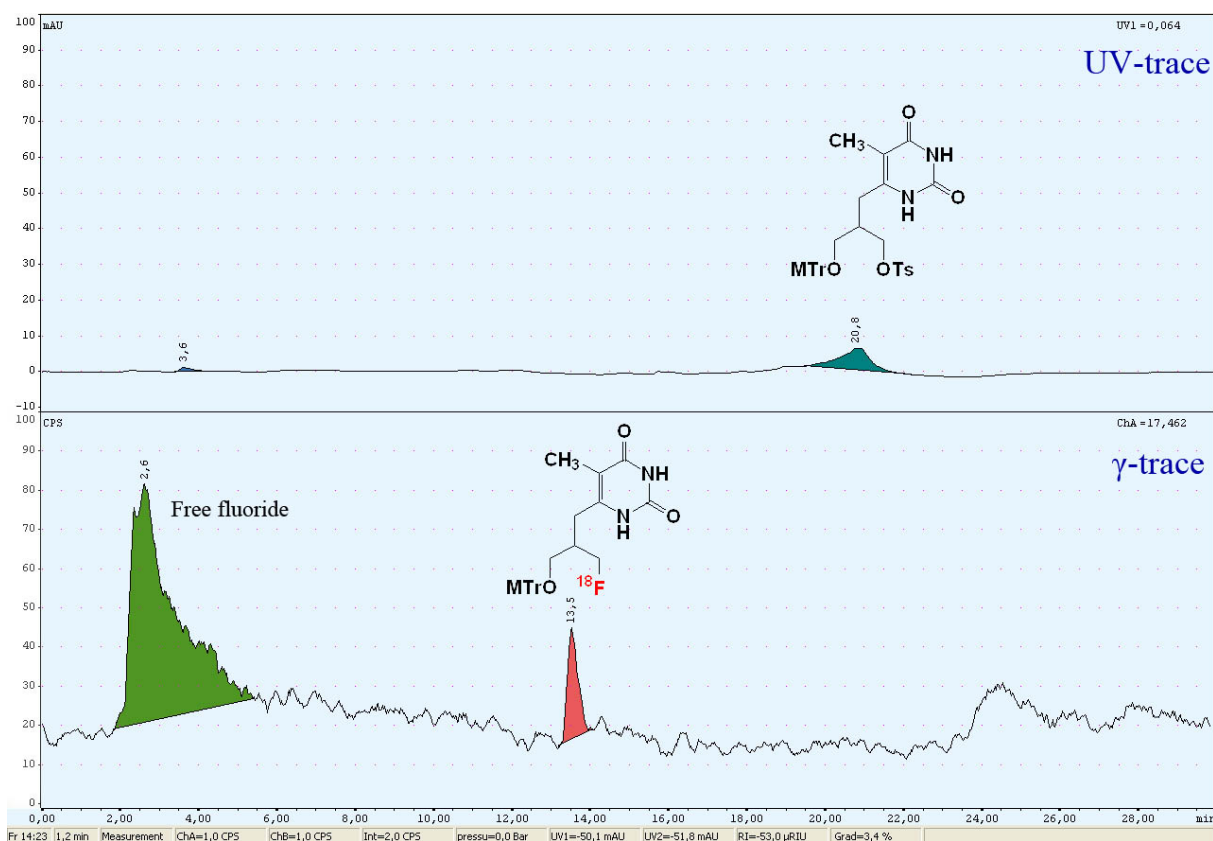

Scheme 2.20: Radiolabeling of compound **19**

Figure 2.4: UV and HPLC radio chromatograms of the reaction mixture after the fluorination of precursor **19**
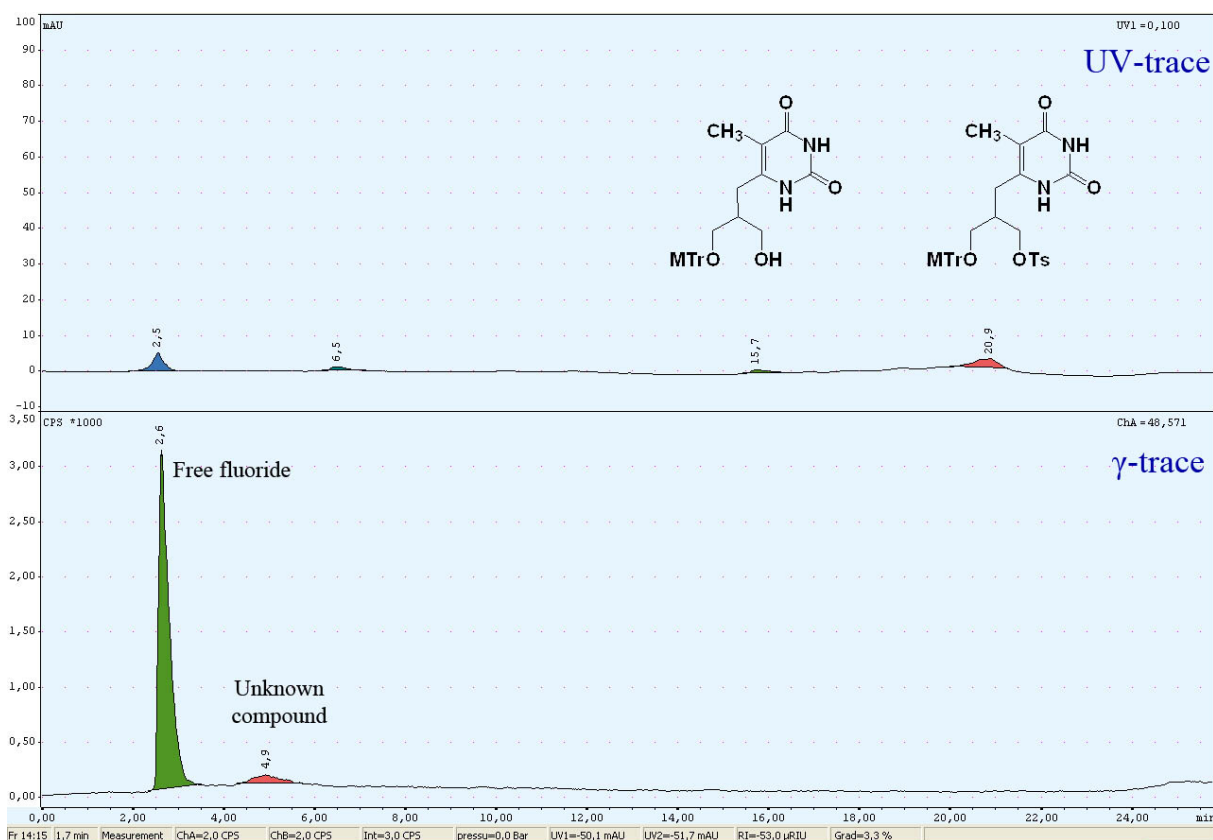

**Figure 2.5:** UV and HPLC radio chromatograms after the hydrolysis of intermediate **20**

2.4. Conclusion and Outlook

The synthetic pathway to lead molecule DHBT was optimized and the overall yield was increased 10-fold, i.e. from 2.5 to 25%. Several synthetic strategies starting from different compound failed to deliver the desired target compound FHBT. In most cases either the intermediates decomposed or an intramolecular cyclization was observed.

Although we successfully produced F-19 and F-18 fluoro derivatives of DHBT in the presence of MTr protecting group, neither FHBT nor [^{18}F]FHBT was isolated.

A novel pathway toward FHBT that would be worth trying, is the one in which the fluorine atom is introduced at the very beginning of the synthesis (Scheme 2.21). The synthesis would start from commercially available glycidol (**A1**), which would be benzylated in one step. Benzylated intermediate **A2** would be transformed into fluoro intermediate **A3** with KHF_2. In analogy to Scheme 2.3, reference compound FHBT could be obtained in reasonable yield (Scheme 2.21).

A drawback of this approach is that it is only applicable for the preparation of the reference compound and cannot be used for the synthesis of radiolabeled FHBT. A possibility could be to use chlorine instead of fluorine. Chlorine could act either as a leaving group or could be converted to a sulfonate [65, 66]. With chlorine, intramolecular cyclization would be less probable since chloride is a poor leaving group.
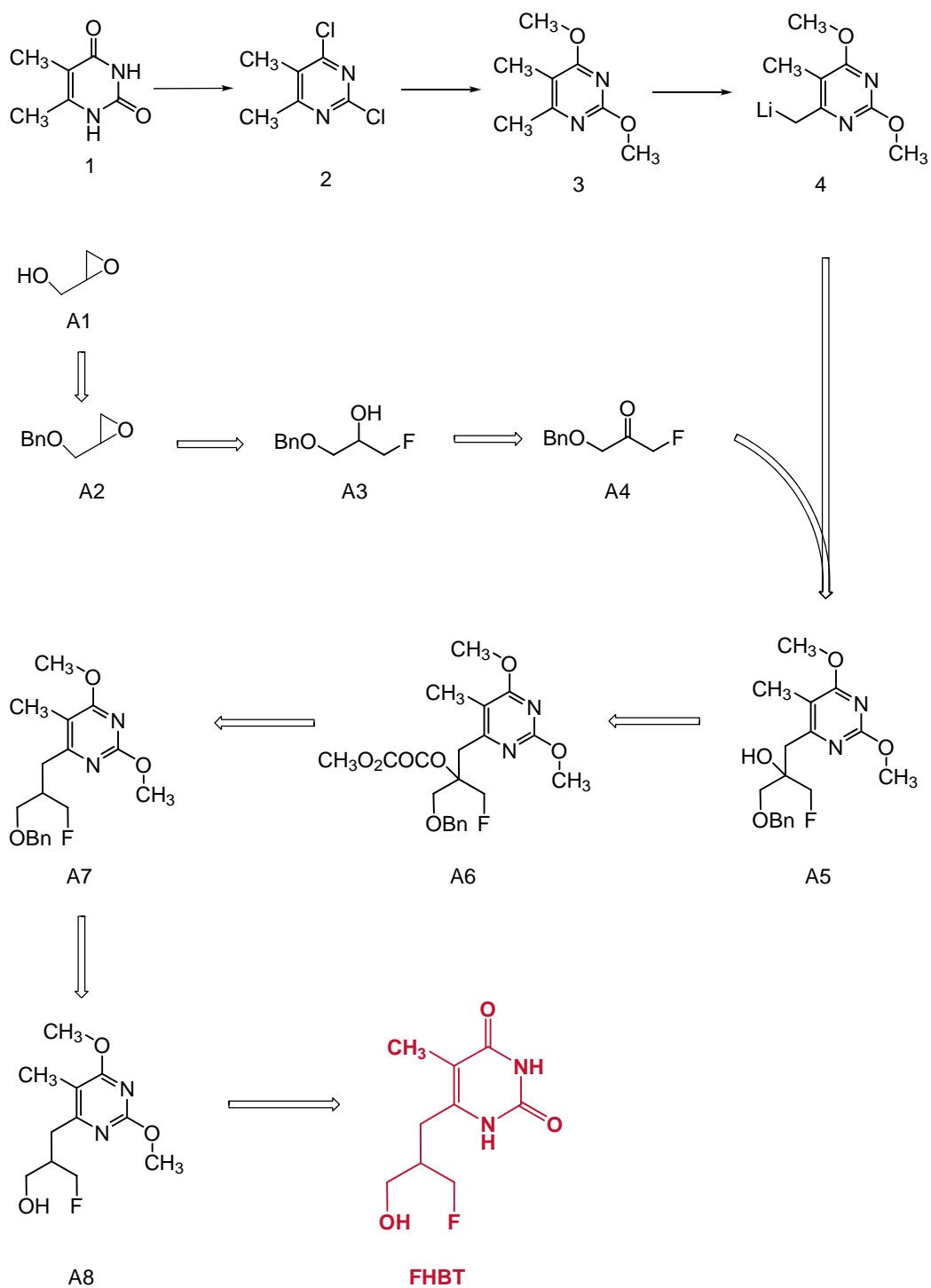
Scheme 2.21: Synthetic approach in which fluorine atom is introduced in the early stage of the synthesis

2.5 Materials and Methods

The ^1H NMR and ^{13}C NMR spectra were recorded on a 300 MHz Varian Gemini 2000 or a Bruker 400 MHz spectrometer with tetramethylsilane as an internal standard. Chemical shifts (δ) are reported in parts per million, and signals are expressed as s (singlet), d (doublet), t (triplet), q (quartet), m (multiplet) or br (broad).

The samples were dissolved in DMSO-d_6, D_2O or CD_3OD and measured in 5mm NMR tubes. The ^1H, ^{13}C NMR chemical shift values (δ) are expressed in ppm referred to TMS and coupling constants (J) in Hz.

Mass spectroscopy analysis was performed with a Micromass Quattro micro TM API LC-ESI or a LCT Premier ESI-TOF from Waters.

TLC was done on Merck silica gel 60 F_{254} precoated plates. Compounds were visualized under UV light (254 nm).

Silica gel used for column chromatography was Silica gel 60, particle size 0.040-0.063 mm (230-400 mesh ASTM), Fluka, Germany.

Evaporations were performed using Büchi Rotavapor R-215 system at 40°C.

Production of [^{18}F] fluoride: No-carrier-added aqueous [^{18}F]fluoride ion was produced on an IBA Cyclone 18/9 cyclotron by irradiation of 2.0 ml water target (for a large volume target) or 0.585 ml (for a small volume target), using a 18 MeV proton beam on 98% enriched [^{18}O]water by the [$^{18}O(p,n)^{18}F$] nuclear reaction.

HPLC 1 (analytical): Hitachi LaChrom Elite system equipped with UV diode array detector (DAD) and a column oven; column: analytical Merck LiChrospher C18 RP-18E, pore size: 100Å, particle size: 5 μm; flow rate: 1ml/min; temperature: 37°C; UV detection 220-400 nm.

HPLC analytical lab: Equipment: Agilent 1100 system equipped with a UV multi-wavelength detector; the radioactivity was monitored with a Raytest Gabi Star detector using a Gina software; column: analytical Merck LiChrospher RP-18E, pore size: 100Å, particle size: 5 μm; flow rate: 1ml/min; temperature: rt; UV detection at 254 nm.

HPLC 2 (analytical): Merck-Hitachi L6200A system equipped with UV multi-wavelength detector; column: analytical Merck LiChrospher RP-18E, Pore Size: 100Å, particle size: 5 μm; flow rate: 1ml/min; temperature: rt; UV detection at 254 nm or 275 nm.

HPLC 3 (semiprep): Merck-Hitachi system equipped with L6200A pump, Knauer variable wavelength detector and Eberline radiation monitor; column: semi-preparative Phenomenex Gemini C18, pore size: 110Å, particle size: 5 μm; flow rate: 5ml/min; temperature: rt; UV detection at 254 or 275 nm.

2,4-Dichloro-5,6-dimethylpyrimidine (2)

A mixture of 2,4-dihydroxy-5,6-dimethylpyrimidine **1** (6.33 g, 45 mmol) and $POCl_3$ (30 ml, 328 mmol) was heated under reflux for 4 h. Excess of $POCl_3$ was then removed under reduced pressure and the residue was added to ice, washed with ether and dried over sodium sulphate. The crude product was recrystallized from ethanol to give **2** (7.54 g, 94.3 %, mp 70-71 °C); ($C_6H_6N_2Cl_2$), $R_f = 0.65$ (n-hexane/EtOAc = 5/1).

^1H NMR (DMSO-d_6) 2.26 (s, 3H, CH_3); 2.47 (s, 3H, CH_3).

^{13}C NMR (DMSO-d_6) δ 155.24 (C-2), 171.48 (C-4), 127.74 (C-5), 160.54 (C-6), 22.83 (CH_3), 14.40 (CH_3).

2,4-Dimethoxy-5,6-dimethylpyrimidine (3)

To a solution of sodium (2 g, 87.0 mol) in methanol (50 ml) was added **2** (7.54 g, 42.6 mmol). The reaction mixture was refluxed for 6 h. The solvent was evaporated and water was added to dissolve NaCl. The oily layer was extracted with dichloromethane, dried over sodium sulphate and concentrated under reduced pressure. The residue was kept in refrigerator and gave colorless crystals of **3** (7.10 g, 99.1 %, mp 39-40 °C).

^1H NMR (DMSO-d_6) 1.98 (s, 3H, CH_3); 2.29 (s, 3H, CH_3); 3.82 (s, 3H, OCH_3); 3.87 (s, 3H, CH_3).

^{13}C NMR (DMSO-d_6) δ 162.10 (C-2), 168.67 (C-4), 107.25 (C-5), 165.67 (C-6), 53.96 (OCH_3), 53.74 (OCH_3), 21.46 (CH_3), 9.67 (CH_3).

1,3-bis(benzyloxy)propan-2-one (6)

N-Chlorosuccinimide (18.0 g, 134.8 mmol) was suspended in dry toluene (210 ml), and the mixture was cooled in dry ice bath. Dimethyl sulfide (15 ml, 204.2 mmol) was added, and the mixture was cooled to -25°C in a dry ice-CH_2Cl_2 bath. 1,3-bis (benzyloxy)-2-propanol **5** (25.0 g, 91.8 mmol) in toluene (21 ml) was added to the mixture, and the mixture was kept under argon for 4 h. Triethylamine (100 ml, 717.5 mol) was added, and the reaction was allowed to warm to rt. After 30 min of stirring at rt, the solution was passed through a filter paper. The residue was washed with diethyl ether (250 ml). The filtrate and the washings were combined, neutralized with 5% aqueous HCl to pH 7, washed with saturated NaCl solution (3 x 50 ml) and then with water (3 x 50 ml), and finally dried over sodium sulphate. The solvent was removed in vacuum, and the resulting oil was purified by column chromatograpy (n-hexane/EtOAc = 4/1) to give 13.5 g (54.4 % yield) of compound **6** ($C_{17}H_{18}O_3$). mp 40 °C.

MS m/z: 270 (M^+).

^1H NMR (DMSO-d_6) 7.23 (10H, Ph); 4.46 (s, 4H, CH_2Ph); 4.13 (s, 4H, CH_2O).

6-[[2-[1,3-bis(benzyloxy)-2-hydroxypropyl]]methyl]-2,4-dimethoxy-5-methylpyrimidine (7)

LDA (1.5 M, 45 ml, 113 mmol) was added dropwise to a solution of 2,4 dimethoxy-5,6-dimethylpyrimidine **3** (7.50 g, 44.6 mmol) in THF (90 ml) at -70°C. The temperature was raised to -55°C, and the solution was stirred for 30 min. **6** (12.00 g, 44.4 mmol) in THF (65 ml) was added dropwise to this solution, and stirring was continued for 2.5 h while the temperature was maintained at -55°C. The solution was neutralized by the addition of AcOH to pH 7 and then the temperature was raised to 25°C, and the solvent removed. The residue was partitioned between AcOEt and H_2O. The organic layer was separated, dried over sodium sulfate and removed by evaporation. The residue was chromatographed on silica gel column, eluting with *n*-hexane/EtOAc = 3/1. The desired fractions were concentrated in vacuum to afford compound **7** in 59% yield (1.25 g).

MS m/z: 439.3 (M^+).

^{1}H NMR (DMSO-d_6) 7.28 (10H, Ph); 5.09 (s, 1H, OH); 4.48 (s, 4H, CH_2Ph); 3.87 (s, 2H, CH_2O); 3.76 (s, 3H, OCH_3); 3.44 (s, 3H, OCH_3); 2.83 (s, 2H, CH_2); 1.99 (s, 3H, CH_3).

6-(3-Benzyloxy-2- benzyloxymethyl-propyl) 2,4-dimethoxy-5-methyl pyrimidine (9)

Methyl oxalyl chloride (5.9 ml, 63.7 mmol) was added to a mixture of 6-[[2-[1,3-bis(benzyloxy)-2-hydroxypropyl]]methyl]-2,4-dimethoxy-5-methyl-pyrimidine **7** (6.00 g, 13.7 mmol) and 4-(dimethylamino) pyridine (DMAP, 3.7 g, 29.6 mmol) in dry CH_3CN (50 ml) at 0°C under argon. The mixture was stirred for 14 h under argon at rt and then diluted with EtOAc (400 ml). The mixture was washed successively with saturated aqueous $NaHCO_3$ solution (120 ml) and H_2O (120 ml). The separated organic phase was dried over sodium sulfate and the solvent was removed under reduced pressure. The residue was coevaporated twice with dried toluene (40 ml) to afford the methyl oxalyl ester **8**. MS m/z: 481 (M+).

A mixture of Bu_3SnH (9.0 ml, 36 mmol) and 2,2'-azobis (isobutyronitrile) (AIBN; 180 mg) in dry toluene (50 ml) was added to a solution of **8** in dry toluene (130 ml) under an argon atmosphere. The mixture was heated at 110°C for 3 h and the solvent was removed by evaporation under reduced pressure. The residue was purified by column chromatography (mixture of n-hexane/EtOAc = 4/1 as mobile phase) to afford 2.77 g of 6-[3-benzyloxy-2-[(benzyloxy) methyl] propyl] thymine **9** in 48 % yield.

MS m/z: 423.3 (M^+).

^{1}H NMR (DMSO-d_6) 7.29 (10H, Ph); 4.42 (s, 4H, CH_2Ph); 3.87 (s, 3H, OCH_3); 3.79 (s, 3H, OCH_3); 3.43 (d, 4H, OCH_2); 2.68 (d, 2H, CH_2); 1.97 (s, 3H, CH_3).

6-(1,3-dihydroxy-isobutyl) 2, 4-dimethoxy-5- methyl pyrimidine (10).

A mixture of **9** (1.44 g, 3.4 mmol) in dry CH_2Cl_2 (20 ml) was cooled to $-78°C$. BCl_3 (1M in CH_2Cl_2, 17.5 ml, 17.5 mmol) was added via syringe and under argon. The mixture was stirred at -78°C for 4h, and then the temperature was raised to -40°C. A mixture of CH_2Cl_2/MeOH (1/1; 60 ml) was added, and the cooling bath was removed. The solution was neutralized with saturated $NaHCO_3$ solution to pH 7 and stirred for additional 30 min. The organic layer was separated and dried over magnesium sulfate. The solvent was removed under reduced pressure and then purified on a silica column ($CHCl_3$/*i*-PrOH = 95/5) to give 0.64 g of compound **10** (77.9% yield).

MS m/z: 243.23 (M^+)

^{1}H NMR ($CDCl_3$) 3.98 (s, 3H, CH_3O); 3.94 (s, 3H, CH_3O); 2.84 (d, 4H, OCH_2); 2.08 (s, 3H, CH_3); 2.04 (m, 2H, CH_2).

2-((5-methyl-2,6-dioxo-1,2,3,6-tetrahydropyrimidin-4-yl)methyl)-propane-1,3-diyl diacetate (11)

A solution of **10** (2.5 g, 10.3 mmol) dissolved in acetyl chloride (10 ml) and containing a few drops of water was stirred at reflux 48 hrs after which was evaporated to dryness. Raw **11** was purified by column chromatography (mixture EtOAC/CH3OH=95/5) to afford 2.3 g of pure **11** (75% yield)

MS m/z= 299.01 (M^+)

^{1}H NMR ($CDCl_3$) 10.72 (s, 1H, NH); 10.04 (s, 1H, NH); 4.13 (m, 4H, CH_2O); 2.15 (s, 3H, CH_3); 2.05 (s, 1H, CH_2).

6-(1,3-dihydroxy-isobutyl)-thymine (DHBT) (12).

A solution of **10** (2.5 g, 10.3 mmol) dissolved in acetyl chloride (10 ml) and containing a few drops of water was stirred at reflux 48 hrs after which was evaporated to dryness. Residue was dissolved in saturated methanolic ammonia, stirred at rt for additional 4 h, and then evaporated to dryness. The product was collected and washed with EtOAc/MeOH = 95/5 to give pure DHBT in 75 % yield.

MS m/z: 215.1 (M^+).

^{1}H NMR (DMSO-d_6) 7.28 (s, 1H, NH); 6.67 (s, 1H, NH); 3.40 (m, 4H, CH_2O); 2.40 (d, 2H, CH_2); 1.86 (s, 1H, CH); 1.75 (s, 3H, CH_3)

^{13}C NMR (DMSO-d_6) δ 171.54 (C-2), 164.71 (C-4), 150.06 (C-6), 104.80 (C-5), 60.67 (C`-3), 42.69 (C`-2), 29.03 (C`-1), 9.72 (CH_3).

Di-tert-butyl 6-(3-acetoxy-2-(acetoxymethyl)propyl)-5-methyl-2,4-dioxopyrimidine-1,3(2H,4H)-dicarboxylate (13)

A solution of **11** (100 mg, 0.33 mmol) in dry pyridine (5.0 ml) was sitrred at rt 10 minutes after which a solution of Boc$_2$O (220 mg, 1.0 mmol in 1.0 ml dry pyridine) was added dropwise to the reaction flask. Obtained mixture was additionally stirred at rt for 90 minutes and solvent was removed. Further purification by column chromatography (n-hexane/EtOAC=1/1) afforded 150 mg of pure **13** (94 % yield).

MS m/z: 521.24 (M + Na$^+$)

^{1}H NMR (CDCl$_3$): 1.55 (d, 18H, Boc); 2.04 (d, 6H, Ac); 2.19 (s, 3H, CH3); 2.89 (m, 2H, CH2); 4.13 (m, 4H, CH2+CH2).

Tert-butyl 2-((5-methyl-2,6-dioxo-1,2,3,6-tetrahydropyrimidin-4-yl)methyl)propane-1,3-diyl dicarbonate (14) (DHBT+2 Boc)

A solution of **12** (23.0 mg, 0.11 mmol) in dry pyridine (5.0 ml) was stirred at rt 10 minutes after which a solution of Boc2O (53.9 mg, 0.24 mol in 0.5 ml dry pyridine) was added dropwise. Obtained mixture was additionally stirred at rt for 1.5 hrs and solvent was removed. Purification by column chromatography (pure EtOAC) afforded 31.2 mg of pure **14** in 72% yield.

MS m/z: 415.16 (M$^+$)

^{1}H NMR (CDCl$_3$): 10.4 (1H, NH); 9.62 (1H, NH); 4.13 (s, 2H, CH$_2$O); 4.11 (s, 2H, CH$_2$O); 2.61 (m, 1H, CH); 1.90 (s, 3H, CH$_3$); 1.47 (m, 18H, CH$_3$).

Di-tert-butyl 6-(3-(tert-butoxycarbonyloxy)-2-((tert-butoxycarbonyloxy)methyl) propyl)-5-methyl-2,4-dioxopyrimidine-1,3(2H,4H)-dicarboxylate (16) (DHBT+4 Boc)

A solution of **12** (22.3 mg, 0.10 mmol) in dry pyridine (1.0 ml) was stirred at rt 10 minutes after which a solution of Boc2O (134 mg, 0.61 mmol in 0.3 ml dry pyridine) was added dropwise. Obtained mixture was additionally stirred at rt for 1.5 hrs and solvent was removed. Further purification by column chromatography (n-hexane/EtOAC=5/2) afforded 39.4 mg of pure **16** in 62% yield.

MS m/z: 615.34 (M$^+$)

^{1}H NMR (CDCl$_3$): 4.15 (s, 2H, CH$_2$O); 4.13 (s, 2H, CH$_2$O); 2.89 (m, 1H, CH); 2.17 (s, 3H, CH$_3$); 1.55 (m, 9H, CH$_3$); 1.54 (m, 9H, CH$_3$); 1.47 (m, 18H, CH$_3$).

6-(3-Hydroxy-2-(((4-methoxyphenyl)diphenylmethoxy)methyl)propyl)-5-methylpyrimidine-2,4(1H,3H)-dione (17)

A solution of **12** (5.0 mg, 23.3 μmol) in dry pyridine (1.5 ml) was stirred with 2.9 mg of DMAP (23.5 μmol) at rt for 10 minutes after which MTr-Cl was added (8.0 mg, 25.7 μmol. Obtained mixture was additionally stirred at 50°C for 1.5 hrs and solvent was removed. Further purification by column chromatography (CH3Cl/i-PrOH=9/1) afforded 4.1 mg of pure **17** in 36% yield.

MS m/z: 485.44 (M$^-$)

^{1}H NMR (CDCl$_3$): 1.78 (s, 3H, CH$_3$); 2.04 (s, 1H, CH); 2.57 (d, 2H, CH$_2$); 3.18 (m, 2H, CH$_2$); 3.74 (m, 2H, CH$_2$); 3.76 (s, 3H, OCH$_3$); 6.80-7.39 (m, 14H, Ph).

3-((4-Methoxyphenyl)diphenylmethoxy)-2-((5-methyl-2,6-dioxo-1,2,3,6-tetrahydropyrimidin-4-yl)methyl)propyl 4-methylbenzenesulfonate (19)

A solution of **17** (3.0 mg, 6.2 μmol), Me$_3$N·HCl (0.1 mg) and Et$_3$N (10 μL) in dry CH$_2$Cl$_2$ (0.5 ml) was stirred at rt 5 minutes after which a solution of Ts-Cl (1.4 mg, 7.4 μmol in 150 μL) was added dropwise. Obtained mixture was additionally stirred at rt for 1 hr and solvent was removed. Further purification by semi-preparative HPLC afforded 3.5 mg of pure **19** in 88% yield.

MS m/z: 611.13 (M$^+$)

^{1}H NMR (CDCl$_3$): 1.90 (m, 1H, CH); 2.43 (s, 9H); 3.06 (m, 2H, CH$_2$); 7.10-7.90 (m, 18H, Ph), 11.43 (s, 1H, NH).

6-(3-Fluoro-2-(hydroxymethyl)propyl)-5-methylpyrimidine-2,4(1H,3H)-dione (FHBT)

Solution of **17** (1.8 mg, 3.7 μmol) in dry CH$_2$Cl$_2$ (3 ml) under argon, was cooled down to -78°C and stirred for 15 min. (Dimethylamino)sulfur trifluoride (20μl, 151 μmol) was added dropwise and reaction was kept at -78°C for additional 15 min after which cooling was removed. After 45 min of stirring at rt, saturated aqueous solution of NaHCO$_3$ was added (3 ml) and reaction was partitioned. Organic layer was separated and evaporated to afford 1.5 mg of raw **18** (83% yield).

Solution of raw **18** was dissolved in 5% HCl in CH$_3$OH (1.5 ml) was refluxed 15 min at 90°C under argon after which the solvent was removed. Possible FHBT was purified using semi-preparative HPLC, however not in sufficient amounts for the analysis.

Radiolabeling of 3-((4-Methoxyphenyl)diphenylmethoxy)-2-((5-methyl-2,6-dioxo-1,2,3,6-tetrahydropyri-midin-4-yl)methyl)propyl 4-methylbenzenesulfonate (19)

To a 10-mL Pyrex brand tube with screw cap containing 5 mg Kryptofix 2.2.2 and 2 mg of K_2CO_3 was added 15 GBq ^{18}F-fluoride. Water was azeotropically evaporated from the mixture using dry CH_3CN (3 x 1.0 mL) at 90°C under a stream of nitrogen. After the final drying sequence, 2 mg of **19** dissolved in 350 μl dry CH_3CN were added to the F-18 residue. The reaction was carried out at 90°C for 30 min. 300 μl of HCl (5% in CH_3OH) were added and the reaction was kept for 10 min at 90°C after which it was allowed to cool to rt. Water (4.7 ml) was added and the mixture was purified by HPLC. The fraction containing the F-18 labeled compound unfortunately did not correspond to [^{18}F]FHBT.

2.6 References

[1] Tjuvajev JG, Doubrovin M, Akhurst T, Cai S, Balatoni J, Alauddin MM, et al. Comparison of radiolabeled nucleoside probes (FIAU, FHBG, and FHPG) for PET imaging of HSV1-tk gene expression. J Nucl Med 2002;43:1072-83.

[2] Gambhir SS, Herschman HR, Cherry SR, Barrio JR, Satyamurthy N, Toyokuni T, Phelps ME, Larson SM, Balatoni J, Finn R, Sadelain M, Tjuvajev J, Blasberg R. Imaging transgene expression with radionuclide imaging technologies. Neoplasia. 2000;2:118-38.

[3] Serganova I, Ponomarev V, Blasberg R. Human reporter genes: potential use in clinical studies. Nucl Med Biol. 2007;34:791-807.

[4] Johayem A, Raić-Malić S, Lazzati K, Schubiger PA, Scapozza L, Ametamey SM. Chem Biodivers. 2006;3:274-83.

[5] Seimbille Y, Bénard F, Rousseau J, Pepin E, Aliaga A, Tessier G, van Lier JE. Impact on estrogen receptor binding and target tissue uptake of [^{18}F]fluorine substitution at the 16α-position of fulvestrant (faslodex; ICI 182,780). Nucl Med Biol 2004; 31:691-8

[6] Lim JL, Zheng L, Berridge MS, Tewson TJ. The use of 3-methoxymethyl-16β, 17β-epiestriol-O-cyclic sulfone as the precursor in the synthesis of F-18 16α-fluoroestradiol. Nucl Med Biol 1996;23:911-5

[7] Berridge MS, Franceschini MP, Rosenfeld E, Tewson TJ. Cyclic Sulfates: Useful substrates for Selective Nucleophilic Substitution. J Org Chem 1990;55:1211-7

[8] He L, Byun H-S, Bittman R. A New Synthetic Route to Chiral Glycerolipid Precursors Using a Cyclic Sulfate Synthon: Preparation of 1-*O*-Hexadecyl-3-*O*-(4'-methoxyphenyl)- *sn*-glycerol and Its 1-Thio and 1-Aza Analogues. J Org Chem 1998; 63:5696-9

[9] Byun H-S, He L, Bittman R. Cyclic Sulfites and Cyclic Sulfates in Organic Synthesis. Tetrahedron 2000;56:7051-91

[10] Tewson TJ. Cyclic Sulfur Esters as Substrates for Nucleophilic Substitution. A New Synthesis of 2-Deoxy-2-fluoro-D-glucose. J Org Chem 1983;48:3507-10

[11] Gao Y, Sharpless KB. Vicinal Diol Cyclic Sulfates: Like Epoxides Only More Reactive. J Am Chem Soc 1988;110:7538-9

[12] Hoffmann RW, Stiasny HS. Diastereoselective Bromine/Lithium-Exchange Applied to the Synthesis of a C-1/C-9-Segmant of the Bryostatins. Tetrahedron Lett 1995;36: 4595-8

[13] Lyle TA, Magill CA, Pitzenberger SM. Fluorine-Induced Formation and Ring Opening of Cyclic Sulfamates from Hydroxy Triflamides. Synthetic and Mechanistic Studies. J Am Chem Soc 1987;109:7890-1

[14] Rebiere F, Samuel O, Ricard L, Kagan HB. A General Route to Enantiomerically Pure Sulfoxides from Chiral Sulfite. J Org Chem 1991;56:5991-9

[15] Singh RP, Shreeve JM. Nucleophilic fluorination of amino alcohols and diols using Deoxofluor. J Fluorine Chem 2002;116:23-6

[16] Hallett DJ, Gerhard U, Goodacre SC, Hitzel L, Sparey TJ, Rowley TSM, Ball RG. Neighboring Group Participation of the Indole Nucleus: An Unusual DAST-Mediated Rearrangement Reaction. J Org Chem 2000;65:4984-93

[17] Sutherland A, Vederas JC. The first isolation of an alkoxy-N,N-dialkylaminodifluorosulfane from the reaction of an alcohol and DAST: an efficient synthesis of (2S,3R,6S)-3-fluoro-2,6-diaminopimelic acid. Chem. Commun 1999; 1739-41

[18] De Jonghe S, Overmeire IV, Calenbergh SV, Hendrix C, Busson R, De Keukeleire D, Herdewijn P. Synthesis of Fluorinated Sphinganine and Dihydroceramide Analogues. Eur J Org Chem 2000;3177-76.

[19] Huang H, Han W, Noodleman L, Grynszpan F. Multiple reactive immunization towards the hydrolysis of organophosphorus nerve agents: hapten design and synthesis. Bioorg Med Chem 2001;9:3185-95.

[20] Taing M, Keng Y, Shen K, Wu L,Lawrence DS, Zhang Z. Potent and Highly Selective Inhibitors of the Protein Tyrosine Phosphatase 1B. Biochemistry 1999;38: 3793-803.

[21] Inoue M, Hiratake J, Suzuki H, Kumagai H, Sakata K. Biochemical Analysis of the Saccharomyces cerevisiae SEC18 Gene Product: Implications for the Molecular Mechanism of Membrane Fusion. Biochemistry 2000;39:7764-72

[22] Shabat D, Itzhaky H, Reymond J-L, Keinan E. Antibody catalysis of a reaction otherwise strongly disfavoured in water. Nature (London) 1995;374:143-6.

[23] Ryberg P, Matsson O. The Mechanism of Base-Promoted HF Elimination from 4-Fluoro-4-(4-nitrophenyl)butan-2-one Is E1cB. Evidence from Double Isotopic Fractionation Experiments. J Org Chem 2002;67:811-4.

[24] Kende AS, Hernando JIM, Milbank JBJ, Total synthesis of (±)-stemonamide and (±)-isostemonamide. Tetrahedron 2002;58:61-74

[25] Smith AB, Leahy JW, Noda I, Remiszewski SW, Liverton NJ, Zibuck R. Total synthesis of the latrunculins. J Am Chem Soc 1992;114:2995-3007

[26] Smith AB III, Friestad GK, Barbosa J, Bertounesque E, Duan JJ-W, Hull KG, Iwashima M, Qiu Y, Spoors PG, Salvatore BA. Total Synthesis of (+)-Calyculin A and (-)-Calyculin B: Cyanotetraene Construction, Asymmetric Synthesis of the C(26-37) Oxazole, Fragment Assembly, and Final Elaboration. J Am Chem Soc 1999; 121:10478-86

[27] Smith AB III, Rano TA, Chida N, Sulikowski GA, Wood JL. Total Synthesis of Cytotoxiy Macrocycle (+)-Hitachimycin. J Am Chem Soc 1992;114:8008-22

[28] Louwrier S, Ostendorf M, Boom A, Hiemstra H, Speckamp WN. Studies towards the synthesis of (+)-ptilomycalin A; Stereoselective N-acyliminium ion coupling reactions to enantiopure C-2 substituted lactams. Tetrahedron 1996;52:2603-28

[29] Hamada Y, Tanada Y, Yokokawa F, Shioiri T. Stereoselective Synthesis of 2,3-dihydroxy-4-dimethylamino-5-methoxypentanoic acid, a fragment of calyculins ------- determination of the absolute configuration of calyculins. Tetrahedron Lett 1991; 32:5983-6

[30] Chida N, Ohtsuka M, Ogawa S. Total Synthesis of (+)-Lycoricidine and Its 2-Epimer from D-Glucose. J Org Chem 1993;58:4441-7

[31] Bolli MH, Marfurt J, Grisostomi C, Boss C, Binkert C, Hess P, Treiber A, Thorin E, Morrison K, Buchmann S, Bur D, Ramuz H, Clozel M, Fischli W, Weller T. Novel Benzo[1,4]diazepin-2-one Derivatives as Endothelin Receptor Antagonists. J Med Chem 2004;47:2776-95

[32] Williams RM, Armstrong RW, Dung J-S. Synthesis and Antimicrobial Evaluation of Bicyclomycin Analogues. J Med Chem 1985;28:733-40

[33] Williams RM, Kwast E. Carbanion-mediated Oxydative Deprotection of Non-Enolizable Benzylated Amides. Tetrahedron Lett 1989;30:451-4

[34] Horita K, Yoshioka T, Tanaka T, Oikawa Y, Yonemitsu O. On the selectivity of deprotection of benzyl, mpm (4-methoxybenzyl) and dmpm (3,4-dimethoxybenzyl) protecting groups for hydroxy functions. Tetrahedron 1986;42:3021-8

[35] Martin JC, McGee DP, Jeffrey GA, Hobbs DW, Smee DF, Matthews TR, Verheyden JP, Synthesis and Anti-Herpes-Virus Activity of Acyclic 2'-

Deoxyguanosine Analogues Related to 9-[(1,3-Dihydroxy-2-propoxy)methyl] guanine. J Med Chem 1986;29:1384-9

[36] Kim JN, Im YJ, Kim JM. Synthesis of ortho-hydroxyacetophenone derivatives from Baylis-Hillman acetates. Tetrahedron Lett 2002;43:6597-6600

[37] Kim N-C, Kinghorn AD, Kim DSLH. Semisynthesis of Abrusoside A Methyl Ester. Org Lett 1999;1:223-4

[38] Zou R, Ayres KR, Drach JC, Townsend LB. Synthesis and Antiviral Evaluation of Certain Disubstituted Benzimidazole Ribonucleosides. J Med Chem 1996;39: 3477-82

[39] Plattner JJ, Gless RD, Rapoport H. Synthesis of Some DE and CDE Ring Analogues of Campotothecin. J Am Chem Soc 1972: 94:8613-5

[40] Haeckel R, Troll C, FischerH, Schmidt RR. Synthesis of Unprotected O-Glycosyl Trichloroacetimidates Structure Assignment and New Results. Synlett 1994;1994: 84-6

[41] Yagi H, Thakker DR, Lehr RE, Jerina DM. Removal of Benzyl-type Protecting Groups from Peptides by Catalytic Transfer Hydrogenation with Formic acid. J Org Chem 1979;44:3442-4

[42] Valerio RM, Alewood PF, Johns RB. Synthesis of Optically Active 2-(*tert*-Butyloxycarbonylamino)-4-dialkoxyphosphorylbutanoate Protected Isosteres of *O*-Phosphonoserine for Peptide Synthesis. Synthesis 1988, 1988:786-9

[43] Fuentes J, Cuevas T, Pradera MA. Syntheses of O-Protected 2-amino-2-deoxy-gentiobioside hydrohalides, Tetrahedron 1993;49:6235-50

[44] Yajima H, Fujii N, Ogawa H, Kawatani H. Trifluoromethanesulphonic Acid, as a Deprotecting Reagent in Peptide Chemistry. J Chem Soc Chem Comm 1974;107-8

[45] Yajima H, Ogawa H, Sakurai H. Synthesis of the nonacosapeptide corresponding to the entire amino acid sequence of duck glucagon. J Chem Soc Chem Comm 1977;909-10

[46] Walker DM, McDonald JF, Logusch EW. Synthesis of D-L-gamma-Hydroxyphosphinothricin, a Potent New Inhibitor of Glutamine Synthetase. J Chem Soc Chem Comm 1987;1710-1

[47] Ihara M, Taniguchi N, Noguchi K, Fukumoto K. Total Synthesis of Hydrocinchonidine and Hydrocinchonine via Photooxygenation of an Indole Derivative. J Chem Soc Perkin Trans 1988;1277-81

[48] Bolos J, Perez-Beroy A, Gubert S, Anglada L, Sacristian A, Ortiz JA. Asymmetric Synthesis of Pyrrolo[2,1-b][1,3,4]thiadiazepine Derivates. Tetrahedron 1992;48:9567-76

[49] Evans DA, Ellman JA. The Total Syntheses of the Isodityrosine-Derived Cyclic Tripeptides OF4949-III and K-13. Determination of the Absolute Configuration of K-13. J Am Chem Soc 1989;111:1063-72

[50] Heffner RJ, Jiang J, Joullie MM, Total Synthesis of (-)-Nummularine F. J Am Chem Soc 1992;114:10181-9

[51] Downing SV, Aguilar E, Meyers AI. Total Synthesis of Bistratamide D. J Org Chem 1999;64:826-31

[52] Sajiki H, Hattori K, Hirota K. The Formation of a Novel Pd/C-Ethylenediamine Complex Catalyst: Chemoselective Hydrogenation without Deprotection of the *O*-Benzyl and *N*-Cbz Groups. J Org Chem 1998;63:7990-2

[53] Felix AM, Heimer EP, Lambros TJ, Tzougraki C, Meienhofer J. Rapid Removal Of Protecting Groups from Peptides by Catalytic Transfer Hydrogenation with 1,4-Cyclohexadiene. J Org Chem 1978;43:4194-6

[54] Berkowitz DB, Pedersen ML. Simultanous Amino and Carboxyl Group Protection for alpha-Branched Amino Acids. J Org Chem 1994;59:5476-8

[55] Samnick S, Ametamey S, Gold MR, Schubiger PA. Synthesis and preliminary in vitro evaluation of a new memantine derivative 1-amino-3-[^{18}F]fluoromethyl-5-methyl-adamantane: A potential ligand for mapping the N-methyl-D-aspartate receptor complex. . Labelled Compd Radiopharm 1997;39:241-50

[56] Berts W, Luthman K. Synthesis of a complete series of C-4 fluorinated Phe-Gly mimetics. Tetrahedron 1999;55:13819-30

[57] Govek SP, Overman LE. Total Synthesis of Asperazine. J Am Chem Soc 2001;123: 9468-9

[58] Beecher JE, Tirrell DA. Synthesis of Protected derivatives of 3-Pyrrolylalanine. Tetrahedron Lett 1998;39:3927-30

[59] Yun M, Oh SJ, Ha H-J, Ryu JS, Moon DH. High radiochemical yield synthesis of 3′-deoxy-3′-[^{18}F]fluorothymidine using (5′-O-dimethoxytrityl-2′-deoxy-3′-O-nosyl-β-D-threo pentofuranosyl)thymine and its 3-N-BOC-protected analogue as a labeling precursor. Nucl Med Biol 2003;30: 151-7

[60] Horita K, Yoshioka T, Tanaka T, Oikawa Y, Yonemitsu O. On the selectivity of deprotection of benzyl, mpm (4-methoxybenzyl) and dmpm (3,4-dimethoxybenzyl) protecting groups for hydroxy functions. Tetrahedron 1986;42:3021-8

[61] Williams RM, Sinclair PJ, Zhai D, Chen D. Practical asymmetric syntheses of alpha-amino acids through carbon-carbon bond constructions on electrophilic glycine templates. J Am Chem Soc 1988;110:1547-57

[62] Grote M, Noll S. Synthesis of ^{18}F-labeled acyclic purine and pyrimidine nucleosides intended for monitoring gene expression. Radiochim Acta 2005;93:585-8

[63] Alauddin MM, Conti PS. Synthesis and Preliminary Evaluation of 9-(4-[^{18}F]-Fluoro-3-Hydroxymethylbutyl)Guanine ([^{18}F]FHBG): A New Potential Imaging Agent for Viral Infection and Gene Therapy Using PET. Nucl Med Biol 1998;25:175-80

[64] Shiue GG, Shiue C-Y, Lee RL, MacDonald D, Hustinx R, Eck SL, Alavi AA. A simplified one-pot synthesis of 9-[(3-[^{18}F]Fluoro-1-hydroxy-2-propoxy)methyl]guanine([^{18}F]FHPG) and 9-(4-[^{18}F]Fluoro-3-hydroxymethylbutyl)guanine ([^{18}F]FHBG) for gene therapy. Nucl Med Biol 2001;28:875-83

[65] Klok RP, Klein PJ, Herscheid JDM, Windhorst AD. Synthesis of N-(3-[^{18}F]Fluoropropyl)-2β-carbomethoxy-3β-(4-iodophenyl)nortropane([^{18}F]FP-β-CIT). J Label Compd Radiopharm 2006;49:77–89.

[66] Shimadzu H, Suemoto T, Suzuki M, Shiomitsu T, Okamura N, Kudo N, Sawada T. A novel probe for imaging amyloid-b: Synthesis of F-18 labelled BF-108, an Acridine Orange analog. J Label Compd Radiopharm 2003;46:765–72.

3 Development of a Novel C-6 Substituted Pyrimidine Derivative for Gene Therapy Monitoring

# 1. Introduction

Non-fluorinated acyclic nucleoside analogues are known to be potent anti-herpes virus agents.[1] The most efficient ones, aciclovir (ACV) and ganciclovir (GCV) possess low host toxicity and are active against herpes simplex virus type 1 (HSV1) and 2 (HSV2) [1]. The selectivity of these acyclic nucleoside analogues is due, in part, to the fact that they are phosphorylated only in virus-infected cells, where a virus specific thymidine kinase of low substrate specificity converts the nucleoside analogues to their monophosphate derivatives. Fluoro derivatives of ganciclovir and penciclovir, i.e. 9-[(3-fluoro-1-hydroxy-2-propoxy)methyl]guanine (FGCV) and 9-(4-fluoro-3-hydroxymethyl-butyl)guanine (FPCV) were evaluated as tracers for non-invasive positron emission tomography (PET) imaging of herpes simplex virus type 1 thymidine kinase (HSV1 TK) gene expression [2,3]. To be considered a suitable agent for monitoring HSV-1 TK expression *in vivo* by PET, compound has to fulfill several requirements [4]: good catalytic efficacy for HSV1 TK, high specificity towards the HSV1-TK enzyme, low specificity toward other enzymes, low cytotoxicity in normal and TK-transfected cells, suitable structure for radiolabeling and favorable pharmacokinetics.

In a previous work, we described lead compound DHBT (Figure 1) and discussed its advantages [5]. The promising results obtained prompted us to pursue the development of a fluorinated derivative of DHBT (Figure 1) for evaluation as a ligand for monitoring HSV1 TK expression.

Herein we describe docking studies and the synthesis of the key compound N-Me DHBT (Figure 1), its binding affinity to HSV-1 TK, kinetic turnover constant and cytotoxicity in B16F1 cell lines. In addition, we report on the fluoro derivative preparation of N-Me DHBT, N-Me FFBT (Figure 1), as well as the fluorine-18 radiolabeling of [^{18}F]N-Me FHBT.
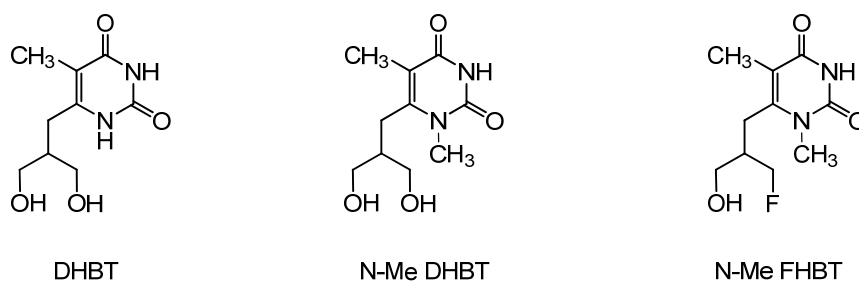
**Figure 1.** Structures of DHBT, N-Me DHBT and N-Me FHBT

2. Results and Discussion

Docking studies using GOLD

The choice of the docking program among the ones available in our lab (Autodock, Dock, Gold, FlexX) was made based on a study of Kellenberger et al. (2004) stating that both the capacity of reproducing the X-ray pose (accuracy) as well as the discrimination of known thymidine kinase lignads were best achieved with the docking program Gold [6].

Gold 2.2 (Genetic Optimisation for Ligand Docking) is especially suited for complexes displaying predominantly H-bonds [7]. Apart from visual inspection, the main parameter to estimate if the docking was successful is the fitness function, which has been optimised for the prediction of ligand binding positions rather than affinity.

Docking studies were performed in order to investigate whether N-Me DHBT would, indeed, be a substrate for HSV1 TK. The docking model was tested by examining binding modes of thymidine, penciclovir (PCV), ganciclovir (GCV) and DHBT. It was successfully validated since all binding modes corresponded to the binding modes seen in their respective crystal structures with HSV1 TK. Root mean square deviation (RMSD) values were always close to 1 Å. An example of a docking validation can be seen in Figure 2.
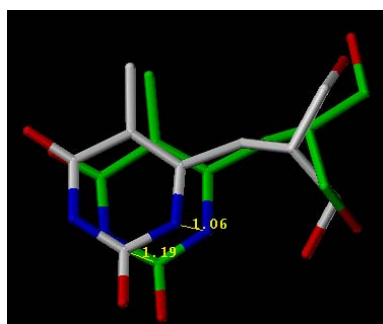
Figure 2. Binding mode comparison between the docking pose of DHBT (green carbons) and the X-ray structure determined one (white carbons). Oxygen and nitrogen are shown in red and blue, respectively. The RMSD value is around 1 Å. For clarity, the surrounding protein has not been displayed.

The docking results predicted that N-Me DHBT would indeed, be a HSV1 TK substrate since N-Me DHBT shows the same interactions known to thymidine and

DHBT. Specifically, the OH groups of N-Me DHBT and N-Me FHBT point towards the catalytic center of the enzyme, formed by E83 and R163. Due to these interactions, it was predicted that N-Me DHBT and N-Me FHBT would undergo phosphorylation since their hydroxyl functionalities mimic the 5'-hydroxyl group of thymidine. The second OH group of N-Me DHBT and the F atom of N-Me FHBT point towards the LID domain (residues 219-226) of HSV1 TK (Figure 3). Based on these results, both compounds fulfill the prerequisite for being HSV1 TK substrates.
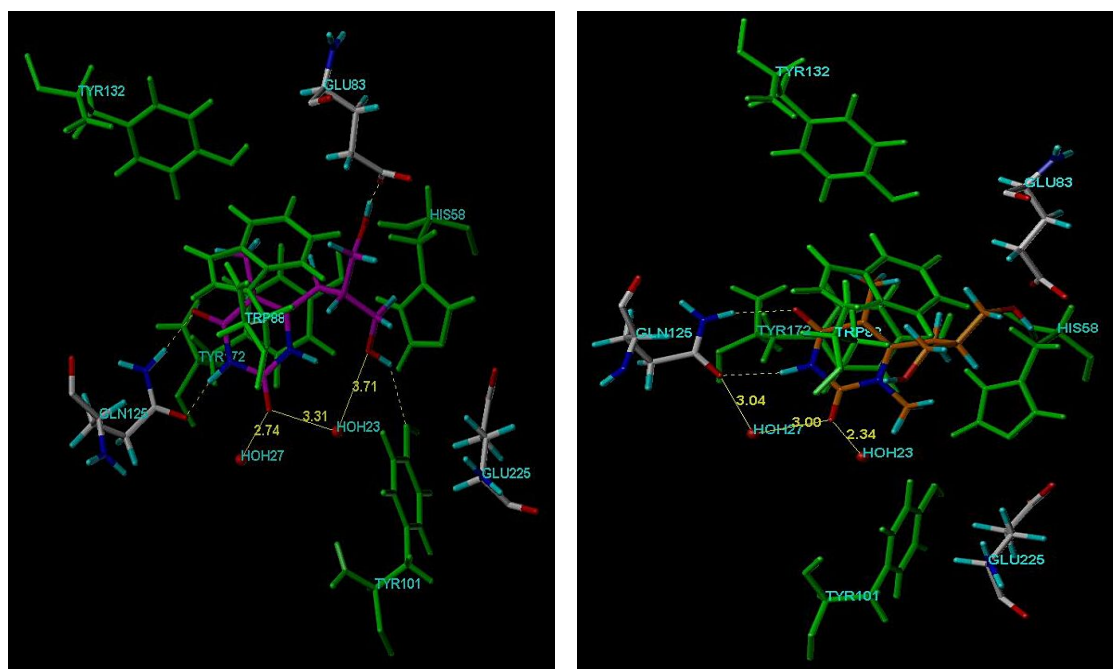
Figure 3. Binding modes of DHBT (left) and N-Me FHBT (right)

Synthesis of N-Me FHBT

The synthesis of the key intermediate N-Me DHBT (Scheme 1) was accomplished in analogy to published procedures with slight modifications in the work-up [8, 9]. The starting compound, 2,4-dihydroxy-5,6-dimethylpyrimidine (**1**), was converted to the corresponding chloride **2** which was used without further purification. Treatement of **2** with sodium methanolate gave dimethoxy compound **3** in 95% yield after purification by column chromatography. In parallel, 1,3-dibenzyloxy-2-propanol (**5**) was oxidized using Corey oxidation to yield ketone **6**. The product of the reaction between lithiated compound **4** and ketone **6** was the C-6 substituted pyrimidine **7**. Removal of the tertiary hydroxyl group was accomplished using radical deoxygenation via oxalyl ester **8**. Introduction of the methyl group in the N-1 position

of pyrimidine ring was achieved by the reaction of **9** with methyl iodide. Cleavage of two benzyl protecting groups, followed by the removal of the methoxy group gave N-Me DHBT in 13 % overall yield.
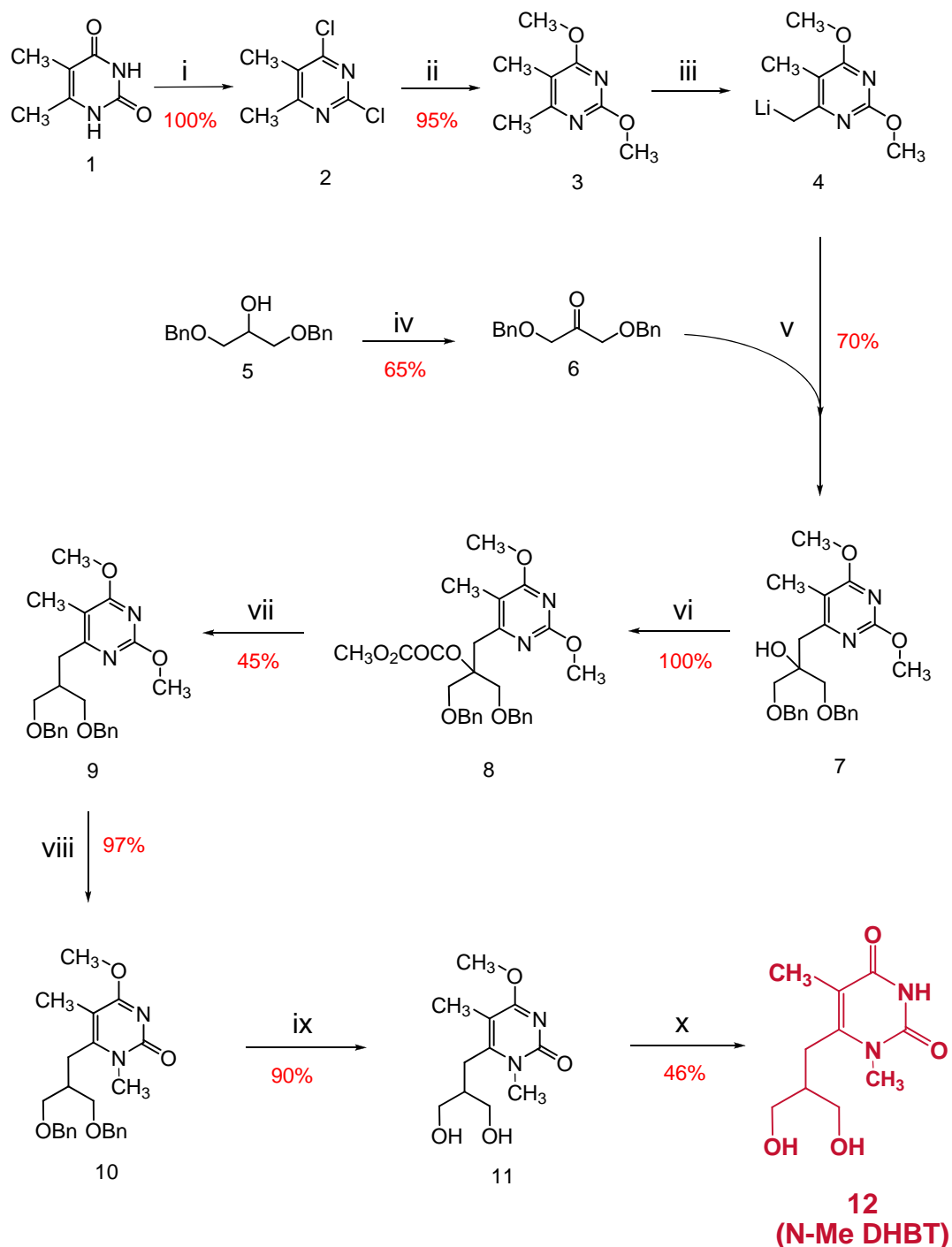
Scheme 1. Synthetic pathway to novel lead compound N-Me DHBT. Reagents and conditions: (*i*) POCl$_3$, reflux; (*ii*) NaOCH$_3$, MeOH; (*iii*) LDA, THF; (*iv*) N-Chlorosuccinimide, Et$_3$N, Toluene ; (*v*) -55°C, THF; (*vi*) C$_3$H$_3$ClO$_3$, DMAP, CH$_3$CN; (*vii*) Bu$_3$SnH, AIBN, Toluene; (*viii*) CH$_3$I; (*ix*) -78°C, BCl$_3$, CH$_2$Cl$_2$; (*x*) AcCl, H$_2$O; NH$_3$, MeOH.

N-Me FHBT was prepared in a three-step reaction sequence (Scheme 2) starting from the key intermediate N-Me DHBT (**12**). In the first step, one of the two hydroxyl groups was selectively protected with MTr (4-**M**ethoxy**tr**ityl) protecting group. Fluorination was performed using DAST to give compound **14**. The removal of MTr group was accomplished using 5% HCl in methanol. Pure reference compound, N-Me FHBT, was obtained in an overall yield of 2.8 %. The structures of all compounds were confirmed with mass spectroscopy, ^{1}H NMR, ^{13}C NMR or ^{19}F NMR spectroscopy.
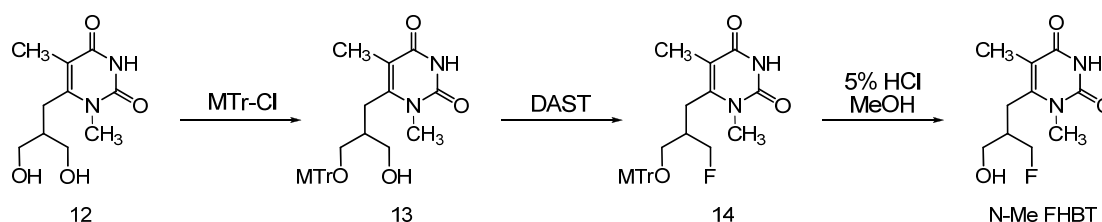
Scheme 2. Preparation of reference compound N-ME FHBT from N-Me DHBT (**12**)

The stability of N-Me FHBT in aqueous solution at room temperature was assessed over a period of 12 months during which no decomposition was observed.

In vitro validation of N-Me DHBT

In analogy to the previously published protocol [10], we initially investigated whether N-Me DHBT would be phosphorylated by HSV1 TK. Prior to assessing the phosphorylation of N-Me DHBT, we additionally validated the protocol using thymidine and DHBT as positive controls. As shown in Figure 4, thymidine (dT) and DHBT were readily phosphorylated be HSV1 TK. Formation of ADP and monophosphorylated substrate, as well as disappearance of the substrate over time are clearly visible. The retention times of N-Me DHBT and ADP are differed only by 0.2 minutes, making a clear distinction between the two components difficult. However, by magnifying a part of DAD (Diode Array Detector) chromatogram corresponding to the region with the retention times of N-Me DHBT and ADP (Figures 4 and 5), it was clearly seen that N-Me DHBT and ADP peaks overlap (Figure 5). As can be seen from Figure 4 (B), the absorption patterns at the beginning and at the end of the

overlapping peak belong to two distinct chemically different compounds. The maxima at 267 nm and 258 nm correspond to ADP and N-Me DHBT, respectively.

The incubation of N-Me DHBT with HSV1 TK, also revealed the presence of a new peak at 7.05 minutes which corresponds to the monophosphorylated N-Me DHBT (Figure 4). An increase over time of this newly formed peak provided another evidence that N-Me DHBT is indeed a substrate of HSV1 TK.

All reactions were done in triplicates and the spontaneous hydrolysis of ATP was taken into consideration.
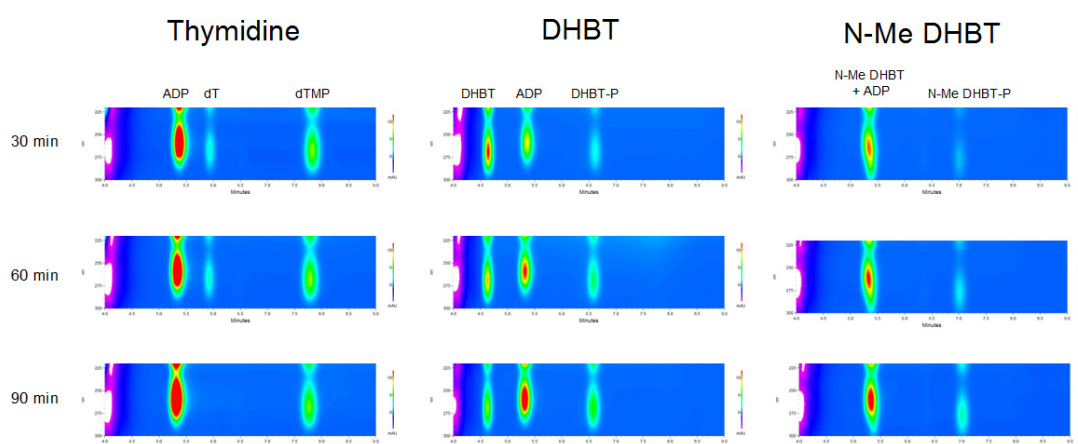

Figure 4. Phosphorylation pattern assay. The formation of new peaks (ADP and monophosphorylated product) has been monitored by HPLC coupled with diode array detector. To assess the functionality of the HSV1 TK enzyme, thymidine (dT) and DHBT were used as positive controls. These chromatogram clearly show the formation of ADP and monophosphorylated products dTMP and DHBT-P, respectively. For N-Me DHBT, the formation of N-Me DHBT monophosphate (N-Me DHBT-P) is clearly visible, while the peaks of N-Me DHBT and ADP overlap.
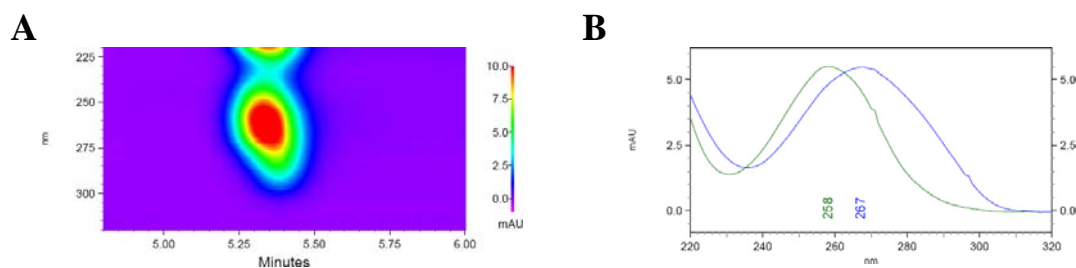
Figure 5. Presence of N-Me DHBT and ADP was confirmed by examining absorption patterns (B) at the beginning and at the and of the overlapping peak (A).

Quantitative enzyme kinetics measurements to determine K_m and K_{cat} were performed by spectrophotometric assay using a previously published protocol [11]. The experiments, performed in triplicate, showed that N-Methyl DHBT was phosphorylated at a similar rate to FHBG ($K_m=10\pm0.3\mu M$, $K_{cat}=0.036\pm0.015$ sec^{-1}). Compared to DHBT ($K_i=35.3 \pm 1.3\mu M$; $K_{cat}=0.035 \pm 0.01$ sec^{-1}), N-Me DHBT exhibits a similar affinity value suggesting that the introduction of a methyl group at the N-1 position of the pyrimidine ring of DHBT has no dramatic influence on the binding affinity of N-Me DHBT.

Cytotoxicity measurements were performed on B16F1 cells using XTT proliferation assay protocol [10,12]. No cytotoxic effect was observed using B16F1 TK+ and B16F1 wt cells even at concentrations where ganciclovir shows high cytotoxicity (Figure 7).

A   **B**
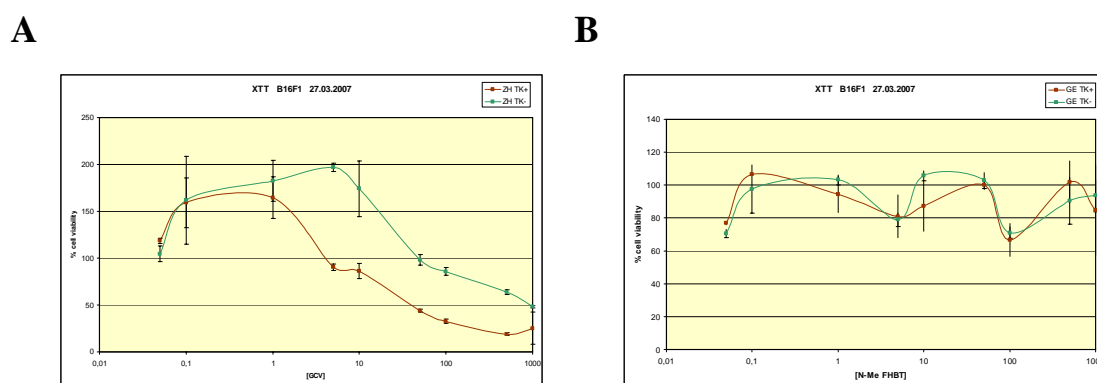
**Figure 7.** Cytotoxicity comparison of ganciclovir (A) and N-Me DHBT (B) using B16F1 TK+ and B16F1 wt cells

Radiolabeling of [^{18}F] N-Me FHBT

For the radiolabeling of [^{18}F]N-Me FHBT it was important to prepare a suitable precursor with a good leaving group. We decided for a tosyl leaving group since this precursor is potentially more lipophilic and can be well separated from the fluorinated product by HPLC. The tosylate precursor **15** was prepared by treating compound **13** with tosyl chloride in 30 % yield. Radiolabeling was carried out under classical conditions using potassium fluoride and kryptofix 2.2.2 in acetonitrile at 90°C (Scheme 3). Purification of the F-18 labeled intermediate **16** was achieved by passing the reaction mixture through a SepPak silica cartridge. The MTr protecting group was easily removed by 5% HCl in methanol during 10 minutes at reflux. Product was obtained by passing reaction mixture first through SepPak C-18 cartridge followed by purification on semi-preparative HPLC. Radiochemically pure [^{18}F]N-Me FHBT (>99 %) was obtained in 25 % RCY (decay corrected) after HPLC purification (Figure 9). In Figures 8 and 9 are shown the HPLC chromatograms of the reaction mixture before and after hydrolysis, respectively. Co-injection with the reference compound confirmed the identity of [^{18}F]N-Me FHBT.
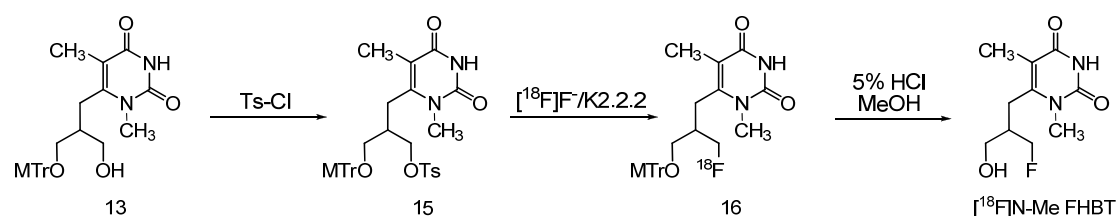
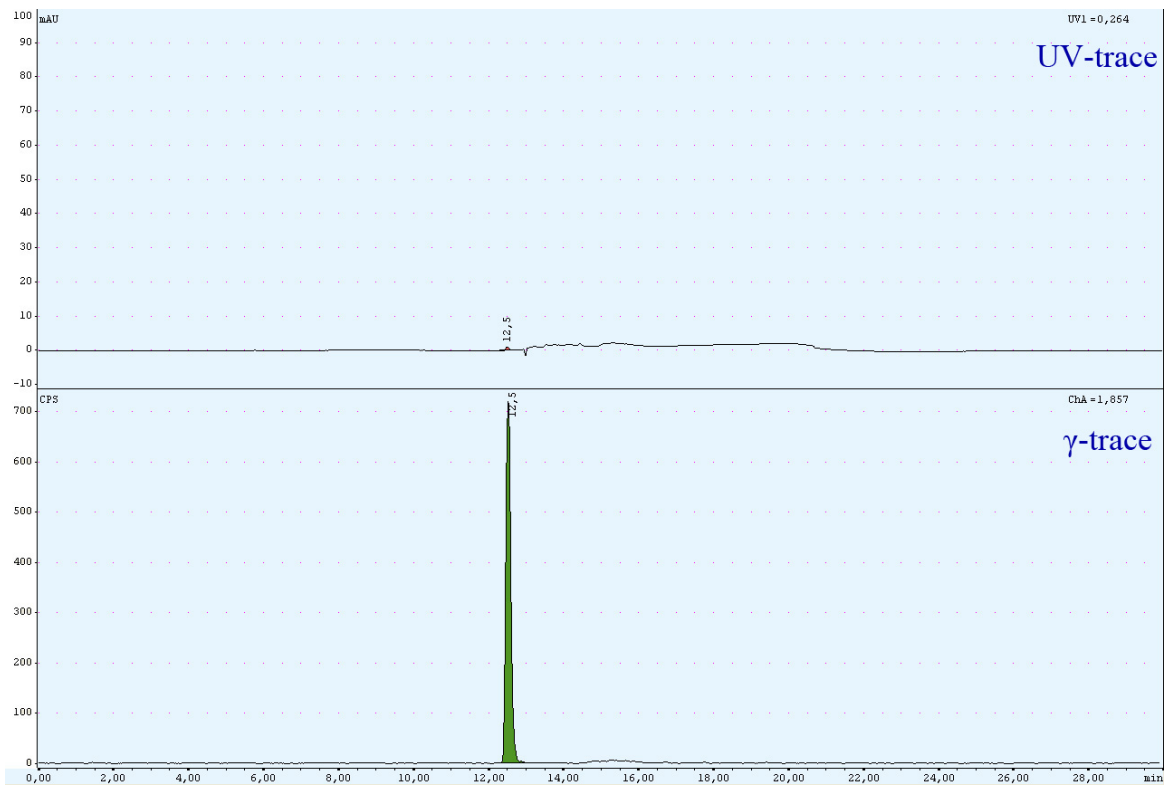**Scheme 3:** Synthesis of [^{18}F]N-Me FHBT
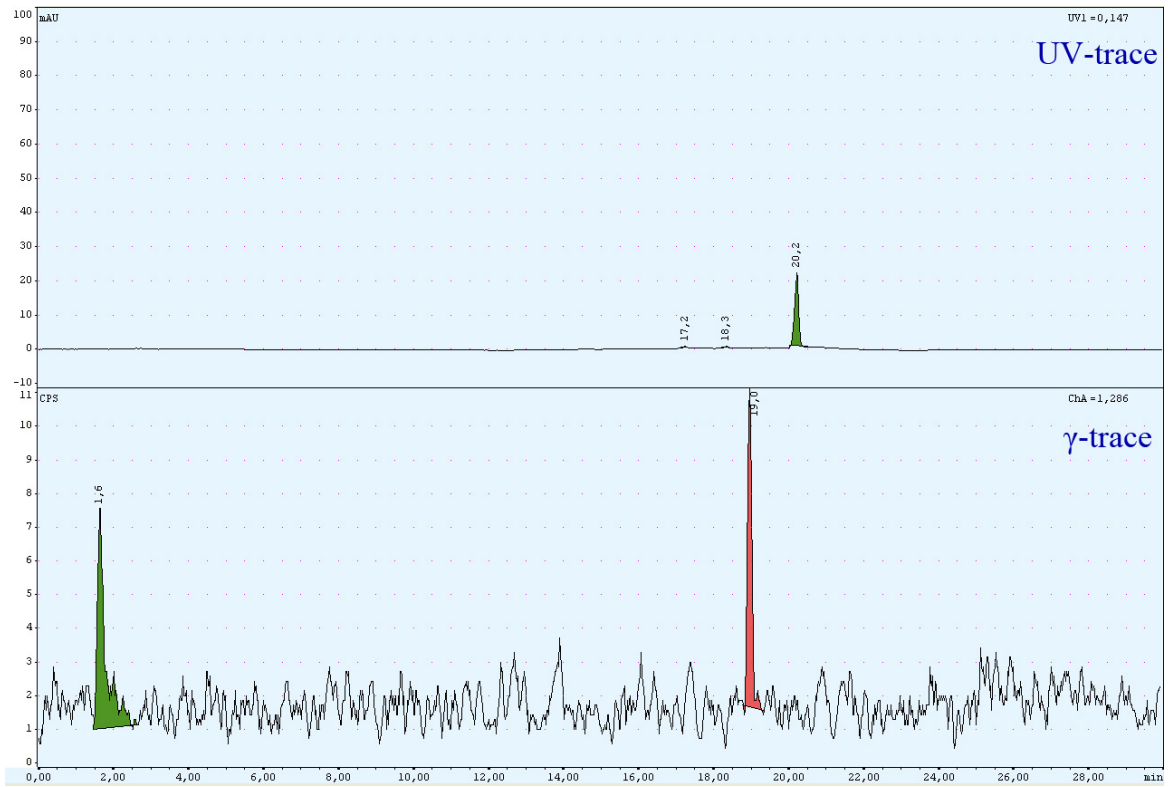
Figure 8. UV and radio HPLC chromatograms before hydrolysis

Figure 9. UV and radio HPLC chromatograms after hydrolysis

3. Conclusions

Molecular modeling was successfully employed to select a novel C-6 substituted pyrimidine derivative for development as a PET ligand for gene expression monitoring. The introduction of a methyl group at the N-1 position of the pyrimidine ring, did not have any dramatic effect on the binding properties of the methylated derivative. N-1 methylation of DHBT effectively prevented intramolecular cyclization and undesired side reactions. Novel lead compound, N-Me DHBT was shown to be a non-cytotoxic substrate for HSV1 TK. The radiosynthesis of [^{18}F]N-Me FHBT was accomplished in good radiochemical yield.

In vitro validation including cell uptake studies, as well as *in vivo* PET studies are necessary to fully assess the biological properties of [^{18}F]N-Me FHBT for monitoring HSV1 TK expression *in vivo*.

The fluorinated derivative is expected to have similar biochemical properties towards HSV-1 TK as N-methyl DHBT.

4. Materials and Methods

The ^{1}H-NMR, ^{13}C-NMR and ^{19}F-NMR spectra were recorded on a 300 MHz Varian Gemini 2000 or a Bruker 400 MHz spectrometer with tetramethylsilane as an internal standard. Chemical shifts (δ) are reported in parts per million, and signals are expressed as s (singlet), d (doublet), t (triplet), q (quartet), m (multiplet) or br (broad). The samples were dissolved in DMSO-d$_6$, D$_2$O or CD$_3$OD and measured in 5mm NMR tubes. The ^{1}H, ^{13}C and ^{19}F NMR chemical shift values (δ) are expressed in ppm referred to TMS and coupling constants (J) in Hz.

Mass spectroscopy analysis was performed with a Micromass Quattro micro TM API LC-ESI or a LCT Premier ESI-TOF from Waters.

TLC was done on Merck silica gel 60 F$_{254}$ precoated plates. Compound was visualized under UV light (254 nm).

Silica gel used for column chromatography was Silica gel 60, particle size 0.040-0.063 mm (230-400 mesh ASTM), Fluka, Germany.

Evaporations were performed using Büchi Rotavapor R-215 system at 40°C.

Production of [^{18}F] fluoride: No-carrier-added aqueous [^{18}F]fluoride ion was produced on an IBA Cyclone 18/9 cyclotron by irradiation of 2.0 ml water target (for a large volume target) or 0. 585 ml (for a small volume target), using a 18 MeV proton beam on 98% enriched [^{18}O]water using the [^{18}O(p,n)^{18}F] nuclear reaction.

HPLC 1 (analytical): Hitachi LaChrom Elite system equipped with UV diode array detector (DAD) and a column oven; column: analytical Merck LiChrospher C18 RP-18E, pore size: 100Å, particle size: 5 μm; flow rate: 1ml/min; temperature: 37°C; UV detection 220-400 nm.

HPLC 2 (analytical): Merck-Hitachi L6200A system equipped with UV multi-wavelength detector; column: analytical Merck LiChrospher RP-18E, pore size: 100Å, particle size: 5 μm; flow rate: 1ml/min; temperature: rt; UV detection at 254 nm or 275 nm.

HPLC 3 (analytical – radiolabeled compounds): Equipment: Agilent 1100 system equipped with a UV multi-wavelength detector; the radioactivity was monitored with a Raytest Gabi Star detector using a Gina software; column: analytical Merck LiChrospher RP-18E, pore size: 100Å, particle size: 5 μm; flow rate: 1ml/min; temperature: rt; UV detection at 254 nm.

HPLC 4 (semiprep): Merck-Hitachi system equipped with L6200A pump, Knauer variable wavelength detector and Eberline radiation monitor; column: semi-preparative Phenomenex Gemini C18, Pore size: 110Å, particle size: 5 μm; flow rate: 5ml/min; temperature: rt; UV detection at 254 or 275 nm.

Docking studies using GOLD

The hTK1 (PDB-ID: 1W4R) and HSV1-TK (PDB-ID: 1VTK) X-ray structures were retrieved from the PDB in pdb format. For each structure, monomer A was kept and hydrogens and Gasteiger charges added using Sybyl 7.2. Then, both structures were stored in mol2 format. For the putative ligands of hTK1 and HSV1-TK, hydrogens and Gasteiger-Huckel partial charges were assigned. Subsequently, the energy of each ligand was minimized using the Powell method with an initial Simplex optimization. The termination criterion was set to a gradient of 0.05 kcal/mol*A and the number of maximal iterations was 1000.

Standard Gold parameters (stored in gold.conf) were applied, except for the definition of the active site, where an origin was defined as center of a sphere with 6.5 A radius.

For hTK, its coordinates were 37.6736, 93.5756 and -19.4822 for x, y and z respectively. This corresponds to the centroid (centre of mass) of dTTP in subunit A of 1W4R. For HSV1-TK, these coordinates were set to 39.502, 16.7312 and 31.9443 (reflecting the centroid of dTMP in subunit A of 1VTK). For each compound, 10 gold runs were done.

2,4-Dichloro-5,6-dimethylpyrimidine (2)

A mixture of 2,4-dihydroxy-5,6-dimethylpyrimidine **1** (6.33 g, 45 mmol) and $POCl_3$ (30 ml, 328 mmol) was heated under reflux for 4 h. Excess of $POCl_3$ was then removed under reduced pressure and the residue was added to ice, washed with ether and dried over sodium sulphate. The crude product was recrystallized from ethanol to give **2** (7.54 g, 94.3 %, mp 70-71 °C); ($C_6H_6N_2Cl_2$), R_f = 0.65 (n-hexane/EtOAc = 5/1).

^{1}H NMR (DMSO-d_6): 2.26 (s, 3H, CH_3); 2.47 (s, 3H, CH_3).

^{13}C NMR (DMSO-d_6): δ 155.24 (C-2), 171.48 (C-4), 127.74 (C-5), 160.54 (C-6), 22.83 (CH_3), 14.40 (CH_3).

2,4-Dimethoxy-5,6-dimethylpyrimidine (3)

To a solution of sodium (2 g, 87.0 mol) in methanol (50 ml) was added **2** (7.54 g, 42.6 mmol). The reaction mixture was refluxed for 6 h. The solvent was evaporated and water was added to dissolve NaCl. The oily layer was extracted with dichloromethane, dried over sodium sulphate and concentrated under reduced pressure. The residue was kept in refrigerator and gave colorless crystals of **3** (7.10 g, 99.1 %, mp 39-40 °C).

^{1}H NMR (DMSO-d_6): 1.98 (s, 3H, CH_3); 2.29 (s, 3H, CH_3); 3.82 (s, 3H, OCH_3); 3.87 (s, 3H, CH_3).

^{13}C NMR (DMSO-d_6): δ 162.10 (C-2), 168.67 (C-4), 107.25 (C-5), 165.67 (C-6), 53.96 (OCH_3), 53.74 (OCH_3), 21.46 (CH_3), 9.67 (CH_3).

1,3-bis(benzyloxy)propan-2-one (6)

N-Chlorosuccinimide (18.0 g, 134.8 mmol) was suspended in dry toluene (210 ml), and the mixture was cooled in dry ice bath. Dimethyl sulfide (15 ml, 204.2 mmol) was added, and the mixture was cooled to -25°C in a dry ice-CH_2Cl_2 bath. 1,3-bis (benzyloxy)-2-propanol **5** (25.0 g, 91.8 mmol) in toluene (21 ml) was added to the mixture, and the mixture was kept under argon for 4 h. Triethylamine (100 ml, 717.5 mol) was added, and the reaction was allowed to warm to room temperature. After 30 min of stirring at room temperature, the solution was passed through a filter paper. The residue was washed with diethyl ether (250 ml). The filtrate and the washings were combined, neutralized with 5% aqueous HCl to pH 7, washed with saturated NaCl solution (3 x 50 ml) and then with water (3 x 50 ml), and finally dried over sodium sulphate. The solvent was removed in vacuum, and the resulting oil was purified by column chromatograpy (n-hexane/EtOAc = 4/1) to give 13.5 g (54.4 % yield) of compound **6** ($C_{17}H_{18}O_3$). mp 40 °C.

MS m/z: 270.1 (M^+).

^{1}H NMR (DMSO-d_6): 7.23 (10H, Ph); 4.46 (s, 4H, CH_2Ph); 4.13 (s, 4H, CH_2O).

6-[[2-[1,3-bis(benzyloxy)-2-hydroxypropyl]]methyl]-2,4-dimethoxy-5-methylpyrimidine (7)

LDA (1.5 M, 45 ml, 113 mmol) was added dropwise to a solution of 2,4 dimethoxy-5,6-dimethylpyrimidine **3** (7.50 g, 44.6 mmol) in THF (90 ml) at -70°C. The temperature was raised to -55°C, and the solution was stirred for 30 min. **6** (12.00 g, 44.4 mmol) in THF (65 ml) was added dropwise to this solution, and stirring was continued for 2.5 h while the temperature was maintained at -55°C. The solution was neutralized by the addition of AcOH to pH 7 and then the temperature was raised to 25°C, and the solvent removed. The residue was partitioned between AcOEt and H_2O. The organic layer was separated, dried over sodium sulfate and removed by evaporation. The residue was chromatographed on silica gel column, eluting with *n*-hexane/EtOAc = 3/1. The desired fractions were concentrated in vacuum to afford compound **7** in 59% yield (1.25 g).

MS m/z: 439.3 (M^+).

^{1}H NMR (DMSO-d_6): 7.28 (10H, Ph); 5.09 (s, 1H, OH); 4.48 (s, 4H, CH_2Ph); 3.87 (s, 2H, CH_2O); 3.76 (s, 3H, OCH_3); 3.44 (s, 3H, OCH_3); 2.83 (s, 2H, CH_2); 1.99 (s, 3H, CH_3).

6-(3-Benzyloxy-2- benzyloxymethyl-propyl) 2,4-dimethoxy-5-methyl pyrimidine (9)

Methyl oxalyl chloride (5.9 ml, 63.7 mmol) was added to a mixture of 6-[[2-[1,3-bis(benzyloxy)-2-hydroxypropyl]]methyl]-2,4-dimethoxy-5-methyl-pyrimidine **7** (6.00g, 13.7 mmol) and 4-(dimethylamino) pyridine (DMAP, 3.7 g, 29.6 mmol) in dry CH_3CN (50ml) at 0°C under argon. The mixture was stirred for 14h under argon at room temperature and then diluted with EtOAc (400ml). The mixture was washed successively with saturated aqueous $NaHCO_3$ solution (120ml) and H_2O (120ml). The separated organic phase was dried over sodium sulfate and the solvent was removed under reduced pressure. The residue was coevaporated twice with dried toluene (40 ml) to afford the methyl oxalyl ester **8**. MS m/z: 481 (M+).

A mixture of Bu_3SnH (9.0 ml, 36 mmol) and 2,2'-azobis (isobutyronitrile) (AIBN; 180 mg, 1.1 mmol) in dry toluene (50 ml) was added to a solution of **8** in dry toluene (130 ml) under an argon atmosphere. The mixture was heated at 110°C for 3h and the solvent was removed by evaporation under reduced pressure. The residue was purified by column chromatography (mixture of n-hexane/EtOAc = 4/1 as mobile phase) to afford 2.77 g of 6-[3-benzyloxy-2- [(benzyloxy) methyl] propyl] thymine **9** in 48% yield.

MS m/z: 423.3 (M^+).

^1H NMR (DMSO-d_6): 7.29 (10H, Ph); 4.42 (s, 4H, CH_2Ph); 3.87 (s, 3H, OCH_3); 3.79 (s, 3H, OCH_3); 3.43 (d, 4H, OCH_2); 2.68 (d, 2H, CH_2); 1.97 (s, 3H, CH_3).

6-(3-(benzyloxy)-2-(benzyloxymethyl)propyl)-4-methoxy-1,5-dimethylpyrimidin-2(1H)-one (10)

Mixture of **9** (3.6 g, 7.57 mol) and CH_3I (50 ml, 803 mol) was refluxed at 50°C for 4 days and evaporated to dryness. Raw product was purified on silica column (n-pentane/ EtOAc= 1/1) to afford 3.5g of pure **10** in 97% yield.

MS: 423.3 (M^+)

^1H NMR ($CDCl_3$): 7.24 (m, 10H, Ph); 4.40 (q, 4H, CH_2); 3.88 (s, 3H, CH_3); 3.45 (s, 3H, CH_3); 3.42 (d, 4H, CH_2); 2.78 (d, 2H, CH_2); 2.10 (m, 1H, CH); 2.95 (s, 3H, CH_3).

6-(3-hydroxy-2-(hydroxymethyl)propyl)-4-methoxy-1,5-dimethylpyrimidin-2(1H)-one (11)

A mixture of **10** (3.2 g, 7.57 mmol) in dry CH_2Cl_2 (40 ml) was cooled to –78°C. BCl_3 (1M in CH_2Cl_2, 35 ml, 35 mol) was added via syringe and under argon. The mixture was stirred at -78°C for 2h, and then the temperature was raised to -40°C. A mixture of CH_2Cl_2/MeOH (1/1; 100 ml) was added, and the cooling bath was removed. The solution was neutralized with saturated $NaHCO_3$ solution to pH 7 and stirred for additional 30 min. The water layer was separated and solvent was removed under reduced pressure to give 1.65 g of pure **11** in 90% yield.

MS m/z: 243.3 (M^+).

^{1}H NMR ($CDCl_3$): 1.96 (s, 3H, CH_3); 2.01 (br, 1H, CH), 2.83 (m, 2H, CH_2); 3.47 (s, 3H, CH_3); 3.58 (m, 4H, $CH_2 + CH_2$); 3.87 (s, 3H, OCH_3).

6-(3-hydroxy-2-(hydroxymethyl)propyl)-1,5-dimethylpyrimidine-2,4(1H,3H)-dione (N-Me DHBT) (12)

A solution of **11** (3.0 g, 12.4 mmol) dissolved in acetyl chloride (10 ml) and containing a few drops of water was stirred at reflux for 48 hrs. The solvent was removed under reduced pressure and the residue was dissolved in saturated methanolic ammonia (50 ml), stirred at rt for additional 4 h, and then evaporated to dryness. The product was purified on a silica column ($CHCl_3$/i-PrOH=4/1) to give pure N-Me DHBT (1.3 g) in 46% yield.

MS m/z: 229.17 (M^+).

^{1}H NMR ($CDCl_3$): 1.86 (s, 3H, CH_3); 1.96 (m, 1H, CH); 2.73 (d, 2H, CH_2); 3.35 (s, 3H, CH_3); 3.58 (m, 4H, $CH_2 + CH_2$).

^{13}C NMR ($CDCl_3$): 10.96 (CH_3); 28.08 ($C_{1'}$); 31.80 (N-CH_3); 41.65 ($C_{2'}$); 61.15 ($C_{3'}$,$C_{4'}$); 109.44 (C_5); 153.85 (C_2, C_4).

6-(3-hydroxy-2-(((4-methoxyphenyl)diphenylmethoxy)methyl)propyl)-1,5-dimethylpyrimidine-2,4(1H,3H)-dione (13)

Solution of **12** (100 mg, 0.44 mmol) in dry pyridine (25 ml) under argon, was cooled down to 0°C. 4-Di(methylamino)pyridine (DMAP, 135 mg, 1.1 mmol) was added to the reaction, and obtained mixture was stirred at 0°C for 15 min. 4-Methoxytriphenylmethyl chloride (150 mg, 0.48 mol) was added, reaction is warmed up to 50°C and stirred for 3 hrs. Reaction mixture was partitioned between

CH_2Cl_2 (250 ml) and saturated aqueous solution of $CuSO_4$ (250 ml). Aqueous layer was washed 3 times with CH_2Cl_2 (100 ml). All organic layers were combined and evaporated to dryness. Pure **13** was obtained after purification on a silica column ($CHCl_3$/i-PrOH=9/1) in 20% yield.

MS m/z: 501.3 (M^+).

^{1}H NMR ($CDCl_3$): 1.75 (s, 3H, CH_3); 1.93 (m, 1H, CH); 2.57 (m, 2H, CH_2); 3.20 (m, 2H, CH_2); 3.28 (s, 3H, N-CH_3); 3.60 (m, 2H, CH_2); 3.71 (s, 3H, OCH_3); 6.73-7.34 (m, 14H, Ph).

6-(3-fluoro-2-((((4-methoxyphenyl)diphenylmethoxy)methyl)propyl)-1,5-dimethylpyrimidine-2,4(1H,3H)-dione (14)

Solution of **13** (37 mg, 73.9 μmol) in dry CH_2Cl_2 (15 ml) under argon, was cooled down to -78°C and stirred for 10 min. (Dimethylamino)sulfur trifluoride (50μl, 378 μmol) was added dropwise and reaction was kept at -78°C for additional 10 min and cooling was removed. After 45 min of stirring at room temperature, saturated aqueous solution of $NaHCO_3$ was added (10 ml) and reaction was partitioned. Organic layer was separated and evaporated to afford 33 mg of raw **14** (89% yield).

MS m/z: 503.3 (M^+).

6-(3-fluoro-2-(hydroxymethyl)propyl)-1,5-dimethylpyrimidine-2,4(1H,3H)-dione (N-Me FHBT)

Solution of raw **14** (33 mg) was dissolved in 5% HCl in CH_3OH was refluxed 15 min at 90°C under argon after which the solvent was removed. Pure N-Me FHBT (2.1 mg) was obtained after HPLC purification in 12% yield.

^{19}F NMR (DMSO-d6): -224 (m).

3-(3,5-dimethyl-2,6-dioxo-1,2,3,6-tetrahydropyrimidin-4-yl)-2-(((4-methoxy phenyl)diphenylmethoxy)methyl)propyl 4-methylbenzenesulfonate (15)

Solution of **13** (44 mg, 87.9 μmol), triethylamine (30μl, 215 μmol) and trimethylamine hydrochloride (1 mg, 10 μmol) in dry CH_2Cl_2 under argon was cooled down to 0°C. Tosyl chloride (20 mg, 104.9 μmol) was added and reaction mixture was stirred at 0°C for 2 hrs and solvent was removed. After HPLC purification, 17.3 mg of pure **15** were obtained (30% yield).

MS m/z: 655.4 (M^+).

6-(3-[^{18}F] fluoro-2-(hydroxymethyl)propyl)-1,5-dimethylpyrimidine-2,4(1H,3H)-dione ([^{18}F] N-Me FHBT)

To a 10-mL Pyrex brand tube with screw cap containing 10 mg Kryptofix 2.2.2 and 2 mg of K_2CO_3 was added 20 GBq ^{18}F-fluoride. Water was azeotropically evaporated from the mixture using dry CH_3CN (3 x 0.9 mL) at 90°C under a stream of nitrogen. After the final drying sequence, 2 mg of **15** dissolved in 300 μl dry CH_3CN were added to the F-18 residue. Reaction was carried out at 90°C for 30 min. Mixture was passed through Sep Pak Silica cartridge and washed with 3.5 ml of CH_3CN and solvent is evaporated at 90°C under the stream of nitrogen. 300 μl of HCl (5% in CH_3OH) was added and reaction was kept for 10 min at 90°C after which it was allowed to cool down to room temperature. Water (4.7 ml) was added and the mixture was purified on HPLC. 2.4 GBq of pure [^{18}F]N-Me FHBT in 2.0 ml was collected after 23 min (25 % RCY after decay correction).

HPLC assay for monitoring the phosphorylation of N-Me DHBT

Reactions were carried out in a final volume of 75 μl containing H_2O (58.2 μl), 1M Tris buffer, pH 7.4 (3.75 μl), 100 mM ATP (3.75 μl), 100 mM $MgCl_2$ (3.75 μl), 1mM N-Me DHBT (3.75 μl) and 2-10 μg of the HSV1 TK. The reaction were carried at 37°C and were stopped by addition of 2.5 mM EDTA (675 μl) at time-points: 10, 20, 30, 45, 60 and 90. Obtained mixture was then injected into HPLC for the analysis. The formation of the monophosphorilated compound, as well as, ADP was monitored qualitatively. Two different blank reactions (no enzyme or no substrate) were run concurrently to account for the occurring minimal reaction independent ATP hydrolysis. All reactions were performed in triplicates. HPLC System: HPLC 1, using a previously published protocol [13]. (Column, C-18; solvent, 0.2 M NaH_2PO_4, 25 mM tetrabutylammonium hydrogen sulphate, 3% methanol; flow 1.1 ml/min; detection, diode array detector).

Determination of k_{cat} by spectrophotometric assays

The K_{cat} values were determined as described in the literature [11]. Reaction mixture with a final volume of 75 μl containing 50 mM Tris buffer pH 7.2, 1 mM 1,4-dithio-DL-threitol, 0.21 mM phosphoenolpyruvate, 2.5 mM $MgCl_2$, 5 mM ATP, 0.18 mM NaDH, 0.8 μg pyruvate kinase, 0.5 μg L-lactate dehydrogenase, and different concentrations of the substrate (0.01 mM, 0.05 mM, 0.1 mM, 0.25 mM, 0.5 mM, 1

mM) were incubated at 37°C. Two minutes later, 5 μg of HSV1 TK was added in order to initiate the reaction. The changes in absorbance at 340 nm corresponding to ADP formation of the TK-dependent reaction at 37°C were monitored during 20 minutes. The data presented are the results of the measurements performed in triplicate. Control experiments were performed in order to take into account the spontaneous hydrolysis of ATP under the experimental conditions.

Cell proliferation assay

Confluent B16F1 TK+ (HSV-1 TK transduced cells) and wt cells were trypsinisated and ingested in 10 ml of fresh RPMI 1640 medium with 10% foetal calf serum and 1% antibiotic PSF solution. The cell concentration of a 1:1 dilution with trypan blue was determined using a Neubauer's counting chamber. The suspension was diluted with medium to a final concentration of 20000 cells per ml.

100 μl of the suspension (2000 cells) were seeded in each well of a 96 well NunclonTM Surface plate from NuncTM. After 1.5 h incubation at 37°C, the cells were attached to the bottom of the wells. 100 μl of sterile solutions of GCV and N-Me DHBT in RPMI 1640 were added to the cells leading to final substrate concentrations of 0.05, 0.1, 1, 5, 10, 50, 100, 500, and 1000 μM. All samples were prepared in triplicate for each cell line. The wells with no thymidine analogue allow calculating the standard value of 100% of cell growth. The plates were incubated for 3.5 days at 37°C in presence of 5% CO_2. Viability of the cells was measured using XTT reagent. 50 μl of the XTT reagent were added to each well. While the plates were incubated at 37°C in presence of 5% CO_2, the living cells converted the XTT (tetrazolin derivative) by biodegradation to a water-soluble reddish formazan derivative [10, 12]. After 9 h incubation the number of viable cells in each vial was determined by colorimetric UV absorption measurement of the converted XTT with an ELISA reader at a wavelength of 450 nm. To account for absorbance due to the presence of varying numbers of cells and non-metabolized XXT, the optical density (OD) at a reference wavelength of 750nm was subtracted [10,12].

5. References

[1]   Tjuvajev JG, Doubrovin M, Akhurst T, Cai S, Balatoni J, Alauddin MM, et al. Comparison of radiolabeled nucleoside probes (FIAU, FHBG, and FHPG) for PET imaging of HSV1-tk gene expression. J Nucl Med 2002;43:1072-83.

[2]   Iyer M, Barrio JR, Namavari M, Bauer E, Satyamurthy N, Nguyen K, Toyokuni T, Phelps ME, Herschman HR, Gambhir SS. 8-[18F]Fluoropenciclovir: an improved reporter probe for imaging HSV1-tk reporter gene expression in vivo using PET. J Nucl Med 2001;42:96-105.

[3]   Cai H, Yin D, Zhang L, Yang X, Xu X, Liu W, Zheng X, Zhang H, Wang J, Xu Y, Cheng D, Zheng M, Han Y, Wu M, Wang Y. Preparation and biological evaluation of 2-amino-6-[18F]fluoro-9-(4-hydroxy-3-hydroxy-methylbutyl) purine (6-[18F]FPCV) as a novel PET probe for imaging HSV1-tk reporter gene expression. Nucl Med Biol. 2007;34:717-25.

[4]   Serganova I, Ponomarev V, Blasberg R. Human reporter genes: potential use in clinical studies. Nucl Med Biol. 2007;34:791-807.

[5]   Johayem A, Raić-Malić S, Lazzati K, Schubiger PA, Scapozza L, Ametamey SM. Synthesis and characterization of a C6 nucleoside analogue for the in vivo imaging of the gene expression of herpes simplex virus type-1 thymidine kinase (HSV1 TK). Chem Biodivers 2006;3:274-83.

[6]   Kellenberger E, Rodrigo J, Muller P, Rognan D. Comparative Evaluation of Eight Docking Tools for Docking and Virtual Screening Accuracy. Proteins 2004;57: 225-42.

[7]   Jones G, Willett P, Glen RC, Leach AR, Taylor R. Development and validation of a genetic algorithm for flexible docking. J Mol Biol 1997; 267:727-48.

[8]   Hsu L-Y, Wise DS, Shannon WM, Drach JC, Townsend LB. Synthesis of C-6 pyrimidine acyclic nucleoside analogs as potential antiviral agents. Nucleosides & Nucleotides 1994;13:563-584.

[9]   Hsu L-Y, Wise DS, Kucera LS, Drach JC, Townsend LB. Synthesis of Anti-Restricted pyrimidine acyclic Nucleosides. J Org Chem 1992;57:3354-8.

[10] Roehm NW, Rodgers GH, Hatfield SM, Glasebrook AL. An improved colorimetric assay for cell proliferation and viability utilizing the tetrazolium salt XTT. J Immunol Methods 1991;142:257-65.

[11] Schelling P, Folkers G, Scapozza L. A spectrophotometric assay for quantitative determination of kcat of herpes simplex virus type 1 thymidine kinase substrates.

[12] Jost LM., Kirkwood JM, Whiteside TL. Improved short- and long-term XTT-based colorimetric cellular cytotoxicity assay for melanoma and other tumor cells. J Immunol Methods, 1992;147:153-65.

[13] Pilger BD, Perozzo R, Alber F, Wurth C, Folkers G, Scapozza L. J Biol Chem. 1999;274:31967-73.

4 Overall Conclusions & Outlook

An optimized synthesis of the key intermediate DHBT was a necessary prerequisite for the development of FHBT. The 10-step synthesis of DHBT was successfully optimized and the overall yield was increased 10-fold. Using numerous synthetic approaches from different starting compounds, the preparation of target compound FHBT was unsuccessful. Although we successfully produced F-19 and F-18 fluoro derivatives of DHBT in the presence of MTr protecting group, neither FHBT nor [^{18}F]FHBT were isolated.

As suggested in Chapter 2, one novel possibility to prepare FHBT would be by introduction of the fluorine atom at the very beginning of the synthesis (Scheme 2.21). Additionally, it should be possible to use chlorine instead of fluorine, since chlorine could be substituted with ^{18}F (see page 54).

N-1 methylated DHBT (N-Me DHBT) was successfully synthesized in 10-step reaction sequence. Enzyme kinetics confirmed that N-Me DHBT is indeed a substrate for HSV1 TK. Methylation on N-1 position effectively prevented intramolecular cyclization and undesired side reactions, thus making the synthesis of cold reference and radiolabeling with F-18 possible. Further *in vitro* validation (cell uptake studies) as well as *in vivo* studies are necessary to fully assess the biological properties of [^{18}F]N-Me FHBT for the monitoring of HSV1 TK expression *in vivo*.

A pool of new compounds is necessary to fully assess the binding affinity of C-5 and C-6 substituted N-1 methylated class of compounds. A novel method for preparing C-5 and C-6 substituted pyrimidine derivatives from acetoacetate derivatives and urea is shown in Scheme 4.2.
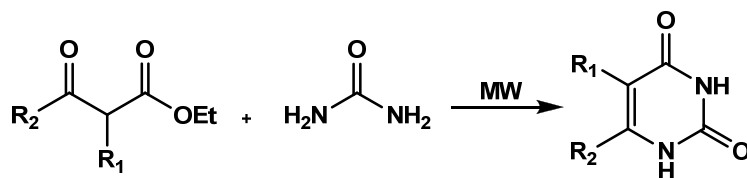

Scheme 4.2 A microwave approach to C-5 and C-6 pyrimidine derivatives from acetoacetate esters and urea

One example which could be tried in future synthesis, starts from commercially available ester **M1. M1** would then react with urea (**M2**) to produce C-5 and C-6 substituted derivative **M3**. Methylation at the N-1 position followed by removal of the methoxy group would give key intermediate **M4** (Scheme 4.3).
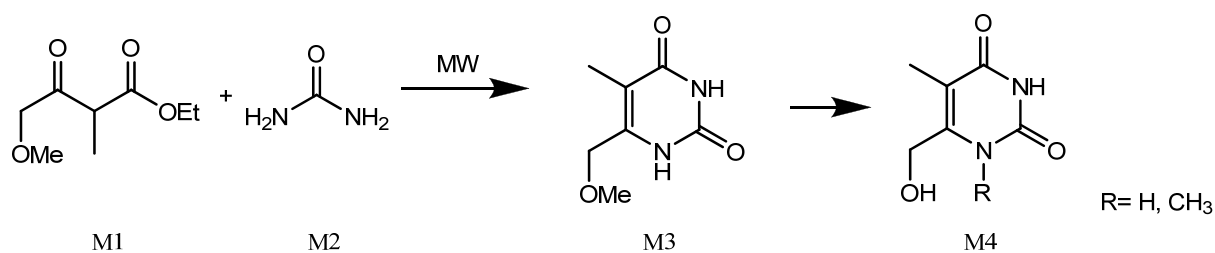
Scheme 4.3 Microwave approach to the preparation of key intermediate **M4**

Free hydroxyl group of **M4** provides excellent opportunities to prepare a series of compounds using relatively simple and straightforward synthetic procedures.
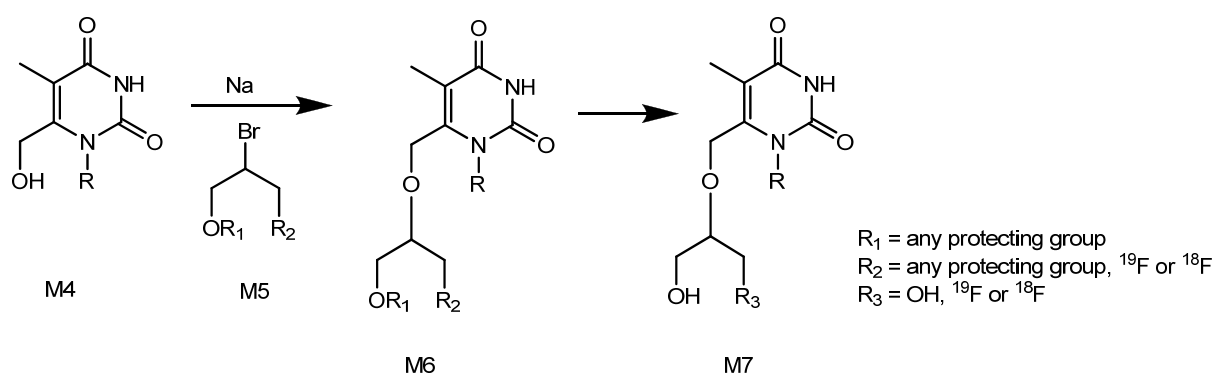
Scheme 4.4 Synthetic approach to prepare a pool of new C-6 substituted N-1 methylated analogues. Method as well provides a possibility to obtain fluorinated analogues

Compounds which would be substrates for viral TK could easily be converted into corresponding fluorinated analogues by using already fluorinated **M5** derivative (Scheme 4.4). Additionally, it would be possible to prepare F-18 labeled **M5** analogues and use them for the synthesis of radiolabeled compounds for gene therapy monitoring and screen their potential as a HSV1 TK substrates.

<div align="center">

Curriculum Vitae

Miljen Martić

</div>

Address: Breitensteinstr. 94
           CH-8037 Zurich, Switzerland
E-mail: miljen.martic@pharma.ethz.ch

Education / Qualifications

2004 – present   **ETH Zurich**, Institute of Pharmaceutical Sciences, Switzerland

PhD in Radiopharmaceutical Sciences

- **Title**: Development of new nucleoside analogues as PET imaging agents for monitoring gene expression
- **Supervisors**: Prof. P. A. Schubiger and Prof. S. M. Ametamey

2005   **Paul Scherrer Institute**, Villigen, Switzerland

Radiation Safety Officer for B- and C-laboratories

1997 – 2002   **University of Zagreb**, Faculty of Science, Croatia

Diploma in chemistry (organic chemistry major)

- **Title**: Synthesis and molecular modeling of 1,1-di-(3-carboxyphenyl)ethane derivatives
- **Supervisors:** Prof. Dr. V. Šunjić and Dr. N. Kujundžić

2002   **Algebra**, Zagreb, Croatia

Internet Application Programmer

International license for programming internet applications using Active Server Pages (ASP), VBScript, JavaScript and integration with MS Access

Languages

Croatian	**Mother tongue**
English	**Fluent**, both spoken and written – **Senior year** of high school spent as an exchange student **in West Chester, PA, USA**
German	**Intermediate** conversational level (B1)

Publications

- <u>M. Martić</u> et al., Synthesis, Biological Activity and Molecular Modeling Studies of Novel COX-1 Inhibitors, Eur. J. Med. Chem. 39 (2004) 141-151.
- <u>M. Martić</u> et al., Development of new F-18 labeled C-6 pyrimidine derivative for gene expression monitoring, manuscript in preparation

Oral and Poster Presentations

Oral

- 17th International Symposium on Radiopharmaceutical Sciences (ISRS), May 2007, Aachen, Germany
- SGR/SGNM, June 2006, Lausanne, Switzerland
- 13. Arbeitstreffen der Arbeitsgemeinschaft Radiochemie / Radiopharmazie, October 2005, Seefeld, Austria
- Doktorandentag, March 2006, ETH Zurich, Switzerland

Poster

- ZNZ Symposium, October 2005, Zurich, Switzerland

Honors & Awards

- U.S. National Chemistry Olympiad, top 15% in Pennsylvania, USA, 1997
- American Chemical Society award certificate for recognition of achievement in high school chemistry, 1997
- Travel grant for the attendance of the 17th International Symposium on Radiopharmaceutical Sciences (ISRS), May 2007, Aachen, Germany